

ENSLAPP-A-473/94
hep-ph/9405359
May 1994

Electroweak Physics Issues at a High Energy Photon Collider *

Marc Baillargeon[#], Geneviève Bélanger[#] and Fawzi Boudjema
*Laboratoire de Physique Théorique ENSLAPP[§]
 B.P.110, 74941 Annecy-Le-Vieux Cedex, France*

Abstract

The main attractions of studying the bosonic sector of the electroweak standard model and its extensions at a future high energy photon collider are reviewed. A presentation of the laser scheme for obtaining such a collider is given where we emphasize the importance of polarised $\gamma\gamma$ spectra. The need for *measuring* the differential luminosities is stressed. We show that, in a large variety of processes, the yield of weak vector bosons is much higher than at the e^+e^- mode but unfortunately, the cross sections are dominated by the transverse modes. Investigation of the physics related to the symmetry breaking sector both in W and Z pair production is given and contrasted with what we expect to obtain in the e^+e^- mode and at the LHC. We reassess the issue of whether an intermediate-mass Higgs can be observed as a resonance when we have a broad spectrum that allows the simultaneous study of a host of electroweak phenomena. This investigation includes the important background of the so-called “resolved” photon. We analyse the important issues of the mass resolution, the b tagging efficiencies, and the polarisation of the beams at two typical e^+e^- energies: 300GeV and 500GeV. New efficient cuts are found to suppress the background. The importance of WWH production at ~ 1 TeV is emphasized and contrasted with other Higgs production mechanisms at both e^+e^- and $e\gamma$. We take into account various backgrounds and look at the effect of polarisation. Finally, we examine the interesting problem of the longitudinal W (W_L) content of the photon. A new set of polarised structure functions for the W_L inside the photon is proposed. We test the validity of the ensuing effective W approximation in the $\gamma\gamma \rightarrow W^+W^-H$ process.

* Based on invited talks given at the “*Two-Photon Physics from DAΦNE to LEP200 and Beyond*”, 2-4 February 1994, Paris.

On leave from *Laboratoire de Physique Nucléaire, Université de Montréal, C.P. 6128, Succ. A, Montréal, Québec, H3C 3J7, Canada*.

§ URA 14-36 du CNRS, associée à l’E.N.S. de Lyon et au LAPP d’Annecy-le-Vieux.

1 Introduction

Photons have, since very long, proved to be an excellent probe of the structure of matter and the forces that govern it. In the area of particle physics a good example is the investigation of the electromagnetic properties (form-factors) of the particles. Analysis of final state photons can also be a unique way of revealing the presence of new physics. Another important on-going area of research is two-photon physics at the various e^+e^- storage rings. These photons are quasi-real photons which give a predominantly soft luminosity spectrum. Here, the bulk of the studies is devoted to various aspects of hadronic interactions and tests of QCD. A new source of highly energetic photons will open up additional possibilities for the investigation of electroweak phenomena, not only because one reaches higher thresholds, but also because the photon is intimately connected to the weak vector bosons. After all, in the $SU(2) \times U(1)$ theory the photon emerges as a combination of W^0 and the hypercharge gauge boson.

The main attractions of $\gamma\gamma$ collisions are:

- $\gamma\gamma$ is a quite “democratic” means of producing any *charged* particle. Phase space allowing, independently of their origin, elementary particles are produced with a predictable cross-section. Signatures of different models/particles reside in their decay. Usually the production mechanisms via e^+e^- are more complicated and model dependent.
- From the point of view of the electroweak physics and most importantly the sector of symmetry breaking, $\gamma\gamma$ allows to access the $J_Z = 0$ directly with the most spectacular manifestation being the production of a scalar as a resonance. This is perhaps the most salient advantage over e^+e^- collisions where chirality highly suppresses this s –channel production.

On the other hand a clear disadvantage is that a $J_Z = 1$ resonance can not occur in the $\gamma\gamma$ mode. This should be viewed as a complementarity between the e^+e^- and the $\gamma\gamma$ modes. At this point it is worth adding a slight “undertone”. While the $J_Z = 1$ resonance in e^+e^- is not suppressed at all, the neutral scalar can not be coupled in a point-like manner to the two photon state. This coupling can be effectively parameterized by a dimension-5 operator, essential for gauge invariance, which involves a factor of α :

$$(S, P)\gamma\gamma \rightarrow \infty \frac{1}{M} \frac{\alpha}{\pi} F_{\mu\nu} (F_{\mu\nu}, \tilde{F}^{\mu\nu}) \quad (1.1)$$

where S is for a scalar and P for a pseudo-scalar and M is a typical scale. Therefore the $S\gamma\gamma$ coupling is suppressed and the peak is not expected to be as prominent as what we

would have with a gauge boson in e^+e^- . For example, the two-photon coupling of the Higgs is only induced at one-loop.

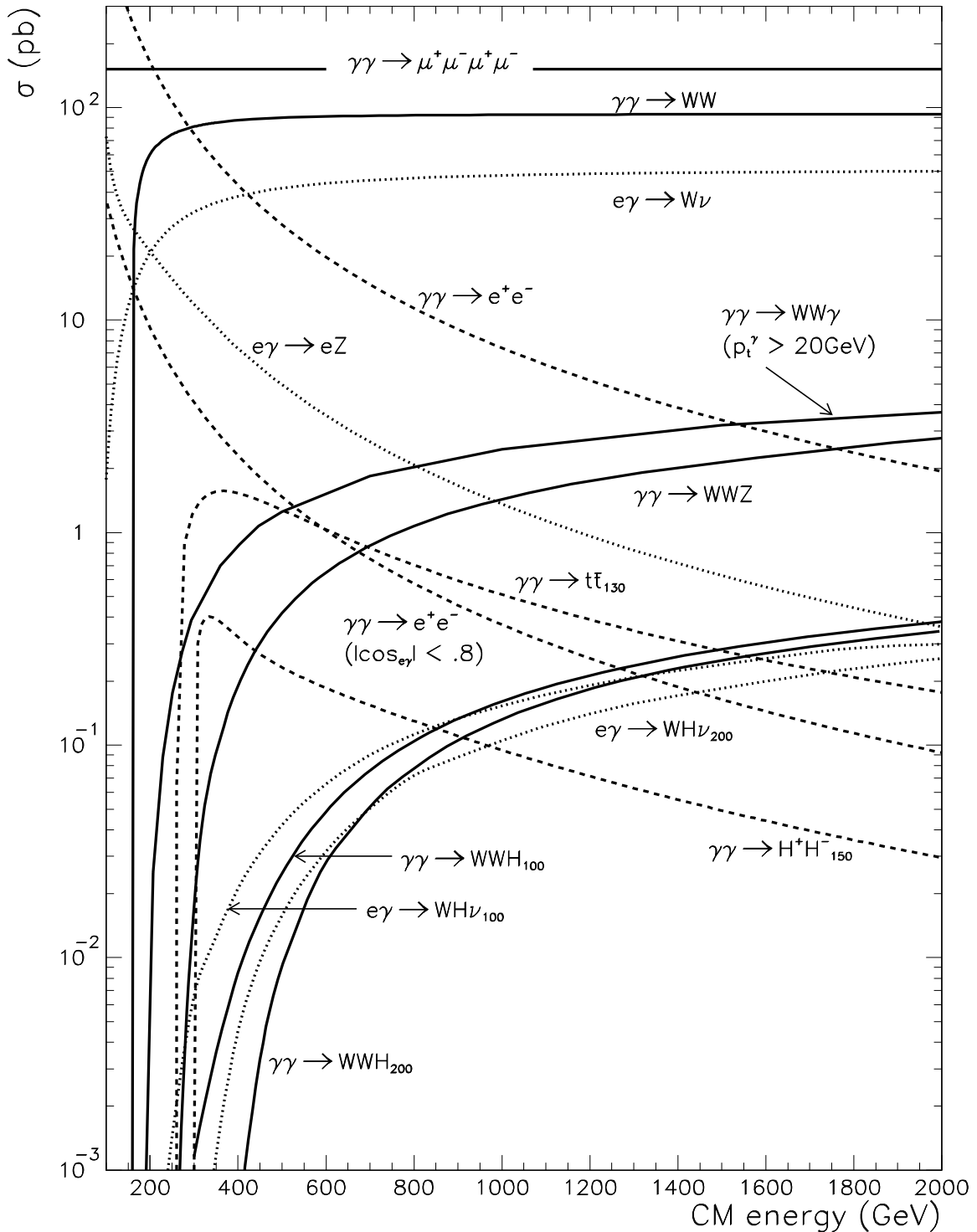
Nonetheless, with the unique possibility of easily accessing the $J_Z = 0$ state and the observation that the photon has an $SU(2)$ part, $\gamma\gamma$ collisions seem to have all the ingredients to study W physics and notably the mechanism of symmetry breaking. If only we had large cross-sections..... and correspondingly very energetic and “luminous” beams.....

2 Typical sizes of electroweak cross-sections

At high enough energies, in fact soon after the opening up of the corresponding thresholds, production of W bosons gives very large cross-sections. In Fig. 1 we show some typical processes that occur in $\gamma\gamma$ collisions. For the sake of comparison we have also included $e\gamma$ processes, although our talks concentrate essentially on $\gamma\gamma$ physics. Vector boson production dominates in $\gamma\gamma$ collisions due the t-channel spin-1 exchanges. Most prominent is the W pair cross-section, which very quickly reaches a plateau of about 90pb[1, 2]. At 500 GeV this cross-section is larger than the total e^+e^- production that scales as $1/s$. At yet higher energies triple vector production, WWZ and $WW\gamma$ (with a fixed $p_t^\gamma > 20$ GeV) become more important than fermion pair production[3]. In fact W pair production is so important that we can envisage to use it to trigger H production. We see that substantial WWH cross-sections are possible[3]. From the experimental point of view one could use the large cross-section for W pair production as a luminosity monitor. The total $\mu^+\mu^-\mu^+\mu^-$ [4] that could also be used as a luminosity monitor is not sensibly larger, while it remains to be seen how well one could tag the extreme forward 4 muons.

To clearly see how important and how rich $\gamma\gamma$ reactions become at TeV energies it is very educating to compare a few characteristic cross-sections with the corresponding same-final-state processes at e^+e^- . The first observation is that independently of the spin of the particle, at the same centre-of-mass energy, $\gamma\gamma$ initiated processes are, at high enough energy, about an order of magnitude larger than the corresponding e^+e^- reactions (Fig. 2). Let us briefly contrast the situation as regards the production of charged scalars, fermions and vector bosons that we will take to be the W . As stated earlier, for $\gamma\gamma$ reactions one only needs to know the electric charge assignment and for the weak vectors we take them to be elementary gauge bosons. We express the cross-section in units of $\sigma_0 = 4\pi\alpha^2/(3s)$ with s being the centre-of-mass energy of either the $\gamma\gamma$ or e^+e^- system. For pair production of a particle of mass M we will also use $\tilde{\sigma}_0 = \sigma_0(s = 4M^2) = \pi\alpha^2/3M^2$.

Figure 1: *Typical sizes of non hadronic $\gamma\gamma$ and $e\gamma$ processes. The subscripts in Higgs processes refer to the mass of the Higgs. For $t\bar{t}$ production the top mass was set to 130 GeV.*



•Scalars

To compute the pair production rate of charged scalars in e^+e^- shown in Fig. 2 we have chosen as an example the charged Higgses of the MSSM which (at tree-level) is like taking a simple two-doublet extension of the standard model (\mathcal{SM}). For $\gamma\gamma$ collisions only the charge assignment is needed. This is a particular example of what we alluded to earlier: tree-level cross-sections in e^+e^- require the knowledge of a model dependent part which is interesting in its own. However, this argument can also be turned to the advantage of the $\gamma\gamma$ mode by arguing that the model dependent part necessarily will show up in the decay patterns leaving us with a cleaner initial state. The Z exchange, though, does not change the features of the comparison between the $\gamma\gamma$ and e^+e^- modes, so for the sake of clarity our discussion only keeps the photonic exchanges in e^+e^- both for the case of scalars and fermions, without any incidence on the unitarity of the cross-section. The first characteristic is the behaviour of the cross-section at threshold

$$\sigma_{thr}(e^+e^- \rightarrow H^+H^-) = \frac{1}{4}\beta^3\tilde{\sigma}_0 \quad \sigma_{thr}(\gamma\gamma \rightarrow H^+H^-) = \frac{3}{2}\beta\tilde{\sigma}_0 \quad (2.1)$$

Clearly the e^+e^- cross-section suffers from the P-wave suppression ($\propto \beta^3$). At higher energies, $s \gg 4M^2$, there is a factor 6 in favour of the $\gamma\gamma$ cross-section:

$$\sigma(e^+e^- \rightarrow H^+H^-) = \frac{1}{4}\sigma_0 \quad \sigma(\gamma\gamma \rightarrow H^+H^-) = \frac{3}{2}\sigma_0 \quad (2.2)$$

•Fermions

Again, only taking the photon exchange in e^+e^- and considering a charged particle with unit charge one has

$$\sigma_{thr}(e^+e^- \rightarrow f\bar{f}) = \frac{3}{2}\beta\tilde{\sigma}_0 \quad \sigma_{thr}(\gamma\gamma \rightarrow f\bar{f}) = 3\beta\tilde{\sigma}_0 \quad (2.3)$$

The cross-section is twice as large, although this threshold enhancement factor can be offset for fermions with less-than-unity charges. Far from threshold the $\gamma\gamma$ cross-section has a logarithmic factor enhancement

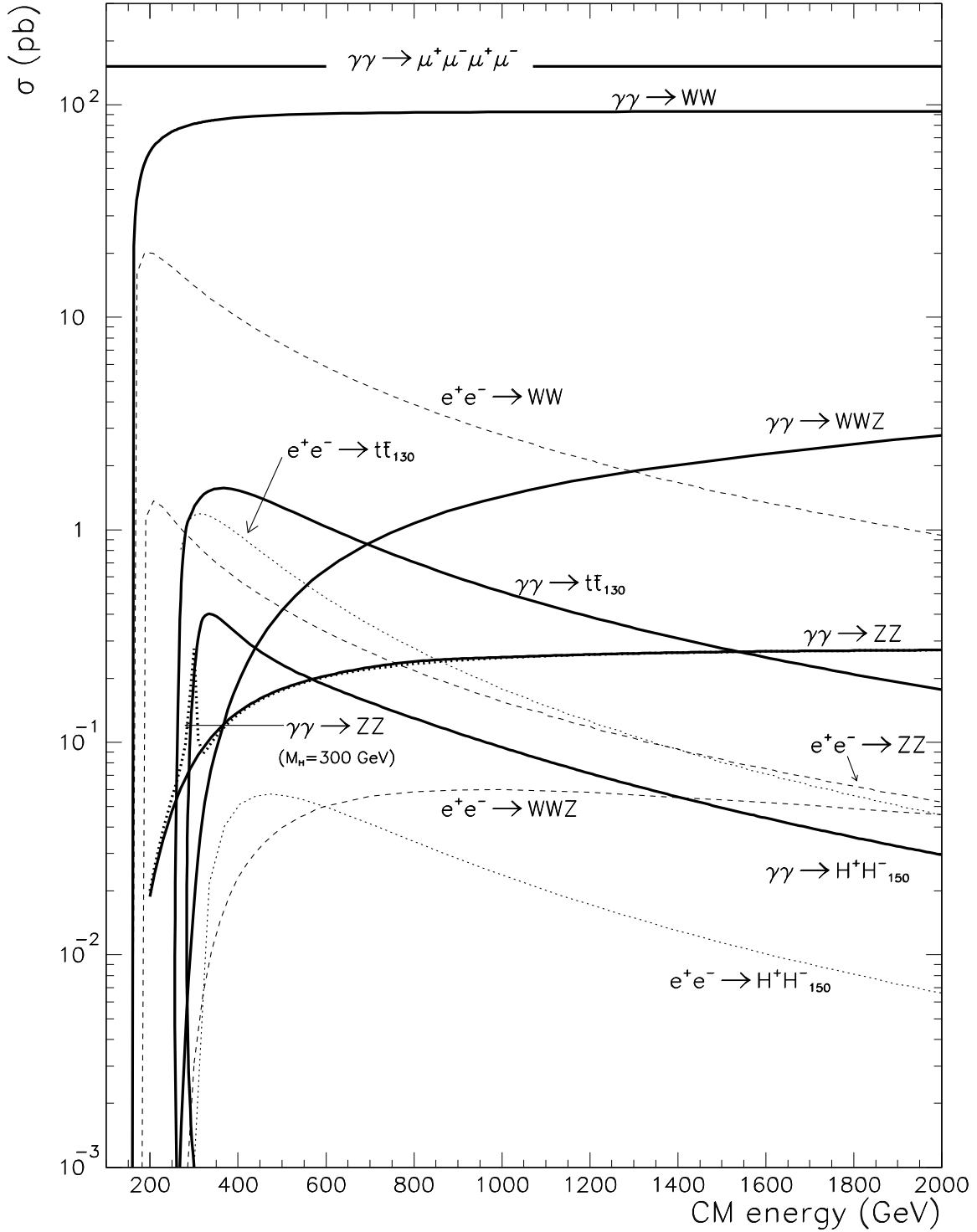
$$\sigma(e^+e^- \rightarrow f\bar{f}) = \sigma_0 \quad \sigma(\gamma\gamma \rightarrow f\bar{f}) = 3(\log(s/M^2) - 1)\sigma_0 \quad (2.4)$$

•Vectors

It is with the vector bosons that we have the most interesting results. Here we include all of the electroweak diagrams. First, at threshold one has

$$\begin{aligned} \sigma_{thr}(e^+e^- \rightarrow W^+W^-) &= \frac{3}{4s_W^4}\beta\tilde{\sigma}_0 \approx 12\beta\tilde{\sigma}_0 \\ \sigma_{thr}(\gamma\gamma \rightarrow W^+W^-) &\approx \frac{57}{2}\beta\tilde{\sigma}_0 \end{aligned} \quad (2.5)$$

Figure 2: Comparison between the sizes of $\gamma\gamma$ and e^+e^- cross-sections with the same final state (All bold curves are for $\gamma\gamma$ processes). The subscripts refer to Higgs and top masses. In the case of ZZ production (from [5]), the dotted line corresponds to $M_H = 300\text{GeV}$ while the plain curve corresponds to the infinite Higgs mass.



Again the $\gamma\gamma$ cross-section is about a factor 2 larger. At asymptotic energies, as advertised earlier, the $\gamma\gamma$ cross-section reaches a plateau while the e^+e^- decreases with energy:

$$\sigma(e^+e^- \rightarrow W^+W^-) = \frac{3}{8s_W^4} \log(s/M_W^2)\sigma_0 \quad \sigma(\gamma\gamma \rightarrow W^+W^-) = \frac{8\pi\alpha^2}{M_W^2} \quad (2.6)$$

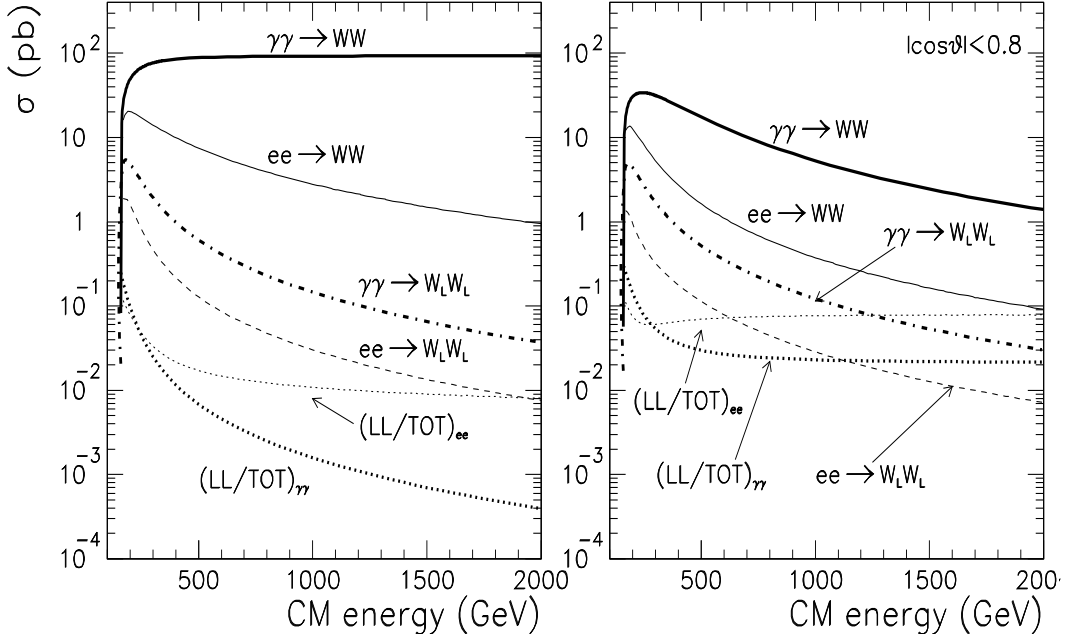
Another very important fact concerns the reaction $\gamma\gamma \rightarrow ZZ$ [5, 6, 7, 8, 9]. While ZZ production in e^+e^- occurs at tree-level and decreases with energy, $\gamma\gamma \rightarrow ZZ$ is a purely quantum effect very akin to the scattering of light-by-light. Even so, at tree-level the cross-section very rapidly picks up and takes over the corresponding e^+e^- process! Again this is due to the rescattering effect, $\gamma\gamma \rightarrow W^+W^- \rightarrow ZZ$. The reaction $\gamma\gamma \rightarrow W^+W^-$ is the backbone reaction for a host of electroweak processes. Even triple vector boson production, WWZ , which can be considered as a Z radiation off W plays an important role at TeV energies in $\gamma\gamma$ [3]. Compared to the same final state in e^+e^- [10, 11, 12], at 2 TeV, there is a factor of two orders of magnitude in favour of the $\gamma\gamma$ mode.

2.1 To be fair: t -channel cross-sections and transverse *versus* longitudinal vector bosons yield

As stressed earlier, the importance of the vector boson pair production and the fact that the cross-section for W pair becomes constant at asymptotic energies is due to the spin-1 t channel exchange. Of course, fusion processes via spin-1 do occur at the e^+e^- collider but the interesting processes with production of vector bosons are generally accompanied with missing momentum (neutrinos or electrons lost in the beam pipe) as in single W or Z production. Even when compared to these cases, the WW in $\gamma\gamma$ has a larger cross-section. It is true that the W 's are produced quite forward and hence once a cut on the scattering angle of the W is imposed the cross-section does decrease with energy. However, even with a cut on the W scattering angle such that $|\cos\theta| < 0.8$, the cross-section is still substantial and one is doing with WW “picobarn physics” all the way up to 1 TeV centre-of-mass. Moreover, even when the W 's are very forward, at sub-TeV energies one could in principle still recognize them through their decay. Therefore, even after angular cuts the WW cross-section is still very large.

Another aspect that must be addressed is to know how much of the W sample would be conducive to interesting electroweak tests. For instance, having in view the mechanism of symmetry breaking (\mathcal{SB}), what is the amount of longitudinal W 's at high energy? The production of W_LW_L in $\gamma\gamma$ is given by the same asymptotic formula for the production of two scalars. This is as much as 5 times more than what we have in e^+e^- . This is the

Figure 3: Comparing the total WW cross-sections and the longitudinal $WLWL$ in e^+e^- versus $\gamma\gamma$ as well as the ratio of longitudinal over total. For the latter, the scale can be read off on the same y axis. The second figure shows what happens when a cut on the scattering is imposed.



good news. However, one has to realize that the extraction of these longitudinals, if the new physics does not substantially increase their yield, is an incredibly tiny portion of all WW 's. From this perspective the situation in e^+e^- is not so bad. To wit,

$$\sigma_{s \gg M_W^2} (e^+e^- \rightarrow W_L^+W_L^-) \sim \frac{1}{3}\sigma_0 \quad \sigma_{s \gg M_W^2} (\gamma\gamma \rightarrow W_L^+W_L^-) = \frac{3}{2}\sigma_0 \quad (2.7)$$

but

$$\frac{\sigma_{s \gg M_W^2} (e^+e^- \rightarrow W_L^+W_L^-)}{\sigma_{s \gg M_W^2} (e^+e^- \rightarrow W^+W^-)} \sim \frac{1}{20} \frac{1}{\log(s/M_W^2)} ; \quad \frac{\sigma_{s \gg M_W^2} (\gamma\gamma \rightarrow W_L^+W_L^-)}{\sigma_{s \gg M_W^2} (\gamma\gamma \rightarrow W^+W^-)} \sim \frac{1}{4} \frac{M_W^2}{s} \quad (2.8)$$

So, as a summary regarding the comparison between e^+e^- and $\gamma\gamma$ processes and before addressing the subject of how so large $\gamma\gamma$ cms energies can be obtained, one could say that the WW cross-section system provides a good example of the characteristics of the electroweak cross-sections in $\gamma\gamma$ in the sense that there would be plenty of electroweak events but we will have to fight very hard to extract the interesting samples of longitudinal vector bosons out of the huge sample of transverse vector bosons. Angular cuts do, though, improve the LL/TT ratio (see Fig. 3).

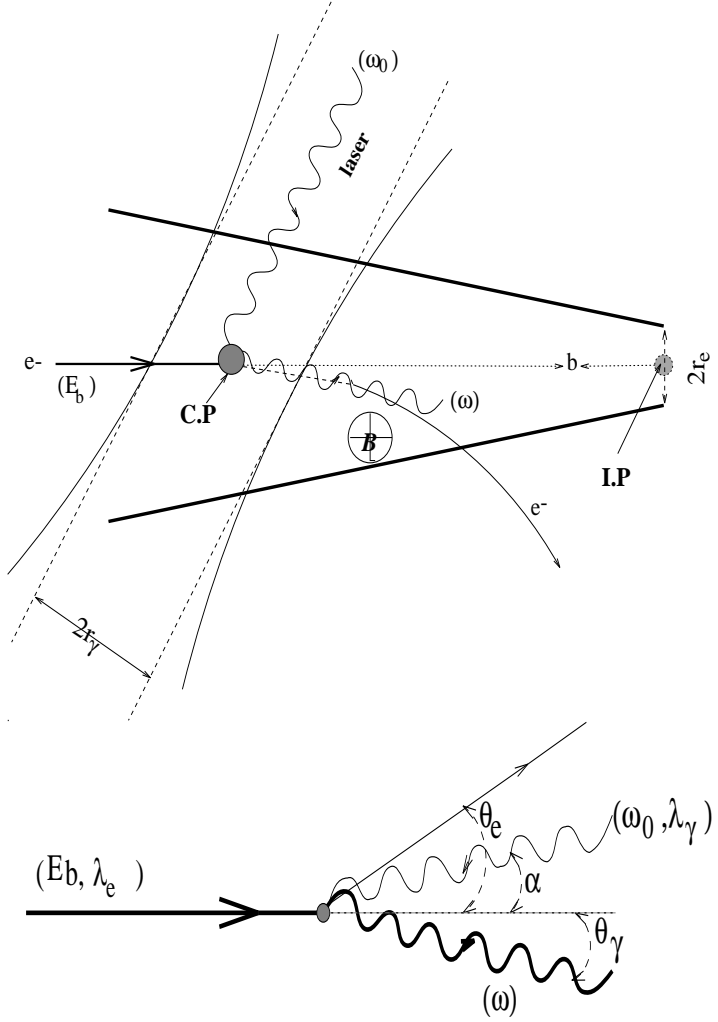
3 The laser set-up for a high energy photon collider and the luminosity spectra

3.1 The laser set-up

Until now, two-photon processes at e^+e^- storage rings have exploited the “Weiszäcker-Williams” spectrum[13], which is essentially a “soft-photons” spectrum. The $\gamma\gamma$ luminosity peaks for very small fractions of the invariant $\gamma\gamma$ mass $\sqrt{s}_{\gamma\gamma}$, i.e., for $\tau = s_{\gamma\gamma}/s_{e^+e^-} \ll 1$. Recently, with the intense activity in the physics of a linear e^+e^- collider there has been a growing interest and some excitement about converting the single pass electron into a very energetic photon through Compton backscattering of an intense laser light. The seeds of the idea are some 30 years old[14] but the most comprehensive analysis of the scheme has been performed by the Novosibirsk group[15]. The detailed analyses of this group have also provided the working basis[16] to investigate new physical processes. The set-up of such a scheme is shown in Fig. 4

The principle of the scheme is quite simple. A laser beam of frequency ω_0 (of order the eV) is focused at an extremely small angle (α) on the electron beam of energy E_b . Compton backscattering occurs at the conversion point (C.P.) which is a distance b (a few cm) away from the interaction point (I.P.), where the electron would have converged. This gives a very energetic photon of energy ω emitted at a very small angle and a soft electron. In order that the “soft” electron does not end up in the interaction region and hence would interact with a hard photon from the opposite arm of the collider or with another soft electron, it is suggested to use a very strong transversal magnetic field between the conversion region and the interaction point[15]. With this suggestion, additional and unnecessary backgrounds due to non- $\gamma\gamma$ initiated processes as well as degradation of the overall $\gamma\gamma$ luminosity are avoided. However, considering that the conversion distance b is only a few cm at best, we will have a highly complicated interaction region where a lot of disruptions can occur as far as placing a detector goes. The whole issue of the interaction requires a dedicated investigation. This particular aspect of the strong magnetic field so close to the interaction region should also be borne in mind when discussing particular processes that are very sensitive on detector performances. We, here, have in mind the issue of b -tagging for instance with a vertex detector which is a pivotal issue in the detection of a Higgs with an intermediate mass. The situation is worse in the case of $e\gamma$ high energy collider. The issue of the choice between converting at some distance from the interaction point or hitting at the interaction point still requires a detailed investigation as the merits of a finite conversion distance are offset by the large magnetic field.

Figure 4: The laser scheme of converting an electron of the linac into a highly energetic photon (see text).



3.2 Parameters of a Photon Collider

A key parameter of the machine, x_0 , is directly related to the maximum energy, ω_{max} , of the “collider” photon. It is introduced through the scaled invariant mass of the original $e\gamma$ system and for a head-on hit of the laser is given by:

$$x_0 = \frac{M_{e\gamma 0}^2}{m_e^2} - 1 = \frac{4E_b\omega_0}{m_e^2} \simeq (15.3) \left(\left(\frac{E_b}{TeV} \right) \left(\frac{\omega_0}{eV} \right) \right) \text{ so that } \omega_{max.} = \frac{x_0}{x_0 + 1} E_b \quad (3.1)$$

Most of the photons are emitted at extremely small angles with the most energetic photons scattered at zero angle. With the typical angle $\theta_0 = (m_e/E_b)\sqrt{x+1}$ of order some μ rd, the spread of the high-energy photon beam is thus of order some 10’s nm. The energy

spread is roughly given by $\omega \approx \omega_{max}/(1 + (\theta/\theta_0)^2)$. It is clear that the further away from the I.P. the conversion occurs, those photons that make it to the I.P. are those with the smallest scattering angle and hence with the maximum energy. These are the ones that will contribute most to the luminosity. Therefore, with a large distance of conversion one has a high monochromaticity at the expense of a small integrated (over the energy spectrum) luminosity. For some processes whose cross-section is largest for the highest possible energy, this particular set-up would be advantageous especially in reducing possible backgrounds that dominate at smaller invariant $\gamma\gamma$ masses.

From Eq. 3.1 it is clear that in order to reach the highest possible photon energies one should aim at having as large a x_0 as possible. However, one should be careful that the produced photon and the laser photon do not interact so that they create a e^+e^- pair (first threshold); the laser frequency should be chosen or tuned such that one is below the e^+e^- threshold[15]. If we want maximum energy, it is by far best to choose the largest x_0 taking into account this restriction. The optimal x_0 is then given by $x_0 \leq 2(1+\sqrt{2}) \sim 4.83$. This value means that the photon can take up as much as 83% of the beam energy.

3.3 The luminosity spectra

Naturally, the luminosity spectrum depends directly on the differential Compton cross-section. The original electron as well as the laser can be polarised, resulting in quite distinctive spectra depending on how one chooses the polarisations. Introducing y , the fraction of the initial electron energy retained by the backscattered photon,

$$y = \frac{\omega}{E_b} \leq \frac{\omega_{max}}{E_b} \quad r = \frac{y}{x_0(1-y)} \leq 1 \quad \bar{\sigma}_0 = \frac{2\pi\alpha^2}{m_e^2 x_0} \quad (3.2)$$

the energy spectrum of the photons is given by [15]

$$\begin{aligned} f_c(y) &= \frac{1}{\sigma_c} \frac{d\sigma_c}{dy} = \frac{\bar{\sigma}_0}{\sigma_c} C_{00}(y) \quad \text{with} \\ C_{00}(y) &= \frac{1}{1-y} + 1 - y - 4r(1-r) - 2 \lambda_e P_c r x_0 (2r-1)(2-y) \end{aligned} \quad (3.3)$$

where λ_e is the average helicity of the initial electron and P_c is the degree of circular polarisation of the initial laser beam. The spectrum is normalised from the Compton cross section (σ_c)

$$\begin{aligned} \sigma_c &= \sigma_c^{n,p} + 2\lambda_e P_c \sigma_1 \\ \sigma_c^{n,p} &= \bar{\sigma}_0 \left[\left(1 - \frac{4}{x_0} - \frac{8}{x_0^2}\right) \log(1+x_0) + \frac{1}{2} + \frac{8}{x} - \frac{1}{2(1+x_0)^2} \right] \\ \sigma_1 &= \bar{\sigma}_0 \left[\left(1 + \frac{2}{x_0}\right) \log(1+x_0) - \frac{5}{2} + \frac{1}{1+x} - \frac{1}{2(1+x_0)^2} \right] \end{aligned} \quad (3.4)$$

One of the important observation is that the spectrum depends on the product of the helicity of the electron *and* the photon. The backscattered photons will retain a certain amount of the polarisation of the laser photon beam. This polarisation, which is energy-dependent is determined by the three Stoke's parameters ξ_i , $\langle \xi_i \rangle = C_{i0}/C_{00}$. The functions C_{i0} are written as

$$C_{10} = 2r^2 P_t \sin 2\phi, \quad C_{30} = 2r^2 P_t \cos 2\phi \quad (3.5)$$

$$C_{20} = 2 \boldsymbol{\lambda}_e r x_0 (1 + (1-y)(2r-1)^2) - \boldsymbol{P}_e (2r-1) \left(\frac{1}{1-y} + 1-y \right) \quad (3.6)$$

where now P_t is the degree of transverse polarisation of the laser photon beam and ϕ specifies the direction of the maximum laser polarisation. The mean helicity of the high energy photon is given by $\langle \xi_2 \rangle$ while its degree of transverse polarisation by $\langle \xi_1 \rangle$ and $\langle \xi_3 \rangle$. We will be dealing with processes that are \mathcal{C} and \mathcal{P} conserving so that there is no need in requiring any transverse polarisation. Such polarisation has been shown to be very useful when looking for \mathcal{CP} violating signals in scalar production[17] or in W pair production [18]. It is very crucial to realise that the mean helicity of the produced photon does not, in contrary to the energy spectrum, depend on the product of the mean initial helicities (eq. 3.6). Therefore, one can get a dominant helicity configuration for the colliding photons by having only the laser polarised, which is very easily obtained.

The $\gamma\gamma$ luminosity spectrum is a convolution involving the differential Compton cross-sections of the two photons as well as a conversion function that depends very sensitively on the conversion distances and the characteristics of the linac beams. The energy dependence of the former function is only through the energy fraction $\sqrt{\tau}$, while the conversion function involves the e^+e^- cm energy explicitly. Realistically other considerations should be taken into account. These have to do with the laser power. In the following it is assumed that the density of the laser photons is such that all the electrons are converted (this assumes a conversion coefficient, $k = 1$) and that multiple scattering is negligible. A compact analytical form for the conversion function is obtained in the case of a Gaussian profile for the electron beam with an azimuthal symmetry. In this case the electron energy density, for a beam with spotsize σ_e can be written as [15]

$$F_e(r) = \frac{1}{2\pi\sigma_e^2} e^{-\frac{r^2}{2\sigma_e^2}} \quad (3.7)$$

Taking the same conversion distances for both arms of the collider and with the same initial electron beams characteristics one gets for the double differential cross-section

$$\begin{aligned}\frac{d^2L}{d\tau d\eta} &= I_0\left(\rho_0^2 \frac{(x_0+1)}{\sqrt{\tau}} X\right) \exp\left(-\rho_0^2 \frac{(x_0+1)}{\sqrt{\tau}} Y\right) f_c(y_1) f_c(y_2) \\ L &= \frac{\mathcal{L}_{\gamma\gamma}}{k^2 \mathcal{L}_{ee}} \quad k \text{ is the conversion coefficient}\end{aligned}\quad (3.8)$$

where $y_{1,2}$ are the energy fractions of the two collider-photons which can be re-expressed in terms of the reduced invariant $\gamma\gamma$ mass and the “rapidity” η through $y_{1,2} = \sqrt{\tau} e^{\pm\eta}$. I_0 is the modified Bessel function of zeroth-order ($I_0(z) = \frac{1}{\pi} \int_0^\pi d\theta e^{-z \cos \theta}$). The effect of a non-zero conversion distance is all contained in ρ_0 whose value is a measure of the (improved) monochromaticity of the spectrum due to the conversion distance:

$$\rho_0 = \frac{b}{\sqrt{2}\sigma_e} \frac{m_e}{E_b} \quad (3.9)$$

while X and Y are given by:

$$X = \sqrt{\left(\frac{x_0}{x_0+1} e^{-\eta} - \sqrt{\tau}\right) \left(\frac{x_0}{x_0+1} e^{\eta} - \sqrt{\tau}\right)}, \quad ; \quad Y = \frac{x_0}{x_0+1} \cosh(\eta) - \sqrt{\tau} \quad (3.10)$$

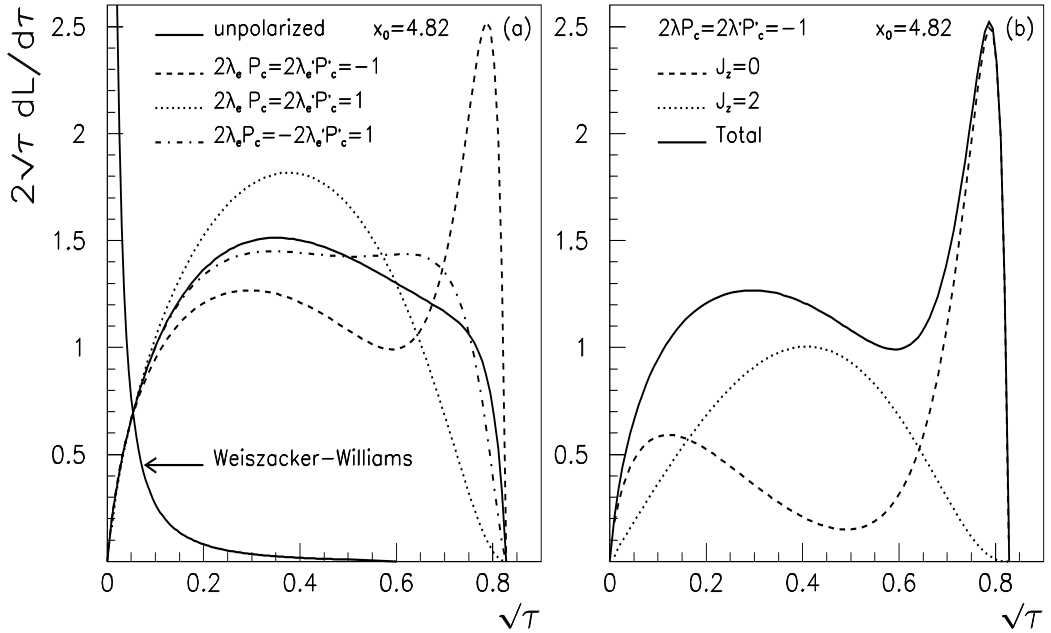
Note that ρ_0 is inversely proportional to the electron spotsize and to the beam energy. Hence increasing the spotsize and the energy degrades the monochromaticity due to the conversion.

3.3.1 Polarised luminosity distributions with zero conversion distance

Almost all of the physics analyses have been done with $b = 0$. We will also conform to this practice. However, we would like to point out that taking $b = 0$ may be too realistic and that taking $b \neq 0$ may have some advantages as it gives a peaked spectrum. In any case what is crucial is to make full use of the availability of polarisation.

In Fig. 5a we compare the luminosity spectrum (as a function of the reduced $\gamma\gamma$ invariant mass) that one obtains by choosing different sets of polarisations for the two arms of the photon collider. First of all, in all cases and as advertised earlier one has a hard spectrum compared to the “classic” Weiszäcker-Williams spectrum. In case of no polarisation at all, one obtains a broad spectrum which is almost a step function that extends nearly all the way to the maximum energy (restricted by the value of x_0). The hardest spectrum is arrived at by choosing the circular polarisation of the laser (P_c) and the mean helicity of the electron (λ_e) to be opposite, i.e., $2\lambda_e P_c = -1$, for *both* arms of the collider. In the case where both arms have $2\lambda_e P_c = +1$ the spectrum has a “bell-like” shape which favours the middle range values of $\sqrt{\tau}$. In the case where the two arms of the collider have an opposite value for the product $2\lambda_e P_c$, the spectrum is almost identical to the

Figure 5: (a) The total luminosity spectra in the case of different combinations of the longitudinal polarisations of the linac electrons and the circular polarisations of the laser. The “classic” Weiszäcker-Williams spectrum is shown for comparison. The spectra assume a distance of conversion, $b = 0$. (b) Projecting the contributions of the $J_Z = 0$ and the $J_Z = 2$ polarised spectrum in the peaked spectrum setting $2\lambda_e P_c = 2\lambda'_e P'_c = -1$.

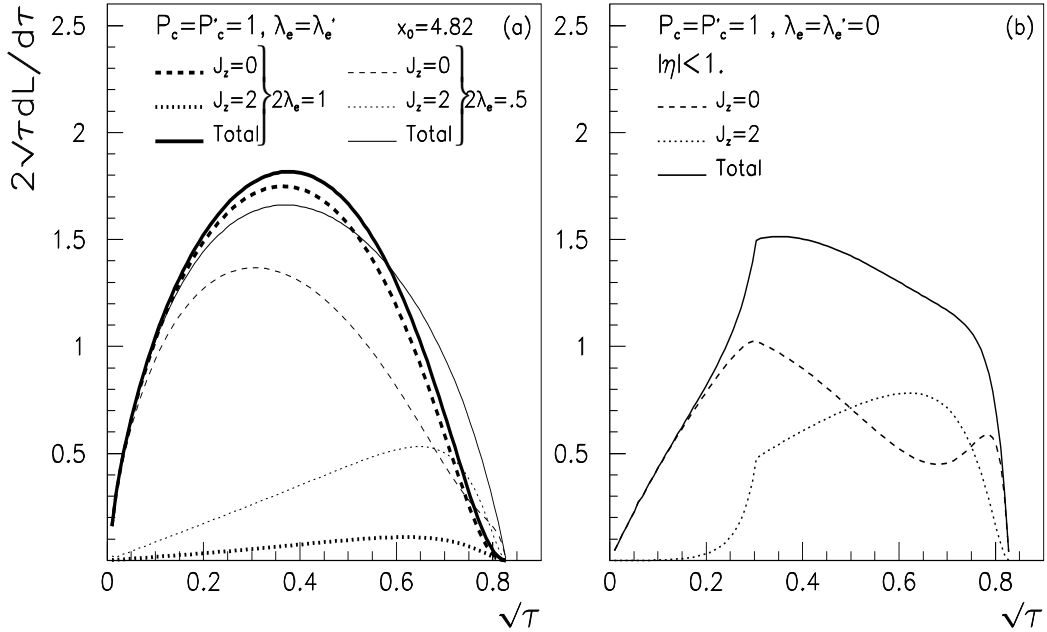


one obtained in case of no polarisation. It is clear that for processes where we need the maximum energy, like those we have encountered with W production processes or those with higher thresholds or again those where the indirect effects of some New Physics grow with energy, the “peaked spectrum”, $2\lambda_e P_c = 2\lambda'_e P'_c = -1$, is best. On the other hand, if one is looking for peaks in the $\gamma\gamma$ invariant mass like in the resonant-scalar production, it is best to take a scheme that explores uniformly the whole energy range. In this case, the spectrum obtained without having any of the beams polarised could do the job.

However, in all situations one should always insist on having some polarisation. This is because polarised laser beams (which are easily obtained) and electron (which should not be too difficult) means that the colliding photons are in a preferred state of polarisation. This is crucially important in favouring some physics channels that occur in $J_Z = 0$ for example rather than for $J_Z = 2$. As one can read from Eq. 3.6 the produced photon has a net mean helicity even if only either the electron or laser beam is polarised. We show in Fig. 5b how the total luminosity is shared between the two states $J_Z = 0$ and $J_Z = 2$. In the “peaked” set-up, i.e. $2\lambda_e P_c = 2\lambda'_e P'_c = -1$ and in the case where both lasers are tuned to have a right-handed circular polarisation ($P_c = P'_c = +1$), one has the added advantage

that the high-energy photons are produced mostly with the same helicity, therefore giving a $J_Z = 0$ dominated environment, for short we will refer to this situation as the “0-dom.” case. The $J_Z = 2$ tail almost disappears for $\sqrt{\tau} > 0.7$. For some processes where the $J_Z = 2$ is dominant, or if one wants to compare the $J_Z = 2$ and the $J_Z = 0$ on an “equal basis”, one would also like to isolate the $J_Z = 2$ at the expense of the $J_Z = 0$ spectrum. We point out[19] that this could be easily achieved by flipping *both* the electron and laser polarisations of *one* of the arms *only* while maintaining $2\lambda_e P_c = -1$ (for a maximum of monochromaticity). In this case, the $J_Z = 0$ and $J_Z = 2$ spectra are simply interchanged. We will refer to this case as the “2-dom.”, for short. For W processes we have preferred, for reasons that should be clear by now, the peaked spectrum.

Figure 6: (a) Projecting the contributions of the $J_Z = 0$ and the $J_Z = 2$ polarised spectrum in the “broad” setting $2\lambda_e P_c = 2\lambda'_e P'_c = 1$ (with a conversion distance $b = 0$). Thick lines are with a 100% longitudinal polarisation for the electron while the light lines are for 50% longitudinal polarisation. The lasers are taken to be fully right-handed. (b) As in (a) but for unpolarised electrons and where we have imposed a rapidity cut of $|\eta| < 1$.

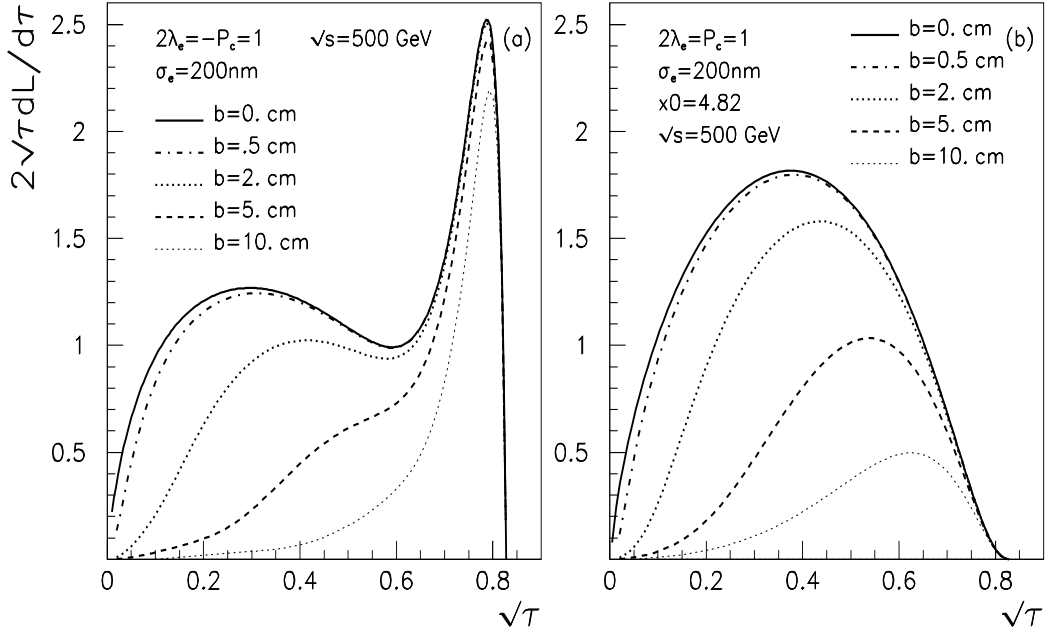


For the Higgs search, that is when we would like to keep an almost constant value for the differential luminosity, the “broad” spectrum that favours the $J_Z = 0$ is highly recommended. What is very gratifying is that with $P_c = P'_c = 2\lambda_e = 2\lambda'_e = 1$ the whole spectrum is accounted for almost totally by the $J_Z = 0$ spectrum(see Fig. 6a); the $J_Z = 2$ contributes slightly only at the higher end. This near purity of the $J_Z = 0$ is not much degraded if the maximum mean helicity of the electron is not achieved. We

show on the same figure (Fig. 6a) what happens when we change both $2\lambda_e$ and $2\lambda'_e$ from 1 to .5, keeping $P_c = P'_c = 1$. There is still a clear dominance of the $J_Z = 0$ especially for the lower values of the centre-of-mass energy. We would like to draw attention to the fact that this effect, (increasing the $\frac{J_Z=0}{J_Z=2}$ ratio), can be further enhanced (when the maximal electron polarisation is not available) by imposing rapidity cuts. The point is that the mean helicity of the final photon, λ_γ , is non zero even in the case of no electron polarisation. Now, if the energy factor multiplying P_c in Eq. 3.6 is the same for both photons, we would expect that the colliding photons have the same degree of polarisation hence producing a $J_Z = 0$ state. This could be achieved by requiring small rapidities. In Fig. 6b we show the luminosity spectrum for the case where only the laser photons have the same maximal circular polarisation but where we have imposed a cut on the rapidity $\eta < 1$. We see that for small centre-of-mass energies $\tau < 0.22$ we have a highly dominant $J_Z = 0$ environment. The relevance of this observation will be fully exploited in the Higgs search section.

3.3.2 Polarised spectra with a finite conversion distance

Figure 7: (a) The total luminosity spectrum with $2\lambda_e P_c = 2\lambda'_e P'_c = -1$ (“peaked spectrum”) for different values of the conversion distance taking a spotsize $\sigma_e = 200$ nm. (b) As in a but with $2\lambda_e P_c = 2\lambda'_e P'_c = 1$ (“broad spectrum”).



For illustration, we take an electron beam with a Gaussian profile. As explained above,

increasing the distance of conversion filters the high energy modes and therefore the spectrum becomes more monochromatic for large values of $\gamma\gamma$ centre-of-mass energy. For the discussion, we take the spotsize of the electron beam to be $\sigma_e = 200$ nm, a e^+e^- cm energy of 500 GeV and consider a few values of the conversion distance. Note that exactly the same features are obtained for a smaller spotsize $\sigma_e = 100$ nm and a proportionally smaller conversion distance. For the peaked spectrum, arrived at by having $2\lambda_e P_c = 2\lambda'_e P'_c = -1$, the peaking is dramatically enhanced for a large conversion distance $b = 10$ cm ($\rho_0 \simeq 0.72$). This means for example that with a conversion distance of 5 cm or 10 cm, there is almost no luminosity below $\sqrt{\tau} < 0.65$. This also means (see Fig. 7a) that the spectrum is a purely $J_Z = 0$ peaked spectrum. This is the most ideal situation to study a $J_Z = 0$ resonance if its mass falls in this energy range, *i.e.* $0.7 < \sqrt{\tau_{res.}} < 0.82$. The $J_Z = 2$ component that was present for the zero-distance of conversion is effectively eliminated for large distances $b > 5$ cm. Note that in this case if one could “manage” with a conversion distance of 0.5 cm then we almost recover the $b = 0$ spectrum.

The situation is not as bright for the broad spectrum case when the interest is on small $\sqrt{\tau}$, like the search of an intermediate-mass Higgs (IMH) at a 500 GeV e^+e^- . The nice features that were unravelled in the last paragraph (an almost pure $J_Z = 0$ for small to moderate $\sqrt{\tau}$) are lost because the luminosity in the energy range of the IMH peak formation is totally negligible for conversion distances of order ~ 5 cm or higher (see Fig. 7b). If one could manage with a conversion distance below 2 cm then we may hope to keep the nice features of the “broad” $J_Z = 0$ scheme.

3.4 Measuring the luminosity

As should have transpired from the previous paragraphs, the interaction region is quite complicated. Whether one chooses to convert the electron at some distance from the I.P, in which case one needs a strong electromagnetic field to sweep away unwanted soft electrons and introduce disruptions, or whether one chooses to hit very close to the I.P, in which case one has additional backgrounds (rendering the machine a mixture of e^+e^- , $e\gamma$ and $\gamma\gamma$) one expects some uncertainties in the true $\gamma\gamma$ luminosity. All this to say that it will be extremely important to *measure* the $\gamma\gamma$ luminosity. This measurement includes in fact various measurements. It will not be sufficient to measure the total luminosity but one should at least measure the differential $\gamma\gamma$ luminosity (as a function of the invariant $\gamma\gamma$ centre-of-mass energy). It will also be very desirable to have the double differential (in rapidity also) luminosity. Moreover, it is very important to “reconstruct” the polarised $J_Z = 0$ and $J_Z = 2$ spectra and make sure that these measurements do not deviate

much from the theoretical luminosity calculations. Otherwise, particular choices of the settings should be reconsidered if the true spectrum does not reproduce the “theoretical” spectrum. For instance, in the Higgs search it should be important to know how much $J_Z = 0$ one actually has in a realistic experimental set-up.

Which reaction could we choose as a luminosity monitor? Few ideas[15, 20, 21] have been suggested but none has received the detailed investigation it deserves. First, the choice of the reaction will sensitively depend on the energy range one wants to cover. For a high energy machine that is going to be devoted to W physics, as Fig. 1 shows, it is not e^+e^- production that is a winner. As a general observation one should, in fact, not choose final states with electrons, especially at the lower energies, since there could be a contamination from non “swept-away” electrons and/or non-converted electrons of the linac. In this respect, muons are best even if the corresponding total cross-sections are smaller. Note that it was suggested to use the e^+e^- final state in order to reconstruct the polarised components[20]. Indeed, once a cut on the scattering angle θ_e^* in the $\gamma\gamma$ cm frame is imposed practically only the $J_Z = 2$ is kept(see eq. 8.2). It is worth pointing that with a cut such that $|\cos\theta_e^*| < 0.8$, it is just as well to use $\mu^+\mu^-$. It should be remarked however, that the e^+e^- or $\mu^+\mu^-$ cross-section for cm energies above 300 GeV is at least two orders of magnitudes less than W pair production. The Novosibirsk group [15] has proposed the 4-fermion processes $\gamma\gamma \rightarrow \mu^+\mu^-e^+e^-$ and $\gamma\gamma \rightarrow e^+e^-e^+e^-$ for the calibration. The disadvantage, apart from the presence of the electrons, is that these processes will not be able to measure the polarisation. From the experimental point of view, taking the muon ($\mu\mu ee$) case as an example, for sub-100 GeV energies it rests to see if one could track down the muons whose average production angle will be below the *mrd*. The large total 4μ cross-section has also the same shortcomings, although if we could track the muons this could be used to measure the total differential cross-section. The advantages of this total cross-section rest on the fact that it is energy independent at high-energy and that it has a large value, $\sim 153 pb$.

We[2] have pointed that the W pair production should also qualify as a good luminosity monitor as one could convince oneself by glancing at Fig. 1 and 2. This has been taken up by [21]. However, a detailed investigation is in order. The needed analysis should be based on a full Monte-Carlo with four fermions in the final states that keeps the correlations between the decay products and that could allow to apply cuts in the laboratory frame directly on the observed fermions (acceptance factors etc...). It has already been shown how one can reduce the effect of non-resonant diagrams to a negligible level[22]. A program within this spirit is being carried out [23]. A drawback, unless one finds good variables, is that at large WW invariant masses the cross-section does not favour a particular initial

polarisation. Another hesitation in using this reaction is that we want to exploit it to uncover new physics that affects the tri-linear $WW\gamma$ as well as the quadrilinear $WW\gamma\gamma$ vertices and hence it might not be as unambiguous as the 4 fermion QED-dominated processes. Nonetheless, we would like to argue that if one is to feel these effects one would probably need the full W sample and therefore when measuring the luminosity this effect could be counted in the systematic error. Moreover, one expects this machine to be running after, or alongside, the high-energy e^+e^- mode where these couplings (at least the tri-linear) would be well measured. Moreover, theoretical arguments (see later) indicate that anomalies would affect the longitudinal and central W 's rather than the preferentially transverse and forward W 's from the \mathcal{SM} .

4 A theoretical technical aside: The importance of a non-linear gauge fixing term for $\gamma\gamma$ electroweak processes

As Fig. 1 and 2 make explicit, production of electroweak bosons is overwhelming especially at high-energies. Since the calculation of these processes involves a large number of diagrams it is highly recommended to simplify the computational task as much as possible. The complication not only arises from the large number of diagrams but also because the non-Abelian gauge nature of the couplings and the ever increasing number of W propagators renders the computation of even a single diagram arduous. Helicity technique methods do help and one can do better by combining these methods with a judicious choice of gauge-fixing. Calculating in the usual unitary gauge is rather awkward because of the cumbersome presence of the “longitudinal” mode (“ $k_\mu k_\nu$ ” term) of the various W propagators. A way out is to use a Feynman gauge. However, with the widespread choice of a linear gauge fixing term, this is done at the expense of having to deal with even more diagrams containing the unphysical Higgs scalars. An indisputable choice of gauge for photonic reactions or for processes involving a mixture of W 's and photons is to quantize with a non-linear gauge fixing term [24] and work with a parameter corresponding to the 't Hooft-Feynman gauge. This type of gauges is also known as the background gauges. Recent developments in the calculation of QCD processes, especially the so-called string inspired organisation[25], can be understood as being (partly) based on the exploitation of similar gauges. This type of gauges can also be efficiently used for tree-level electroweak processes[3] and not just for loop diagrams as has been customarily done till now. For a few of the vector boson processes in $\gamma\gamma$ ($\gamma\gamma \rightarrow WW, Z\gamma, \gamma\gamma; WW\gamma, WW\gamma\gamma, WWZ, WWH, \dots$)

one has, with this choice of gauge-fixing, the same number of diagrams as in the usual unitarity gauge save for the fact that we have no “longitudinal” mode to worry about and that there are no diagrams with unphysical scalars since the virtue of this choice is that the vertex with the photon, the W and the unphysical Higgs field does not exist. In any case the reduction in the number of diagrams is considerable. Of course, one has to allow for small changes in the vertices which turn out to have an even more compact form than in the usual gauges. For instance, all diagrams where the quartic $WW\gamma\gamma$ vertex appears are identically zero when the two incident photons have opposite helicities ($J_Z = \pm 2$). With S^\pm being the unphysical Higgs bosons, the W^\pm -part of the linear gauge fixing condition

$$\mathcal{L}_{\text{linear}}^{\text{Gauge-Fixing}} = -\xi^{-1}|\partial_\mu W^{\mu+} + i\xi M_W S^+|^2 \quad (4.11)$$

is replaced by the “constraint”

$$\mathcal{L}_{\text{non-linear}}^{\text{Gauge-Fixing}} = -\xi^{-1}|(\partial_\mu + ieA_\mu + ig\cos\theta_W Z_\mu)W^{\mu+} + i\xi M_W S^+|^2 \quad (4.12)$$

where θ_W is the usual weak mixing angle. The best choice for ξ is no doubt $\xi = 1$. Note that in the recent calculations of the one-loop process $\gamma\gamma \rightarrow ZZ$, Jikia[5] and Dicus and Kao[8] have used two different variants of this gauge-fixing. We foresee this kind of choices to stand out for applications to W dynamics at a future $\gamma\gamma$ collider as it has proved to be for one-loop weak bosons induced amplitudes for photonic processes [26].

5 Physics with W pairs in $\gamma\gamma$

W pair production has been a recurring theme and its importance can not be over-emphasized. The event sample is just too large! The reaction can be considered as the backbone on which one grafts even more bosons at tree-level or through loops. This reaction was first studied by Pesic[27] within the context of the \mathcal{SM} and by considering W ’s with no magnetic moment. Kim and Tsai[28, 29] extended the study to the case of a W with an arbitrary value of the magnetic moment. A more detailed study by Tupper and Samuel[30] followed. All these studies assumed a Weizsäcker-Williams spectrum. Ginzburg *et al.* [1] were first to study the effect of polarised photon beams.

5.1 Tree-level helicity amplitudes for $\gamma\gamma \rightarrow W^+W^-$ in the \mathcal{SM}

To understand the characteristics of the WW cross-section it is best to give all the helicity amplitudes that contain a maximum of information on the reaction. With $\lambda_1, \lambda_2 = \pm 1$

being the photon helicities, $\lambda_3, \lambda_4 = \pm 1$ the transverse helicities of the W 's and 0 their longitudinal mode, we have[2]¹

$$\mathcal{M}_{\lambda_1\lambda_2;\lambda_3\lambda_4} = \frac{4\pi\alpha}{1 - \beta^2 \cos^2 \theta} \mathcal{N}_{\lambda_1\lambda_2;\lambda_3\lambda_4} ; \quad \beta = \sqrt{1 - 4/\gamma} ; \quad \gamma = s/M_W^2 \quad (5.13)$$

where

$$\begin{aligned} \mathcal{N}_{\lambda_1\lambda_2;00} &= \frac{1}{\gamma} \left\{ -4(1 + \lambda_1\lambda_2) + (1 - \lambda_1\lambda_2)(4 + \gamma) \sin^2 \theta \right\} \\ \mathcal{N}_{\lambda_1\lambda_2;\lambda_30} &= \sqrt{\frac{8}{\gamma}} (\lambda_1 - \lambda_2)(1 + \lambda_1\lambda_3 \cos \theta) \sin \theta \\ \mathcal{N}_{\lambda_1\lambda_2;\lambda_3\lambda_4} &= \beta(\lambda_1 + \lambda_2)(\lambda_3 + \lambda_4) + \frac{1}{2\gamma} \left\{ -8\lambda_1\lambda_2(1 + \lambda_3\lambda_4) + \gamma(1 + \lambda_1\lambda_2\lambda_3\lambda_4)(3 + \lambda_1\lambda_2) \right. \\ &\quad + 2\gamma(\lambda_1 - \lambda_2)(\lambda_3 - \lambda_4) \cos \theta - 4(1 - \lambda_1\lambda_2)(1 + \lambda_3\lambda_4) \cos^2 \theta \\ &\quad \left. + \gamma(1 - \lambda_1\lambda_2)(1 - \lambda_3\lambda_4) \cos^2 \theta \right\} \end{aligned} \quad (5.14)$$

The unpolarised differential and total cross-sections follow

$$\frac{d\sigma_{tot}}{d\cos\theta} = \frac{3\pi\alpha^2}{M_W^2} \frac{\beta}{\gamma} \left\{ 1 - \frac{4}{1 - \beta^2 \cos^2 \theta} \left(\frac{2}{3} + \frac{1}{\gamma} \right) + 2 \left(\frac{4}{1 - \beta^2 \cos^2 \theta} \right)^2 \left(\frac{1}{3} + \frac{1}{\gamma^2} \right) \right\} \quad (5.15)$$

$$\sigma_{tot} = \frac{8\pi\alpha^2}{M_W^2} \beta \left\{ \left(1 + \frac{3}{4\gamma} + \frac{3}{\gamma^2} \right) - \frac{6}{\beta\gamma^2} \left(1 - \frac{2}{\gamma} \right) \text{Arcosh} \frac{\sqrt{\gamma}}{2} \right\} \quad (5.16)$$

Very soon after threshold, the total WW cross-section with either polarised or unpolarised beams increases rapidly with energy until it reaches a plateau, around 400 GeV. In all cases the W pairs are produced near the beam pipe and they are mostly transversely polarised. With a cut on the scattering angle so that W 's along the beam are rejected, the cross-section decreases with energy (see Fig. 3). Note that in the $J_Z = 0$ ($\lambda_1 = \lambda_2$) mode, the \mathcal{SM} does not produce W 's with different helicities, so that either both W 's are longitudinal or if transverse they have the same handedness. This property could be very useful when looking for signals of New Physics, in particular the ones associated with the symmetry-breaking mechanism.

5.2 Tests on the tri-linear anomalous couplings, the “chiral lagrangian” approach and comparison with other machines

Although the bulk of the reaction as we alluded to in our introduction is due to the gauge transverse sector, the fact that there are so many W 's around (one is talking here about a

¹ Yehudai[31] had previously given the complete helicity amplitudes. We find sign differences in some of the standard model helicity amplitudes. This is due to an inconsistent labelling of the polarisation vectors in[31]. Our results have been confirmed by a recent calculation [32].

sample of a million WW pairs with a luminosity of 10fb^{-1}) makes this reaction the ideal place to probe the mechanism of symmetry breaking by trying to reach the Goldstone Bosons, in a sense the longitudinal W 's. With so many transverse W 's one could also attempt to conduct precision tests on the electromagnetic couplings of the W . This aspect of the W physics is more commonly referred to as the anomalous couplings of the weak bosons.

There is an extensive literature (see for instance [33, 34, 35] and references therein) on the effect of anomalous couplings defined through a set of operators that describe deviations from the \mathcal{SM} values of the WWV ($V = \gamma, Z$) vertex. Until very recently, the studies have been devoted to the tri-linear couplings as these could be probed very efficiently in W pair production at the e^+e^- machines or in WZ/γ at the hadron machines. At higher energies, as at the NLC, novel quartic couplings could contribute non-negligibly to triple vector boson production or WW scattering processes. As we have argued [10, 2] elsewhere, it is important to check for these quartic couplings which are more directly related to the scalar sector. Indeed, some of the quartic couplings could be the residual effect of a heavy scalar exchange at tree-level while tri-linear couplings could be thought of as integrating-out heavy fields (at one-loop) or are the effect of mixing with other heavy vectors. In fact, we should draw the analogy between these anomalous couplings and their study in WW and ZZ reactions with the approach that we have heard at the *DAΦNE* sessions where people study, albeit in a totally different energy regime, various predictions of “models” of chiral perturbation theory. Our pions are the Goldstone bosons, of course. This analogy can be put out on more formal ground, but before doing so let us give the by-now “classic” parametrisation of the anomalous tri-linear couplings. This is intended to those who are not familiar with the re-interpretation of these tri-linear couplings within a set of gauge invariant operators. Here, we will only address the issue of the \mathcal{C} and \mathcal{P} conserving couplings (for a discussion of \mathcal{CP} violation in $\gamma\gamma \rightarrow W^+W^-$ see[18, 36]). The oft-used parameterisation of Hagiwara et al. [33], (the *HPZH* parameterisation) for the $WW\gamma$ couplings and their WWZ counterparts, is

$$\begin{aligned}
\mathcal{L}_1 = & -ie \left\{ \left[A_\mu \left(W^{-\mu\nu} W_\nu^+ - W^{+\mu\nu} W_\nu^- \right) + \overbrace{(1 + \Delta\kappa_\gamma)}^{\kappa_\gamma} F_{\mu\nu} W^{+\mu} W^{-\nu} \right] \right. \\
& + \cotg\theta_w \left[\overbrace{(1 + \Delta\mathbf{g}_1^Z)}^{g_1^Z} Z_\mu \left(W^{-\mu\nu} W_\nu^+ - W^{+\mu\nu} W_\nu^- \right) + \overbrace{(1 + \Delta\kappa_Z)}^{\kappa_Z} Z_{\mu\nu} W^{+\mu} W^{-\nu} \right] \\
& \left. + \frac{1}{M_W^2} \left(\boldsymbol{\lambda}_\gamma F^{\nu\lambda} + \boldsymbol{\lambda}_Z \cotg\theta_w Z^{\nu\lambda} \right) W_{\lambda\mu}^+ W_{\nu}^{-\mu} \right\} \tag{5.17}
\end{aligned}$$

The two couplings κ_γ and λ_γ are commonly associated with the magnetic and quadrupole moment of the W [33]. Although here the interest lies with the $WW\gamma$ couplings, the corresponding WWZ couplings are given to illustrate the fact that in $\gamma\gamma$ reactions one has a smaller set of couplings to check than in $e^+e^- \rightarrow W^+W^-$. Hence, we expect a better precision on the measurements (fewer parameters to fit). Furthermore, we will see that when introducing well-motivated symmetry principles, one can relate some WWZ and $WW\gamma$ couplings. Accepting this point of view of a constrained set, the $\gamma\gamma$ mode can probe almost the same parameter space as the e^+e^- .

One of the symmetry principles that we can, in no way, dare to do without is the local gauge symmetry. For instance, as it stands, the above Lagrangian 5.17 is not gauge invariant even in the QED sense. The λ and g_1^Z need appropriate accompanying quartic couplings. This Lagrangian has been written with the specific process $e^+e^- \rightarrow W^+W^-$ in mind. Failing to render it explicitly gauge invariant, one can not apply it to a process such as the one we are interested in: $\gamma\gamma \rightarrow W^+W^-$. There is a simple prescription on how to correct for this if we only want to maintain $U(1)_{QED}$. For instance, some time ago Aronson[37] has shown how we could write the appropriate operator accompanying the parameter λ . For $\gamma\gamma \rightarrow W^+W^-$, λ_γ provides a $WW\gamma\gamma$ vertex. We stress that this is *not a genuine quartic coupling*.

In fact, in view of the beautiful LEP1 results that confirm the \mathcal{SM} to an unsurpassable degree of precision one should embed all the couplings within a set of $SU(2) \times U(1)$ gauge invariant operators. One ends up with a hierarchy of coupling based on the dimensionality of these extra (anomalous) operators. This view has, recently, rallied a large support. In writing these operators, we will also make an additional assumption motivated by the fact that the ρ parameter is, to a very good approximation, equal to 1. We take this to be a consequence of the so-called custodial (global) symmetry, which reflects the fact that, in the absence of mixing with the hypercharge, the W^\pm and W^0 have the same mass. Therefore, we will take the scalar sector to have this additional $SU(2)$ custodial symmetry. For details we refer to [35].

There are two approaches to the construction. In the first approach one assumes the Higgs to be light, in which case one has a linear realisation of symmetry breaking, while in the second approach there is no Higgs. With these few points spelled out, we arrive at the most *probable* set of yet-untested operators, within a linear [38, 39] or a non-linear [40, 41, 42, 43, 44, 45, 46] realisation of \mathcal{SB} .

In Table 1 we have defined

$$\begin{aligned}\mathbf{W}_{\mu\nu} &= \frac{1}{2} \left(\partial_\mu \mathbf{W}_\nu - \partial_\nu \mathbf{W}_\mu + \frac{i}{2} g [\mathbf{W}_\mu, \mathbf{W}_\nu] \right) = \frac{\tau^i}{2} \left(\partial_\mu W_\nu^i - \partial_\nu W_\mu^i - g \epsilon^{ijk} W_\mu^j W_\nu^k \right) \\ \mathbf{B}_{\mu\nu} &= \frac{1}{2} (\partial_\mu B_\nu - \partial_\nu B_\mu) \tau_3 \quad \mathbf{B}_\mu = \tau_3 B_\mu\end{aligned}\quad (5.18)$$

(with $\mathbf{W}_\mu = W_\mu^i \tau^i$, the normalisation for the Pauli matrices is $\text{Tr}(\tau^i \tau^j) = 2\delta^{ij}$). Φ is the usual complex doublet with hypercharge $Y = 1$ while in the non-linear realisation the (dim-0) matrix Σ describes the Goldstone Bosons with the built-in custodial $SU(2)_c$ symmetry:

$$\Sigma = \exp\left(\frac{i\omega^i \tau^i}{v}\right) ; v = 246 \text{ GeV} \quad \text{and} \quad \mathcal{D}_\mu \Sigma = \partial_\mu \Sigma + \frac{i}{2} (g \mathbf{W}_\mu \Sigma - g' B_\mu \Sigma \tau_3) \quad (5.19)$$

Table 1: *The Next-to-leading Operators describing the W Self-Interactions which do not contribute to the 2-point function.*

Linear Realisation , Light Higgs	Non Linear-Realisation , No Higgs
$\mathcal{L}_B = ig' \frac{\epsilon_B}{\Lambda^2} (\mathcal{D}_\mu \Phi)^\dagger B^{\mu\nu} \mathcal{D}_\nu \Phi$	$\mathcal{L}_{9R} = -ig' \frac{L_{9R}}{16\pi^2} \text{Tr}(\mathbf{B}^{\mu\nu} \mathcal{D}_\mu \Sigma^\dagger \mathcal{D}_\nu \Sigma)$
$\mathcal{L}_W = ig' \frac{\epsilon_W}{\Lambda^2} (\mathcal{D}_\mu \Phi)^\dagger (2 \times \mathbf{W}^{\mu\nu}) (\mathcal{D}_\nu \Phi)$	$\mathcal{L}_{9L} = -ig' \frac{L_{9L}}{16\pi^2} \text{Tr}(\mathbf{W}^{\mu\nu} \mathcal{D}_\mu \Sigma \mathcal{D}_\nu \Sigma^\dagger)$
$\mathcal{L}_\lambda = \frac{2i}{3} \frac{L_\lambda}{\Lambda^2} g^3 \text{Tr}(\mathbf{W}_{\mu\nu} \mathbf{W}^{\nu\rho} \mathbf{W}^\mu{}_\rho)$	-----
-----	$\mathcal{L}_1 = \frac{L_1}{16\pi^2} \left(\text{Tr}(D^\mu \Sigma^\dagger D_\mu \Sigma) \right)^2 \equiv \frac{L_1}{16\pi^2} \mathcal{O}_1$
-----	$\mathcal{L}_2 = \frac{L_2}{16\pi^2} \left(\text{Tr}(D^\mu \Sigma^\dagger D_\nu \Sigma) \right)^2 \equiv \frac{L_2}{16\pi^2} \mathcal{O}_2$

The phenomenological parameters are obtained by going to the unitary gauge which, in the non-linear case, corresponds to formally setting $\Sigma \rightarrow \mathbf{1}$. Note that, in the non-linear realisation the counterpart of \mathcal{L}_λ is relegated to a lower cast as it is counted as $\mathcal{O}(p^6)$: $\mathcal{L}_\lambda \propto \text{Tr}([\mathcal{D}_\mu, \mathcal{D}_\nu] [\mathcal{D}^\nu, \mathcal{D}^\rho] [\mathcal{D}_\rho, \mathcal{D}^\mu])$. On the other hand, the operators $\mathcal{L}_{1,2}$ which represent genuine quartic couplings (they do not contribute to the tri-linear couplings) and involve a maximum number of longitudinal modes are sub-sub-dominant in the light Higgs scenario. Unfortunately, they do not contribute to $\gamma\gamma \rightarrow W^+W^-$ at tree-level. By going to the physical gauge, one recovers the phenomenological parameters with the *constraints*:

$$\Delta\kappa_\gamma = \frac{e^2}{s_w^2} \frac{v^2}{4\Lambda^2} (\epsilon_W + \epsilon_B) = \frac{e^2}{s_w^2} \frac{1}{32\pi^2} (L_{9L} + L_{9R})$$

$$\begin{aligned}
\Delta\kappa_Z &= \frac{e^2}{s_w^2} \frac{v^2}{4\Lambda^2} (\epsilon_W - \frac{s_w^2}{c_w^2} \epsilon_B) = \frac{e^2}{s_w^2} \frac{1}{32\pi^2} \left(L_{9L} - \frac{s_w^2}{c_w^2} L_{9R} \right) \\
\Delta g_1^Z &= \frac{e^2}{s_w^2} \frac{v^2}{4\Lambda^2} \left(\frac{\epsilon_W}{c_w^2} \right) = \frac{e^2}{s_w^2} \frac{1}{32\pi^2} \left(\frac{L_{9L}}{c_w^2} \right) \\
\lambda_\gamma &= \lambda_Z = \left(\frac{e^2}{s_w^2} \right) L_\lambda \frac{M_W^2}{\Lambda^2}
\end{aligned} \tag{5.20}$$

In the numerical applications we will take α and “ s_w ” at M_Z^2 , i.e, in Eq. 5.20 $e \rightarrow e(M_Z^2)$ and $s_w^2 \rightarrow s_Z^2 = 0.228$. Note that there is a one-to-one correspondence $L_{9L,9R} \leftrightarrow \epsilon_{W,B}$ for the WWV parts. So, for two bosons production or neglecting Higgs exchanges in $3V$ production, the two sets are equivalent (same constraints). We note that with this set of parameters $\gamma\gamma \rightarrow W^+W^-$ has one little drawback in the sense that $L_{9L,9R}$ are only probed through their sum: the vectorial combination $L_{9L} + L_{9R}$.

5.3 Tri-linear couplings in W pair production

We now turn to the analysis of the signal coming from the tri-linear couplings. We have derived the full set of the helicity amplitudes including both the $\Delta\kappa_\gamma$ and the λ_γ terms. The full expressions are given in the Appendix. There have, in the past, been a few studies including these couplings but only Yehudai[31] has given the helicity amplitudes. For the unpolarised differential cross-section, we recover the results of Choi and Schrempp[47] with either the anomalous $\Delta\kappa_\gamma$ or λ_γ couplings.

We will concentrate mainly on the κ_γ terms as they have a stronger link with the Higgsless scenario ². The results on λ_γ are shown in a pictural form and only succinctly commented upon. We should point out that the chiral Lagrangian route based on the set L_9 has been taken by [48]. In their calculation only the leading $W_L W_L$ contribution, in $\sqrt{s_{\gamma\gamma}}$, has been retained by invoking the equivalence theorem in the chiral limit. We confirm their result in the limit of non-forward processes where the $M_W \rightarrow 0$ limit can be taken and where the leading terms can be unambiguously isolated at the amplitude level ³. Their results are in fact a direct adaptation of the chiral Lagrangian calculation of $\gamma\gamma \rightarrow \pi^+\pi^-$.

The first comment we would like to make is that, for small values of the anomalous couplings, the sensitivity on the measurement of the coupling does not grow much with the increase of energy especially for the $\Delta\kappa_\gamma$ coupling. This is due to the fact that, for small

²Our idiosyncratic choice is also motivated by the fact that a scenario of New Physics that admits a light Higgs (scalar) is, in the $\gamma\gamma$ mode, better studied on top of the scalar resonance.

³There has been a reappraisal [49, 50] of the equivalence theorem as applied to effective Lagrangians with the conclusion that care should be taken when applying the equivalence theorem. In all our studies we avoided the use of the equivalence theorem.

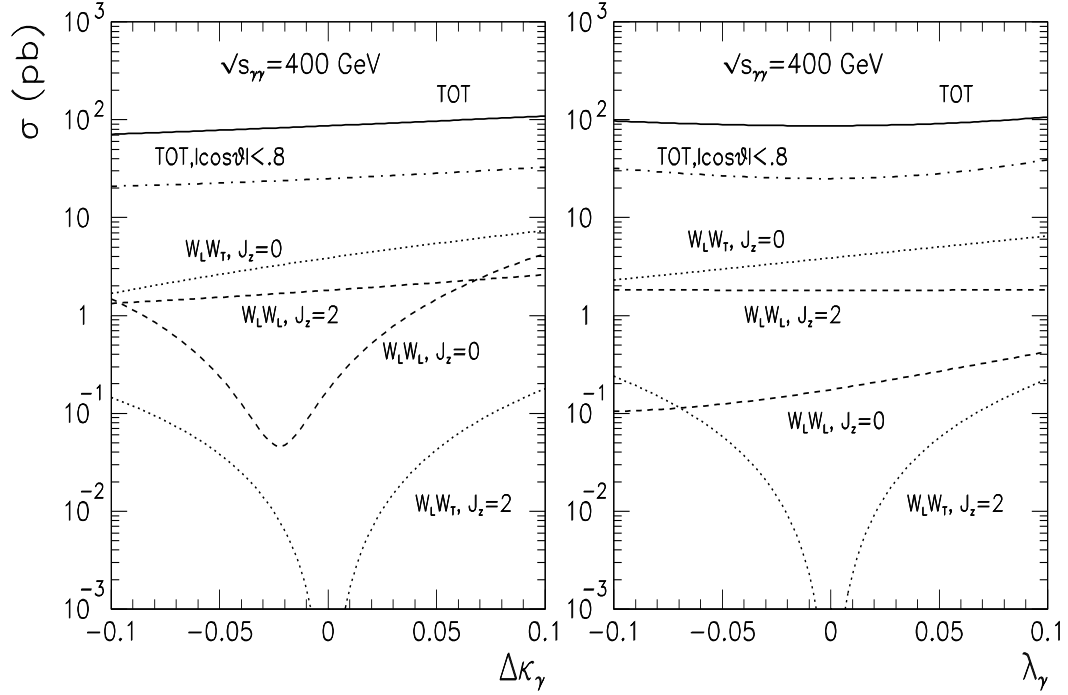
couplings, the main contribution to the cross-section comes from terms that are linear in the anomalous coupling. Unfortunately, the interference between the \mathcal{SM} amplitude and the new coupling is not “effective” in the sense that the energy enhancement brought by the anomalous coupling is tamed by the energy drop of the corresponding \mathcal{SM} amplitude. For instance, with L_9 ($\Delta\kappa_\gamma$) the leading, in $s_{\gamma\gamma}$, contribution is from the $J_Z = 0$ amplitude in $W_L W_L$. The latter, however, decreases as $1/s_{\gamma\gamma}$ for the \mathcal{SM} part. This explains why the net effect is sensibly the same as in the $J_Z = 2$, as far as the interference is concerned. To wit, for central W ’s the leading terms in $W_L W_L$ are

$$\begin{aligned}\mathcal{M}_{++LL}^{\mathcal{SM}} &\sim 4\pi\alpha \times \frac{-8}{\gamma \sin^2 \theta} & \mathcal{M}_{+-LL}^{\mathcal{SM}} &\sim 4\pi\alpha \times 2 \quad \text{while} \\ \mathcal{M}_{++LL}^{\Delta\kappa_\gamma} &\sim 4\pi\alpha \times \gamma & \mathcal{M}_{+-LL}^{\Delta\kappa_\gamma} &\sim -4\pi\alpha \times 4\end{aligned}\quad (5.21)$$

Therefore, for this particular coupling, if we do not reconstruct special correlations that would give information on all the elements of the density matrix, going higher in energy does not pay much. Unless, of course, the couplings are large enough that terms quadratic in $\Delta\kappa_\gamma$ play an important role. However, within the chiral Lagrangian approach, quadratic terms correspond to higher order terms in the energy expansion as those mimicked by the interference terms between the $\mathcal{O}(\sqrt{s})$ and the lowest (universal) terms. The other prominent effect is in the production of $W_L W_T$ states in the $J_Z = 2$ which is *absent* in the \mathcal{SM} at tree-level. Unfortunately, while this is a clear signature of the tri-linear term, the yield in this channel is even smaller than the $W_L W_L$. At the end of the day, the most troublesome feature is the large $W_T W_T$ production which is essentially of a gauge nature. Fig. 8 shows that the largest deviation does occurs for $W_L W_L$ in the $J_Z = 0$ channel. However, this channel is completely buried under the transverse modes even when angular cuts are imposed.

Our analysis is preliminary, in the sense that ultimately we would like to generate the four-fermion final state from the decay of the W ’s keeping the full spin-correlation. We would then apply cuts on the observed fermions. Nonetheless, we applied cuts in the laboratory frame by requiring $p_T^{W^\pm} > 50$ GeV for $\sqrt{s_{ee}} = 500$ GeV. We consider an unpolarised as well as a “0-dom” spectrum Fig. 6. With the latter, due to the fact that the effect of L_9 does not sensibly grow with the energy, we do not gain much with polarisation whose effect is also to give a peaked spectrum at high-energy. This is seen in Fig. 9. To extract the limit on L_9 ($\Delta\kappa_\gamma$) we only considered the sample of WW events that does not consist of double leptonic channels nor of any τ events. We have taken an efficiency of 0.8 and have not aimed at reconstructing the final W polarisation. We take a luminosity of $\int \mathcal{L}_{ee} = 10 \text{fb}^{-1}$. With these values (even with $p_T^W > 50$ GeV) the statistical

Figure 8: *Deviation in the various polarised cross-sections due to the anomalous couplings before folding with the spectrum. The effect of an angular cut on the total cross-section is also shown.*



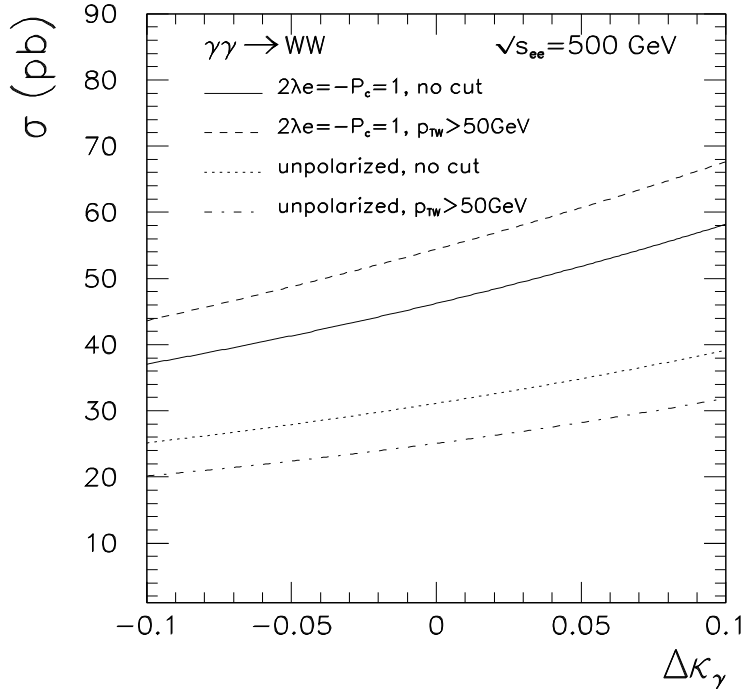
error is too small compared to the systematic error that we have assumed to be 1% with these cuts and the above clean sample. Taking a 3σ deviation our results for both the polarised (“0-dom”) spectrum Fig. 5 and the unpolarised case are

$$\begin{aligned}
 -9.6 &< L_{9L} + L_{9R} < 9.6 \text{ for the unpolarised spectrum} \\
 -10.4 &< L_{9L} + L_{9R} < 9.6 \text{ for the “0-dom” spectrum}
 \end{aligned} \tag{5.22}$$

These values are in qualitative agreement with the ones given by both Yehudai[31] and by Choi and Schrempp [47] (when interpreted as $\Delta\kappa_\gamma$). We have also compared these limits with the ones obtained in the e^+e^- mode[34] and from the LHC[43] within the same constrained set of the dominant operators of the chiral Lagrangian[35].

The conclusion of the comparison, beside the fact that the next e^+e^- at 500 GeV does much better than the LHC and improves considerably on the expected LEP200 bounds, is that the allowed parameter space spanned by the two L_9 would be further reduced (by about 50%) given the availability of the $\gamma\gamma$ mode as shown in Fig. 10.

Figure 9: Variation of the cross-section as a function of $\Delta\kappa_\gamma$ including the unpolarised spectrum and the “0-dom”. The effect of cuts is also shown.

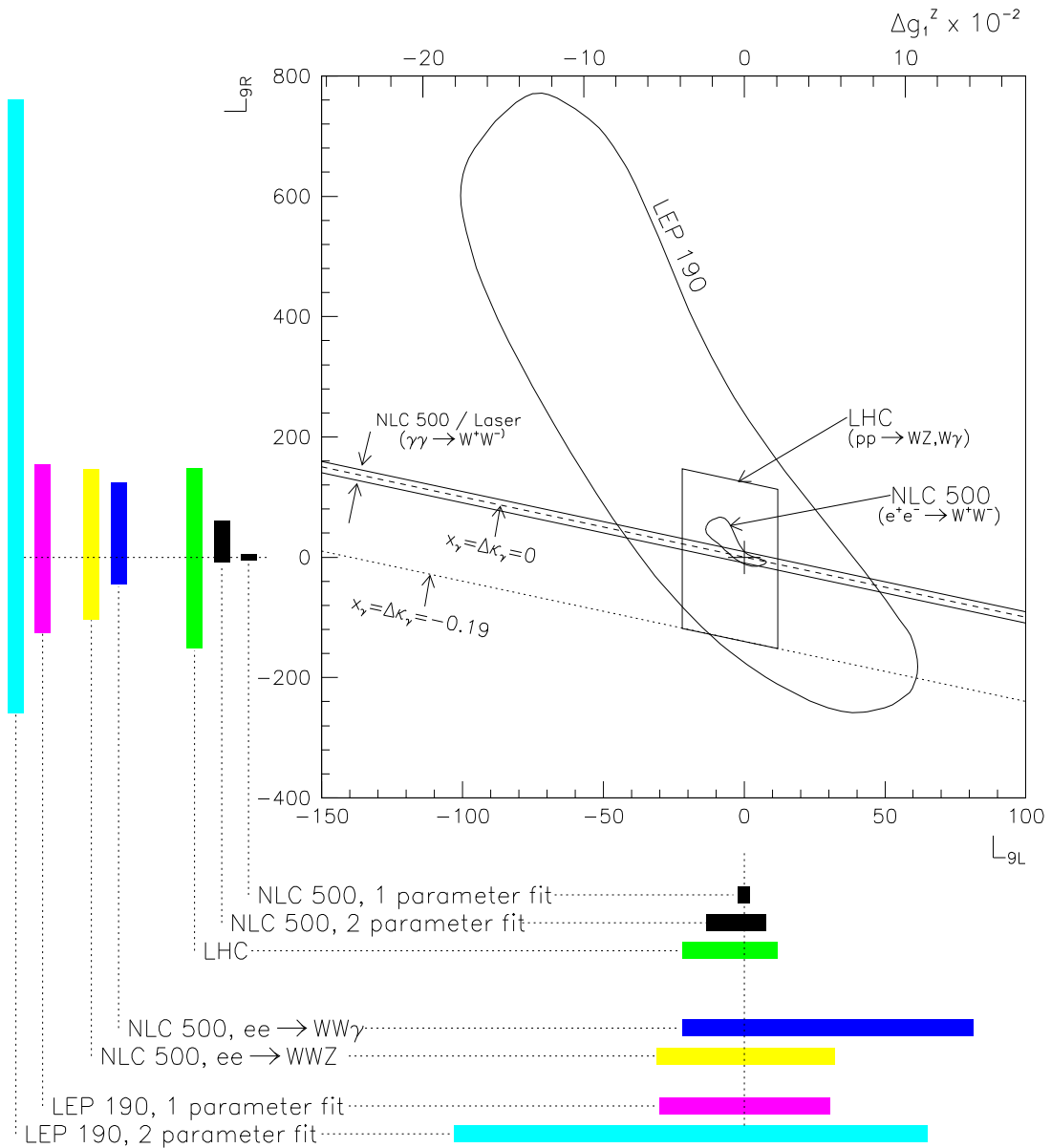


5.4 Effects of genuine quartic couplings and the scalar connection

Within the spirit of the classification of the anomalous couplings based on gauge-invariance and scaling[35], *genuine* quartic couplings, $WW\gamma\gamma$, only appear at the next-to-next-to-leading. We[2, 19]have looked at these operators maintaining the custodial symmetry. Of course, going to the next order one has many more operators contributing to the trilinear couplings so that the above relations between the WWZ and $WW\gamma$ couplings are no longer maintained. This means that one could not make a direct comparison with the two-parameter fits in e^+e^- . Nonetheless, as far as tri-linear couplings are concerned, in the no-Higgs scenario, $\gamma\gamma$ measures only a collective $\Delta\kappa_\gamma$ while λ_γ is already of higher order in the energy expansion and of a purely gauge origin. So, if the measurements at $\gamma\gamma$ are precise enough one may hope to also check the $WW\gamma\gamma$ couplings. There are in fact only two additional $WW\gamma\gamma$ Lorentz structures. In the non-linear realisation these can be embedded in the following sets:

$$\mathcal{L}_0^{2\gamma} = - \frac{L_0^{2\gamma}}{\Lambda^2} \left\{ k_0^W g^2 \text{Tr}(\mathbf{W}_{\mu\nu} \mathbf{W}^{\mu\nu}) + k_0^B g'^2 \text{Tr}(\mathbf{B}_{\mu\nu} \mathbf{B}^{\mu\nu}) + k_0^{WB} gg' \text{Tr}(\mathbf{W}_{\mu\nu} \mathbf{B}^{\mu\nu}) \right\} \times \text{Tr}(\mathcal{D}^\alpha \Sigma^\dagger \mathcal{D}_\alpha \Sigma)$$

Figure 10: Comparison between the expected bounds on the two-parameter space $(L_{9L}, L_{9R}) \equiv (L_W, L_B) \equiv (\Delta g_1^Z, \Delta \kappa_\gamma$ (see text for the conversions) at the NLC500, LHC and LEP2. The NLC bounds are from $e^+e^- \rightarrow W^+W^-$ [34], $W^+W^-\gamma$, W^+W^-Z [2] (for the latter these are one-parameter fits) and $\gamma\gamma \rightarrow W^+W^-$. The LHC bounds are from $pp \rightarrow WZ, W\gamma$ [43]. We also show (“bars”) the limits from a single parameter fit.



$$\mathcal{L}_{2\gamma}^c = - \frac{L_c^{2\gamma}}{\Lambda^2} \left\{ k_c^W g^2 \text{Tr}(\mathbf{W}_{\mu\alpha} \mathbf{W}^{\mu\beta}) + k_c^B g'^2 \text{Tr}(\mathbf{B}_{\mu\alpha} \mathbf{B}^{\mu\beta}) + k_c^{WB} gg' \text{Tr}(\mathbf{W}_{\mu\alpha} \mathbf{B}^{\mu\beta}) \right\} \times \text{Tr}(\mathcal{D}^\alpha \Sigma^\dagger \mathcal{D}_\beta \Sigma) \quad (5.23)$$

For $\gamma\gamma$ reactions, by only making explicit the $U(1)_{QED}$ symmetry, these operators map into the set that we have previously defined through the Lagrangian

$$\begin{aligned} \mathcal{L}_0^{2\gamma} &= - \frac{\pi\alpha}{4\Lambda^2} a_0 g^2 F_{\mu\nu} F^{\mu\nu} \text{Tr}(\mathcal{D}^\alpha \Sigma^\dagger \mathcal{D}_\alpha \Sigma) \\ \mathcal{L}_c^{2\gamma} &= - \frac{\pi\alpha}{4\Lambda^2} a_c g^2 F_{\mu\alpha} F^{\mu\beta} \text{Tr}(\mathcal{D}^\alpha \Sigma^\dagger \mathcal{D}_\beta \Sigma) \end{aligned} \quad (5.24)$$

with

$$a_{0,c} = \frac{4e^2}{s_w^2} L_{0,c}^{2\gamma} \left(k_{a,c}^W + k_{a,c}^B + k_{a,c}^{WB} \right) \quad (5.25)$$

The custodial symmetry imposed on these couplings means that, in leading order in s , they contribute in the same way to the $\gamma\gamma \rightarrow WW$ and to the $\gamma\gamma \rightarrow ZZ$, that is we have

$$\mathcal{A}(\gamma\gamma \rightarrow W_L^+ W_L^-) = \mathcal{A}(\gamma\gamma \rightarrow Z_L Z_L) \quad (5.26)$$

The “neutral” operator, $L_0^{2\gamma}$, only contributes to the $J_Z = 0$ ($\lambda_1 = \lambda_2$) amplitude

$$\begin{aligned} \mathcal{A}_{\lambda_1\lambda_2;00}^0 &= a_0^V (1 + \lambda_1\lambda_2) (2 - \gamma) \quad \text{and} \quad \mathcal{A}_{\lambda_1\lambda_2;\lambda_3\lambda_4}^0 = a_0^V (1 + \lambda_1\lambda_2)(1 + \lambda_3\lambda_4) \\ a_0^W &= \pi\alpha \frac{s}{4\Lambda^2} a_0 \quad , \quad a_0^Z = \frac{a_0^W}{c_W^2} \quad \text{and} \quad \gamma = \frac{s}{M_V^2} \end{aligned} \quad (5.27)$$

For the “charged” operator both the $J_Z = 2$ and $J_Z = 0$ contribute. This property already allows a possible separation of the effects of the two quartic couplings

$$\begin{aligned} \mathcal{A}_{\lambda_1\lambda_2;00}^c &= a_c^V \left[(1 + \lambda_1\lambda_2) (2 - \gamma) + \frac{\gamma}{2} (1 - \lambda_1\lambda_2) \sin^2 \theta \right] \\ \mathcal{A}_{\lambda_1\lambda_2;\lambda_30}^c &= a_c^V \sqrt{\frac{\gamma}{2}} (\lambda_1 - \lambda_2)(1 + \lambda_3 \cos \theta) \sin \theta \\ \mathcal{A}_{\lambda_1\lambda_2;\lambda_3\lambda_4}^c &= a_c^V \left\{ (1 + \lambda_1\lambda_2)(1 + \lambda_3\lambda_4) + \right. \\ &\quad \left. (1 - \lambda_1\lambda_2) \left[(1 - \lambda_3\lambda_4 \cos^2 \theta) + \lambda_1\lambda_3(1 - \lambda_3\lambda_4) \cos \theta \right] \right\} \\ a_c^W &= \pi\alpha \frac{s}{8\Lambda^2} a_c \quad \text{and} \quad a_c^Z = \frac{a_c^W}{c_W^2} \end{aligned} \quad (5.28)$$

Here “effective” interference does take place in the $J_Z = 2$ channel. As in the \mathcal{SM} , neither of the quartic couplings produces W ’s or Z ’s with opposite-helicities in the $J_Z = 0$ mode. This is therefore an obvious way, in W^+W^- , to disentangle their effect from that of the anomalous trilinear couplings $\lambda_\gamma, \kappa_\gamma$, which do not share this property. Furthermore,

the trilinear couplings contribute only to $\gamma\gamma \rightarrow W^+W^-$, whereas the $SU(2)$ symmetric quartic couplings contribute also to $\gamma\gamma \rightarrow ZZ$. It is very important to have polarised photon beams although disentangling the two couplings is possible even if no initial beam polarisation were available either by a careful scan of the angular distribution (the a_0 coupling contributes a flat distribution) or through measurements of the final W and Z polarisations.

To extract limits on the two operators, we use the total cross-section with polarised or unpolarised beams. As for the analysis of the trilinear couplings, a luminosity $\mathcal{L} = 10\text{fb}^{-1}$ is assumed for $\sqrt{s_{ee}} = 500$ GeV and the efficiency for W pair detection is taken to be 80%. We ignore events with tau's or two neutrinos in the final state and a cut on $|\cos\theta_W^*| < .7$ is imposed. Assuming a 1% systematic error and taking $\Lambda = 1\text{TeV}$, a 3σ deviation with unpolarised beams give the limits

$$-25 < a_0 < 9.4 \quad -19 < a_c < 10 \quad (5.29)$$

These can be improved with the use of polarisation, even when taking a 2% systematic error to take into account the additional error introduced by the measurement of the polarisation, we find at 3σ

$$-11 < a_0 < 5.5 \quad -10 < a_c < 6.6 \quad (5.30)$$

These bounds were obtained with the polarisation that gave the optimum sensitivity to each operator. Keeping $2\lambda'_e P'_c = -1$ in both cases, we took $2\lambda_e P_c = -1$, a $J_Z = 0$ -dominated spectrum, for a_0 and $2\lambda_e P_c = 1$, a $J_Z = 2$ spectrum for a_c .

5.4.1 Reconstructing the final polarisations

A reconstruction of the W polarisation, allowing to pull out the longitudinal W 's, could help in establishing as well as confirming signals from the symmetry-breaking sector [23]. To be able to determine the specific sign of the transverse helicity of the W one would use the leptonic (e, μ) decays of the W in order to reconstruct the angular distribution of the charged lepton in the rest frame of the decaying W . The problem is, of course, to boost back from the lab frame to the rest frame. In $e^+e^- \rightarrow W^+W^-$ (with little or no beamstrahlung) this is done simply from the knowledge of the beam energy that is also the energy of the W . In $\gamma\gamma$ the energy must be reconstructed. In WW events where only one of the W decays leptonically this should be possible without much error since the missing p_T of the neutrino could be inferred. On the other hand, for many analyses it may be sufficient to extract the differential cross sections for longitudinal and transverse

vector bosons as well as the spin correlation that do not require charge identification. In the $\gamma\gamma$ mode one could, in this case, use the all-hadronic decays.

5.4.2 Higgs resonance in $\gamma\gamma \rightarrow W^+W^-$?

If the Higgs is heavy it will decay preferentially into a W pair (see Fig. 15). One could then envisage to exploit its $\gamma\gamma$ coupling to produce it as a resonance[51, 52]. The problem will be the incredibly huge WW continuum. A recent[32] study has looked at this aspect by also taking into account the interference between the continuum and the s –channel Higgs exchange. A large destructive interference is found in the $\gamma\gamma \rightarrow W^+W^-$ channel which implies that a Higgs Boson of mass $M_H \geq 200\text{GeV}$ is manifest as a resonant *dip* in the M_{WW} invariant mass distribution. The conclusion is based on a setting that enhances the $J_Z = 0$ component ($P_c = P'_c$ and $\lambda_e = \lambda'_e = 0$) with a cut on the scattering angle of the W measured in the WW cms and by using the all-hadronic decays. Even with the most optimistic value on the resolution of the WW mass, $\Delta M_{WW} = 5\text{GeV}$, and an integrated luminosity of 20fb^{-1} the statistiscal significance of the resonant dip is not encouraging. Doubling the value of the resolution (which is still very hopeful) the signal disappears. Therefore, there seems to be very little (if none) prospect to look for the Higgs in this channel.

6 $\gamma\gamma \rightarrow ZZ$

This is a very interesting process for a variety of reasons. First, it is an effect of totally quantum origin. In its “pure gauge symmetric” manifestation with both Z transverse this reaction is to be likened to the scattering of light-by-light. In its “symmetry breaking phase”, *i.e.*, in the $Z_L Z_L$ case one could draw the analogy with $\gamma\gamma \rightarrow \pi^0\pi^0$. In fact, the early interest in this reaction was in the production of the longitudinal modes. Within the \mathcal{SM} realisation of \mathcal{SB} and for a Higgs with mass above $\sim 2M_Z$, this reaction would, at first, seem more advantageous than WW for revealing such a scalar as a resonance[51]⁴. This is because the WW continuum is overwhelming while $\gamma\gamma \rightarrow ZZ$ only takes place at one-loop. Thus, one expected this contribution to be too small so that ZZ would qualify as an indicator of a clean Higgs signal or else as an unambiguous manifestation of New Physics. In this case, identifying the longitudinal modes with the Goldstone bosons, one is back to the same topic covered here at some length especially in the sessions dedicated to DAΦNE, that is the $\gamma\gamma \rightarrow \pi^0\pi^0$. In the context of chiral perturbation theory, this

⁴The branching ratios as well as the total width of the Higgs as a function of its mass are shown in Fig. 15.

reaction has received a particular attention[53, 54] because it has been regarded to be a good test for the application of the formalism. One has argued so, because as with $\gamma\gamma \rightarrow ZZ$, the leading contribution to $\gamma\gamma \rightarrow \pi^0\pi^0$ occurs at $\mathcal{O}(\sqrt{\epsilon})$ and at this order it is completely predictable solely from the universal $\mathcal{O}(\sqrt{\epsilon})$ Lagrangian and does not require any counterterm. As is known now, it turned out that a naive and straightforward application of the formalism (at least to lowest order) was misleading[55, 56] and did not quite reproduce the data[57].

While this is a first warning if one were tempted to copy *mutatis mutandis* the Goldstone Boson sector of *QCD* to the longitudinal ZZ in $\gamma\gamma$, by all means there is “more to it” in the ZZ than the longitudinals: it is crucial to check the importance of the transverse.

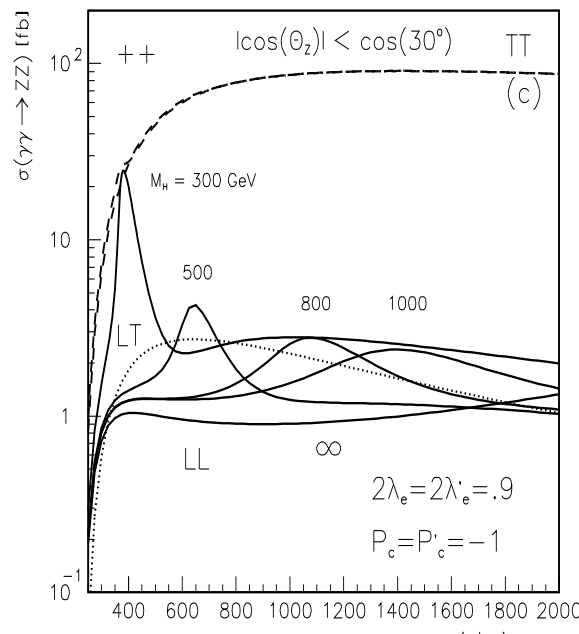
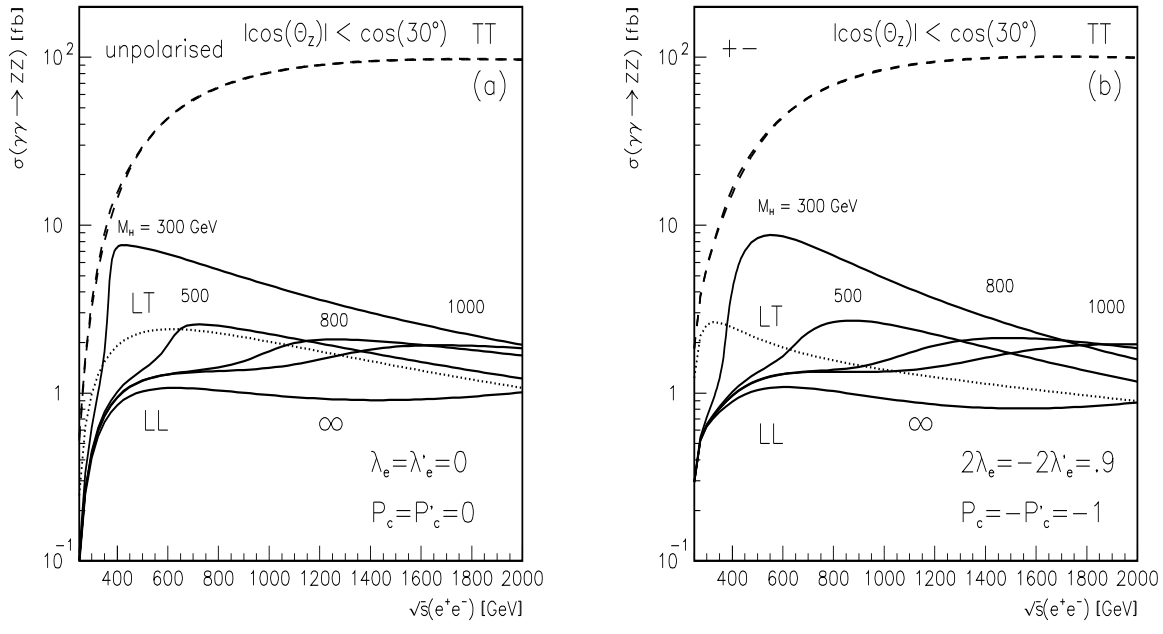
6.1 $\gamma\gamma \rightarrow ZZ$ in the \mathcal{SM} and the Higgs resonance

The first full calculation of the one-loop $\gamma\gamma \rightarrow ZZ$ within the \mathcal{SM} is a beautiful computation by Jikia[5] whose results have been repeatedly confirmed[6, 7, 8, 9]. As one might fear by having the ubiquitous $\gamma\gamma \rightarrow W^+W^-$ in mind, even for this one-loop example it turned out that, once again, the transverse modes are overly dominant, especially at high energy.

As we mentioned, when one examines the transverse modes it is almost as if one were studying the scattering of light-by-light. The most interesting novel aspect, compared to the pure case of QED, is that in the context of the electroweak interaction one has a pure non-Abelian contribution mediated by W loops. This contribution has been looked at some time ago[58, 59]. Already then, we stressed [59] the importance of doing such calculations within the background gauge. Another similar process that has also been calculated within the same spirit is the decay of the Z into three photons [26, 60, 61, 62]. Jikia and Tkabladze have also recently calculated the $\gamma\gamma \rightarrow \gamma\gamma$ [63] and $\gamma\gamma \rightarrow \gamma Z$ [62] cross section in the context of a high energy $\gamma\gamma$ collider.

Although the $\gamma\gamma \rightarrow \gamma\gamma$ and $Z \rightarrow 3\gamma$ processes are quite attractive and have a clear connection with $\gamma\gamma \rightarrow ZZ$, the longitudinal modes for these processes are insignificant and decouple quite trivially. Physics-wise $\gamma\gamma \rightarrow ZZ$ is much “richer” because the longitudinal modes play a crucial role. Our discussion on the characteristics of the $\gamma\gamma \rightarrow ZZ$ reaction within the \mathcal{SM} and the Higgs resonance in ZZ is based almost entirely on the results of Jikia[5]. The main conclusions of the study of $\gamma\gamma \rightarrow ZZ$ are summarised in Fig. 11,12,13 that we have borrowed from [5]. All the figures are with $m_t = 120\text{GeV}$. To produce central events a cut on the Z production angle measured in the $\gamma\gamma$ cms is imposed: $30^\circ < \theta_Z < 120^\circ$. Since, from the point of view of the \mathcal{SM} , the motivations for studying

Figure 11: Cross section for ZZ production after convoluting with different spectra. The cut on the Z scattering angle is shown. The three combinations of the final Z polarisations are shown. The LL curves are indicative of the Higgs whose mass can be read off from the position of the bump/peak: $M_H = 300, 500, 800, 1000$ and ∞ . From [5].



this reaction lie primarily on its ability to bring out the heavy Higgs peak formation[51, 64], the issue of polarising the initial state is central. One must aim at creating a $J_Z = 0$ environment. And, if possible, reconstruct the longitudinal polarisation of the ZZ that signals the Higgs while trying to reduce the transverse.

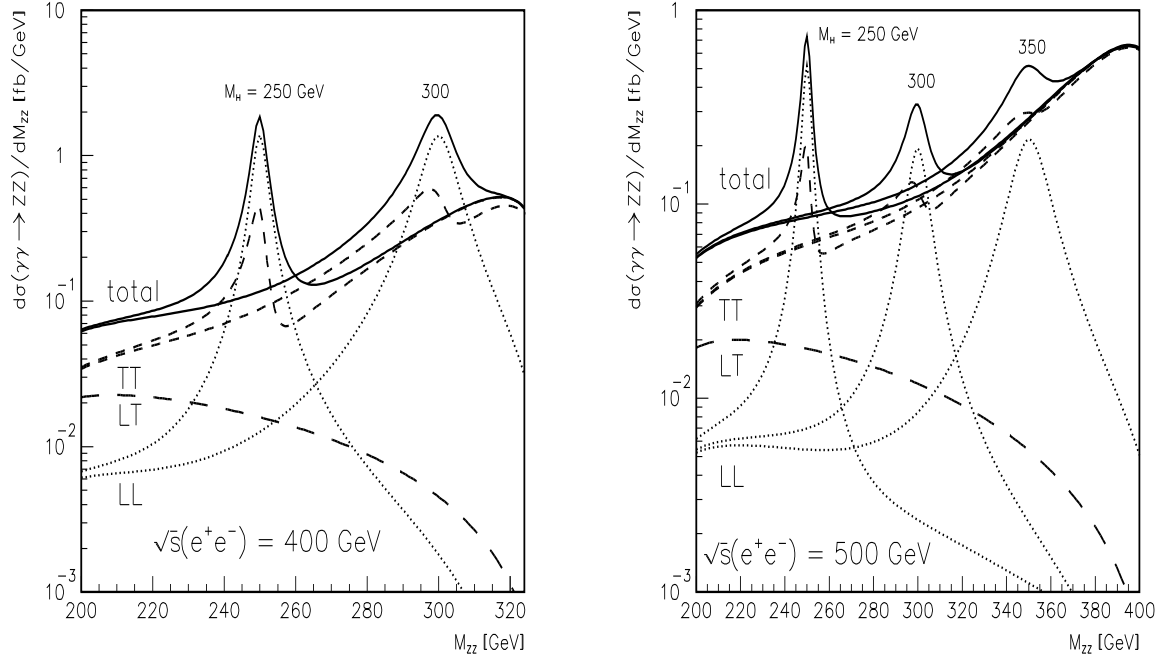
As is the hallmark with $\gamma\gamma \rightarrow W^+W^-$, one sees (Fig. 11) that once again the transverse modes, either in the $J_Z = 0$ or $J_Z = 2$ state dominate, by far, the cross-section especially as the energy increases. This is due essentially to the W loops. We effectively have that the WW produced in $\gamma\gamma$ rescatter into ZZ . This shows, from a different perspective, how $\gamma\gamma \rightarrow W^+W^-$ permeates so many aspects of W physics in the $\gamma\gamma$ collider.

It is clear that unless one recreates a $J_Z = 0$ there would be little hope of extracting a Higgs signal apart, perhaps, if the Higgs mass is below $\sim 300\text{GeV}$ and the e^+e^- energy below 500GeV . Even if the “0-dom” is realised (see Fig. 11c), such that the $J_Z = 0$ part of the $\gamma\gamma$ spectrum is peaked for $\sqrt{s_{\gamma\gamma}}$ values around the Higgs mass, one observes that Higgs masses below $\sim 350\text{GeV}$ could emerge above the Z_TZ_T continuum. For instance, a Higgs mass of 500GeV which would require an optimum set-up in the “0-dom” environment that corresponds to $\sqrt{s_{ee}} = 700\text{GeV}$ would already be completely buried under its intrinsic Z_TZ_T background. Therefore, before addressing the issue of the identification of the ZZ final state, one learns that a high energy e^+e^- machine with $\sqrt{s_{ee}}$ in TeV range would not be of much help in revealing the resonant Higgs formation.

As to what happens in a Higgs search at a given energy, the results are displayed in Fig. 12. The laser set-up is such that one filters out a predominant $J_Z = 0$. In the calculation of Jikia this filtering is obtained through what we have called a “0-dom” spectrum that is peaked towards the maximum $\hat{s}_{\gamma\gamma}$ (see Fig. 5). This may not be the optimal choice of polarisation as we could arrive at a $J_Z = 0$ environment in a flat spectrum set-up that would be more appropriate if one were searching for the Higgs whose mass would not have been determined by another means⁵. Anyhow, we see that at $\sqrt{s_{ee}} = 400\text{GeV}$, the situation is quite bright even with the “0-dom” set up: the Higgs resonance is clearly evident over the TT continuum all the way up to the kinematic limit. With $\sqrt{s_{ee}} = 500\text{GeV}$ in the “0-dom” set-up it becomes already difficult to extract a Higgs with $M_H \sim 350\text{GeV}$. It has been shown[8] that the situation improves for these values of the Higgs mass and the energy if we change the polarisation settings. In fact, if we take what we have called the polarised “broad spectrum” (see Fig. 6a) so that for small M_{ZZ} one has a dominant $J_Z = 0$, one could still see a peak in the M_{ZZ} invariant

⁵As compared to the IMH this seems less justified as Higgs masses with $M_H > 2M_Z$ would be easily discovered at the LHC.

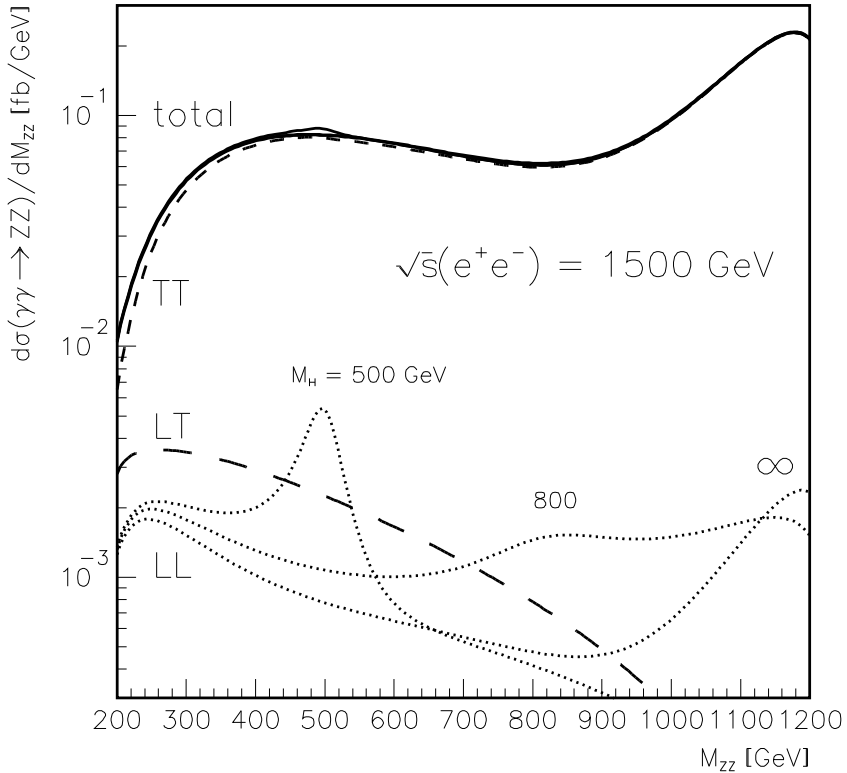
Figure 12: *Searching for the Higgs in the invariant ZZ mass distribution at e^+e^- cms of 400 and 500GeV. The three combinations of the final polarisations as well as the sum over all final helicities are shown. The illustrative masses of the Higgs are shown. From [5].*



mass for Higgs masses below 400GeV at a 1TeV e^+e^- machine. However, it is not clear whether the statistical significance of the signal in this case is satisfactory as the luminosity in the broad spectrum has been uniformly spread over a large energy range[8]. From the perspective of observing the Higgs resonance beyond TeV e^+e^- energies, the situation as displayed in Fig. 13 becomes totally hopeless as the transverse ZZ are awesome.

So far, the pictorial description of the H resonance, if any, lacks a careful investigation of the backgrounds to ZZ . The problem is that the largest branching fraction of a visible Higgs through ZZ is into 4 jets. This signature will be utterly buried under the huge WW that materialise into 4 quarks. A quick look at Fig. 2, that also shows the 300GeV Higgs resonance in ZZ , should be convincing. In the 4 jets topology the only glimmer of hope that we foresee is the decay of (at least one) of the Z into b 's. This requires a very good rejection of charm to disentangle the Z from the W . A very nice signature of the ZZ that has a relatively good branching fraction is when one of the Z decays into

Figure 13: *As in the previous but for $1.5\text{TeV } e^+e^-$. The infinite mass Higgs is also shown. From [5].*



neutrinos. The latter produces a large missing transverse energy, recoiling against an invariant mass $\sim M_Z$ [2, 51, 19]. Basing the analysis of this signature on counting rate should help at small $\sqrt{s_{ee}}$. However, since we can not reconstruct the invariant ZZ mass with these decays, it seems to be difficult to carry this analysis to higher energies. Would a distribution in the transverse mass improve the situation?

The cleanest signal that allows an invariant ZZ mass reconstruction is when at least one of the Z decays leptonically (one should only consider e and μ) while the other decays visibly. Unfortunately, this corresponds to a small combined branching fraction of about 10% of all ZZ events. Nonetheless, it seems to be possible to extract a good signal for low enough e^+e^- cms energy and Higgs masses[65]. It has been pointed out[65] that $f\bar{f}Z$ final state could fake the signal. Fortunately this background could be easily disposed off by requiring a central $f\bar{f}$ pair that reconstructs the Z [65].

6.2 Looking for \mathcal{SB} scenarios in $\gamma\gamma \rightarrow ZZ$

As mentionned earlier, the reaction $\gamma\gamma \rightarrow ZZ$ was not considered to be interesting just from the point of view of the Higgs resonance but also from the perspective of checking the symmetry breaking. The nice proposals all predict an excess of $Z_L Z_L$ events at high M_{ZZ} invariant masses, but the analyses were done with the tacit assumption that the excess was an excess over very negligible ($\sim zero!$) ZZ events. Looking at Fig. 12 once more, it is clear that the conclusions should be reconsidered and the optimism somehow watered down.

Nonetheless, we think that with the proper inclusion of the \mathcal{SM} contribution adapted to the Higgsless limit, this reaction should still be useful. After all, we were able to extract competitive limits on the L_9 parameters of the chiral Lagrangian description of the $WW\gamma$ anomalous couplings through the reaction $\gamma\gamma \rightarrow W^+W^-$ whose cross section is so much larger than the $Z_T Z_T$. Furthermore, since the limits on the various parameters that were extracted from the ZZ process are quadratic in these parameters, we do not expect that the taking into account of the $Z_T Z_T$ mode changes the limits by more than an order of magnitude.

When adapting the \mathcal{SM} results to the search of unconventional scenarios of \mathcal{SB} that do not admit a Higgs, the reference value of $Z_L Z_L$ should correspond to the large Higgs mass limit[66, 5, 9], $M_H^2 \gg s_{\gamma\gamma} \gg M_W^2, M_Z^2$, that can also be more easily obtained by using the equivalence theorem or the chiral limit of the properly ‘‘translated’’ $\gamma\gamma \rightarrow \pi^0\pi^0$ [53, 54, 48].

$$\mathcal{M}_{++LL} \rightarrow \frac{\alpha^2}{s_w^2} \frac{s_{\gamma\gamma}}{2M_W^2} \equiv 8\pi\alpha \frac{s_{\gamma\gamma}}{(4\pi v)^2} \quad (6.31)$$

Once this universal part ($\mathcal{O}(\sqrt{\Delta})$) has been included it turns out that all models of symmetry breaking can be described in terms of their contribution to the helicity amplitudes with only the two parameters a_0 and a_c that we introduced in the previous section[2]. These should be seen as corrections of order $\mathcal{O}(\sqrt{\lambda})$ in the energy expansion. The corresponding operators that describe $\gamma\gamma \rightarrow \pi^0\pi^0$ are the ones first discovered by Terent’ev[67]. Models that correspond to the residual effect of heavy charged scalars contribute to a_0 [54, 68], as well as the effect of a very heavy neutral scalar ($s_{\gamma\gamma} \gg M_S^2$) coupled in a chiral invariant way [69, 70]. Note also that, in effect, the universal term in Eq. 6.31 contribute to the same leading helicity amplitude as a_0 .

It should be realised that if one wished to include the effect of a not-so heavy scalar, which in a sense would be some unconventional Higgs[2], one would modify our non-resonant formulae by providing for the propagator of the scalar (in a sense $\Lambda^2 \rightarrow s - \Lambda^2 + i\Gamma\Lambda$). One could even accommodate the model of Chanowitz[71] that would be interpreted in

the limit that the above unconventional scalar is a light Higgs having enhanced couplings, as a result of some ultra-heavy states. In any case, for all these models there would be no contribution to the $J_Z = 2$ amplitude⁶.

This is not the case of the a_c models that would show up both in the $J_Z = 2$ and the $J_Z = 0$. The case of heavy axial fermions that could be the analog of the nucleons in the chiral picture could also be made[2, 68]. We would then identify this case with $a_0 = -a_c$. Models with heavy vector resonances V constructed on the hadron mould [73, 74] like the so-called BESS model[75] could not contribute in their minimal version to $\gamma\gamma \rightarrow ZZ$. In this particular scenario one can not just rely on the equivalence theorem to replace the longitudinal Z by the “pion” field and apply the result of $\gamma\gamma \rightarrow \pi^0\pi^0$ [68, 76, 70] that gives the same pattern $a_0 = -a_c$. One needs to break \mathcal{C} for the effective γVZ . This entails that the model[77] contains anomalies and loses much of its attraction.

The case with $a_c = -2a_0$ would only contribute to the $J_Z = 2$. We should also note that at high enough energy some unitarisation of the amplitudes should be provided[78] and that for some values of the parameters of $\mathcal{O}(\sqrt{\lambda})$ Lagrangian one has a softening of the growth of the $J_Z = 0$ amplitude for the two longitudinal vector bosons.

6.3 Limits on the $\mathcal{O}(\sqrt{\lambda})$ operators in ZZ .

Before the results of the \mathcal{SM} cross section for $\gamma\gamma \rightarrow ZZ$ were available, the investigations of the symmetry breaking mechanisms [2, 71, 79, 48] concluded that this channel was an ideal testing ground as compared to WW . Unfortunately the optimism has faded somehow, since the \mathcal{SM} provides a non negligible rate completely dominated by $Z_T Z_T$. As we argued above, even when taking into account the \mathcal{SM} contribution, the ZZ still remains a good window for the New Physics. A naive estimate will suffice to get a good idea of what can be achieved in the ZZ channel. First of all, the \mathcal{SM} $Z_L Z_L$ contribution in the very heavy Higgs mass limit (the “universal” term) does not pose much problem as it is quite small at all energies (around $1fb$, see Fig. 11). To have a rough idea on how the limits are changed it will be sufficient to include the \mathcal{SM} $Z_T Z_T$ contribution that is not affected by the effects we are looking at. We have thus based our discussion on the total cross-section only. Another idea that deserves more study should exploit the fact that the TT cross section does not depend much on the J_Z of the initial two photons.

⁶Deviations in the $\gamma\gamma \rightarrow ZZ$, $\gamma\gamma \rightarrow Z\gamma$ and $\gamma\gamma \rightarrow \gamma\gamma$ due to an anomalous operator in the linear (light Higgs) realisation of symmetry breaking have been analysed recently [72]. We wish to point out that since the sole effect of this operator is a modification of the coupling $HVV(V = \gamma, Z, W)$, in principle, we could also test this operator via Higgs production in e^+e^- either in the Bjorken process or the fusion mechanism.

Therefore, by constructing an asymmetry such as ($\Delta\sigma_{02} = \sigma_{J_Z=0} - \sigma_{J_Z=2}$), in a peaked spectrum set-up, Fig. 5, one should reduce the \mathcal{SM} background. This, of course, assumes that the New Physics is such that it does not contribute equally to the two J_Z as is the case with a_0 or a_c taken separately. This also assumes that one can “afford” sharing the luminosity between the two modes while maintaining a good signal.

For our tentative estimate based on the total cross section we only considered the visible unambiguous ZZ signature with one Z decaying hadronically and the other leptonically, with a cut $\cos\theta_Z^* < .866$. The “0-dom” (Fig. 5) setting was assumed so that to reproduce the cut and settings of Jikia[5]. The criterion of observability was based on requiring 3σ statistical deviation from the standard cross-section. Taking $\Lambda = 1TeV$, we obtain the limits

$$\begin{aligned} |a_0| &< 2 \quad |a_c| < 5 \quad \text{with } \sqrt{s_{ee}} = 500GeV ; \int \mathcal{L} = 10fb^{-1} \\ |a_0| &< 0.3 \quad |a_c| < 0.7 \quad \text{with } \sqrt{s_{ee}} = 1TeV ; \int \mathcal{L} = 60fb^{-1} \end{aligned} \quad (6.32)$$

These limits are only a factor 2 (at 500GeV) worse than what we have obtained by neglecting the \mathcal{SM} contribution and about a factor 4 worse at 1TeV. Nonetheless these limits are better than what we would obtain in the e^+e^- mode through three vector production[10] or in the $e\gamma$ mode [80].

7 WWZ and $WW\gamma$ Production

As already pointed out in the introduction, triple vector production at $\gamma\gamma$ is very important. In this section we would like to point at some interesting aspects of these cross-sections. We note that with these reactions one is totally in the non-abelian gauge sector of the \mathcal{SM} .

7.1 $\gamma\gamma \rightarrow W^+W^-\gamma$ [81, 3]

For the $WW\gamma$ final state, a cut on either the final photon energy or transverse momentum is required. With a fixed cut $p_T^\gamma > 20$ GeV for all centre-of-mass energies, the cross-section increases with energy (see Fig. 14a). At 500 GeV one reaches a cross-section of about 1.3pb. This is about 1.6% of the WW cross-section at the same energy. The $J_Z = 0$ obtained when both photons have the same helicity slightly dominates over the $J_Z = 2$ (1.5pb versus 1.1pb). At $\sqrt{s_{\gamma\gamma}} = 2$ TeV the cross-section with the same $p_T^\gamma > 20$ GeV cut reaches 3.7pb. The logarithmic ($\log^2 s$) growth can be understood on the basis that this cross-section can be factorised in terms of $\gamma\gamma \rightarrow WW$, which is constant at

asymptotic M_{WW} invariant masses, times the final state photon radiator which contains the logarithmic s dependence. We note that this logarithmic increase only concerns the production of transverse W . When both W 's are longitudinal ($W_L W_L$) the cross-section decreases. This can also be traced back to the fact that $\gamma\gamma \rightarrow W_L^+ W_L^-$ decreases with energy. We find that the $W_L W_L$ fraction of all W 's is about only 1% at 500 GeV, 0.3% at 1 TeV and a mere 0.07% at 2 TeV. It must be noted that the bulk of the cross-section occurs when all final particles are produced at very small angles: this is a typical example of multiparticle production in the very forward region. For instance, increasing the p_T^γ cut and at the same time imposing a pseudorapidity cut on the photon, the $WW\gamma$ yield, as shown in Table 2, drops considerably, especially at higher energies. The reduction is even more dramatic when we put an isolation cut between all the particles and force them away from the beam. With these strictures the cross-section decreases with energy (See Table 2).

Table 2: *Cross-section for $\gamma\gamma \rightarrow W^+ W^- \gamma$ (in fb) at different energies, including various cuts.*

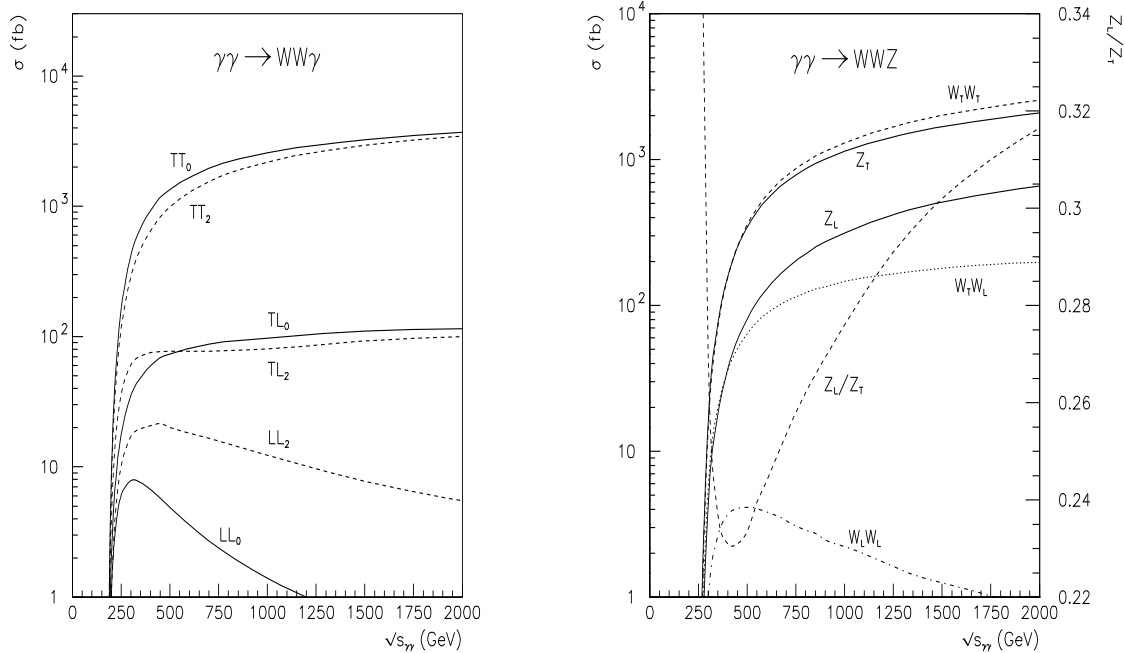
$\sqrt{s}_{\gamma\gamma}$ (TeV)	0.5	1	1.5	2
type of cut				
cut 1: $p_T^\gamma > 20$ GeV	1254	2469	3195	3678
cut 2: $p_T^\gamma > 40$ GeV $\times \sqrt{s}_{\gamma\gamma}$ (in TeV)	1254	1434	1258	1050
cut 3: cut 2 and $ y^\gamma < 2$	1235	1373	1159	930
cut 4: cut 2 and $\cos(\text{between any two particles}) < 0.8$	201	86	47	32

While the $W_L W_L$ production is very much favoured in the $J_Z = 2$ mode, $W_T W_T$ and $W_T W_L$ productions (which are by far the largest contributions) are slightly more favoured in the $J_Z = 0$ channel (see Fig. 14a). This is the same behaviour as in the two body process $\gamma\gamma \rightarrow W^+ W^-$.

7.2 $\gamma\gamma \rightarrow W^+ W^- Z[3]$

Contrary to the previous reaction one can calculate the total cross-section. It exhibits an interesting behaviour at TeV energies. One notes that already at 1 TeV the triple vector boson production is larger than top pair ($m_t \geq 130$ GeV) and charged heavy scalars production (with $m_{H^\pm} \simeq 150$ GeV) as shown in Fig. 2. At 2 TeV the total WWZ cross-section is about 2.8 pb and exceeds the *total* electron-positron pair production! This is a typical example of the increasing importance of multiparticle production in weak

Figure 14: a) Polarised cross-sections for $WW\gamma$ production. The subscripts 0, 2 refer to the two-photon state. b) WWZ with unpolarised photons. When the particle is not indicated this means that we have summed on all its polarisations. We also show the ratio Z_L/Z_T



interactions at higher energies, purely within perturbation theory ⁷. The rising of the cross-section with the centre-of-mass energy is essentially from the very forward region due to the presence of the “non-annihilation” diagrams with the (spin-1) W exchanges. A similar behaviour in e^+e^- reactions is single vector boson production. What is certainly more interesting in $\gamma\gamma \rightarrow W^+W^-Z$ is the fact that it has a purely non-abelian origin. It may be likened to $gg \rightarrow ggg$ in QCD except that we do not need any infrared cut-off (the W and Z mass provide a natural cut-off).

The bulk of the cross-section consists of both W being transverse as is the case with the “parent” process $\gamma\gamma \rightarrow W^+W^-$. While the total cross-section is larger in the $J_Z = 0$ than in the $J_Z = 2$, the production of all three vector bosons being longitudinal occurs mainly in the $J_Z = 2$ channel and accounts for a dismal contribution. For instance, the ratio of LLL/TTT (three longitudinal over three transverse) in the case of unpolarised beams amounts to a mere 2per-mil at 500 GeV and drops to 0.1per-mil at 2 TeV. Nonetheless, the total ⁸ production of longitudinal Z ’s as compared to that of transverse Z ’s is not at

⁷As opposed to the surmise of large W multiplicities due to topological effects at extremely high-energies. For a recent review see [82].

⁸i.e., taking into account all polarisation states of the W .

all negligible. In fact, between 500 GeV and 2 TeV this ratio increases from about 23% to 32% (see Fig. 14b). This is somehow counterintuitive as one expects the longitudinal states to decouple at high energies. The importance of Z_L production (in association with $W_T^+W_T^-$) is, however, an “infrared” rather than an “ultraviolet” phenomenon in this reaction: the Z is not energetic. First, one has to realize that the $\gamma\gamma \rightarrow W^+W^-Z$ amplitude is transverse in the momentum of the Z , q , as is the case with the photons in $\gamma\gamma \rightarrow W^+W^-\gamma$. With k_1 and k_2 being the momenta of the photons, the longitudinal polarisation vector of the Z , with energy E_Z , writes

$$\epsilon_\mu^L = \frac{1}{\sqrt{E_Z^2 - M_Z^2}} \left(\frac{E_Z}{M_Z} q_\mu - \frac{M_Z}{\sqrt{s}} (k_1 + k_2)_\mu \right); \quad \epsilon^L \cdot \epsilon^L = -1 \quad (7.1)$$

The transversality of the amplitude means that the leading (“ultraviolet” $\propto E_Z$) part does not contribute. Only the “infrared” part $\propto M_Z$ does. This contribution should vanish in the limit of vanishing M_Z . However, the amplitude, in analogy with what happens in $WW\gamma$, has the infrared factor $1/E_Z$ and the “soft” term in Eq. 7.1 contributes. Furthermore, more importantly, the bulk of the cross-section is from configurations where both W are transverse (see Fig. 14.b) and all three particles go down the beam. In the limit of vanishing masses this topology leads to collinear divergences⁹. In this dominating configuration, in the exact forward direction, the longitudinal Z contributes maximally. At the same time, angular momentum conservation does not allow the Z to be transverse when all final particles are down the beam (with $p_T = 0$) and both W are transverse. So the “maximal collinear enhancement” is not as operative for the transverse Z as it is for longitudinal Z when both W_T are at zero p_T . However, as soon as one moves away from these singular configurations, the longitudinal Z does decouple and the “smooth” mass limit may be taken. This is well rendered in Table 3 which displays the ratio of Z_L/Z_T without any cut and with the inclusion of cuts. The most drastic of these cuts is when we impose angular separation cuts between the final particles and force them to be away from the beam, with the effect that the Z_L/Z_T decreases with energy and gets dramatically smaller. On the phenomenological side, the study of this reaction is important as, especially for $M_H \sim M_Z$, it is a background to Higgs detection through WWH production¹⁰.

⁹In the limit $M_V \rightarrow 0$, added to the divergence in $\gamma\gamma \rightarrow W^+W^-$, there is the collinear divergence when the Z and a W are collinear.

¹⁰Two calculations of the WWZ cross section have appeared[83, 84]. They deal with the total unpolarised cross section. In [83] we find complete agreement at all energies. In [84] we agree after folding with the unpolarised luminosity spectrum at $s_{ee} = 500\text{GeV}$ and 1TeV and taking into account the same value of the parameters α and $\sin^2\theta_W$. With the same changes our result for the unpolarised $WW\gamma$ are

Table 3: *Cross-section for $\gamma\gamma \rightarrow W^+W^-Z$ and ratio of longitudinal over transverse Z (L/T) including various cuts. “all” means that we require the final particles to be separated and to be away from the beam by an angle θ corresponding to $\cos\theta < 0.8$.*

	$\sqrt{s}_{\gamma\gamma} = 500$ GeV $\sigma(\text{fb})$	$\sqrt{s}_{\gamma\gamma} = 1$ TeV $\sigma(\text{fb})$	$\sqrt{s}_{\gamma\gamma} = 1.5$ $\sigma(\text{fb})$	$\sqrt{s}_{\gamma\gamma} = 2$ TeV $\sigma(\text{fb})$	L/T	L/T	L/T	
no cut	428	24%	1443	27%	2195	30%	2734	32%
$\cos(WZ) < 0.8$	368	19%	1025	18%	1321	19%	1465	19%
$\cos(W\gamma) < 0.8$	164	18%	232	17%	186	17%	145	16%
$\cos(\text{“all”}) < 0.8$	115	11%	140	8%	105	6%	77	5%
$E_Z > 150$ GeV	184	11%	1032	21%	1700	25%	2220	28%

8 Search for the \mathcal{SM} Intermediate-mass Higgs

One of the most attractive motivations for doing physics with very energetic photon beams is the unique capability of this mode for producing a scalar particle as a resonance. In our context this is the Higgs. This resonant Higgs structure is out of reach in the usual e^+e^- mode. However, as we stressed in our general introduction, the coupling of the Higgs to two photons only occurs at the loop-level. Therefore, on the one hand, the rate of production is not as large as with the resonant Z , say. On the other hand, a precision measurement of the $H\gamma\gamma$ coupling is an indirect way of revealing all the massive charged particles that would be present in an extension of the \mathcal{SM} . These heavy quanta would not decouple and would therefore contribute substantially to the production rate in $\gamma\gamma$.

To conduct the precision measurements of the $H\gamma\gamma$ coupling one needs to sit at the Higgs resonance and collect enough luminosity. For the IMH, this would mean operating within a narrow energy range that could be much below the highest accessible energy. Therefore, the question arises whether one should tune the $\gamma\gamma$ machine such that one obtains a spectrum that is peaked at the Higgs mass and that has very little spread. We will refer to this scheme as the narrow-band low-energy $\gamma\gamma$ collider. This is certainly possible, however this choice will preclude the study of a plethora of interesting weak processes and thus it rests to see whether such a decision would be made. For instance, the most important mass range at the NLC is the intermediate mass Higgs, IMH, $M_Z < M_H < 140$ GeV. This mass range is, in a sense the preserves of the NLC, since it is going to be extremely difficult (if at all) to cover this range at the LHC.

The unease with the choice of a peaked $\gamma\gamma$ spectrum is that, within this narrow do-
also confirmed by [84].

main of energy, obtained from an e^+e^- with $\sqrt{s_{ee}} = 500$ GeV or higher ¹¹ it will not be possible to reach the WW threshold (that seems to be a good luminosity monitor) and other W reactions that offer a rich physics program. This could include the direct production of some of those particles that would only be probed indirectly in $H\gamma\gamma$. Of course, one may argue that these would be necessarily produced in the e^+e^- but in view of the known universal character of the production mechanism in $\gamma\gamma$, they may be better studied. Not to mention that it is not excluded that the $\gamma\gamma$ mode when operated in the full range of energy can access scalar particles that would kinematically be out of reach in the e^+e^- mode. This could happen if in e^+e^- they can only be produced in association with another heavy particle. The \mathcal{CP} -odd Higgs of the minimal supersymmetric model is such an example[51].

It is certain that a narrow-band low-energy $\gamma\gamma$ collider has its merits especially if it is achieved with high luminosity, since precision tests on the nature of the light Higgs may be performed. To some degree, this would be a spin-0 version of a polarised LEP1! Moreover, as we will see, with a low-energy scheme many backgrounds are drastically suppressed. Investing enough running time in such a mode to be able to switch between different polarisation settings (circular/linear polarisation,...) one could, for instance, *directly* test the parity of the Higgs [85, 86] or perform \mathcal{CP} tests from probing the $H\gamma\gamma$ coupling[17]. These are undoubtedly quite interesting studies to do, but we should stress that they do call for very high luminosities and would be done at the expense of a rich program. In addition, keeping in mind that this “narrow-band” scheme presupposes that it is in the e^+e^- mode that the mass of the Higgs has been determined and used to tune the laser, the e^+e^- would also give a good clue on some of the above issues that one wants scrutinized in the peaked $\gamma\gamma$ mode. For instance, the parity of the scalar will, in a large degree, be inferred from its rate of production in the e^+e^- . A spin-0 either standard or supersymmetric produced through the VVH vertex is \mathcal{CP} even. As pointed out in [51] it may also happen that a measurement of the $h^0\gamma\gamma$ if not very precise would not provide much more insight. This could occur if in the e^+e^- mode of a 500GeV only the lightest Higgs of the minimal supersymmetric model is discovered while the other susy particles are above threshold. Eventually, the choice will depend on the priority of the time and how the e^+e^- collider is operating. For instance if we will have two interaction regions, one devoted to $\gamma\gamma$ physics as suggested in[87], then one should search in both modes with a later (long) run dedicated to precision measurements.

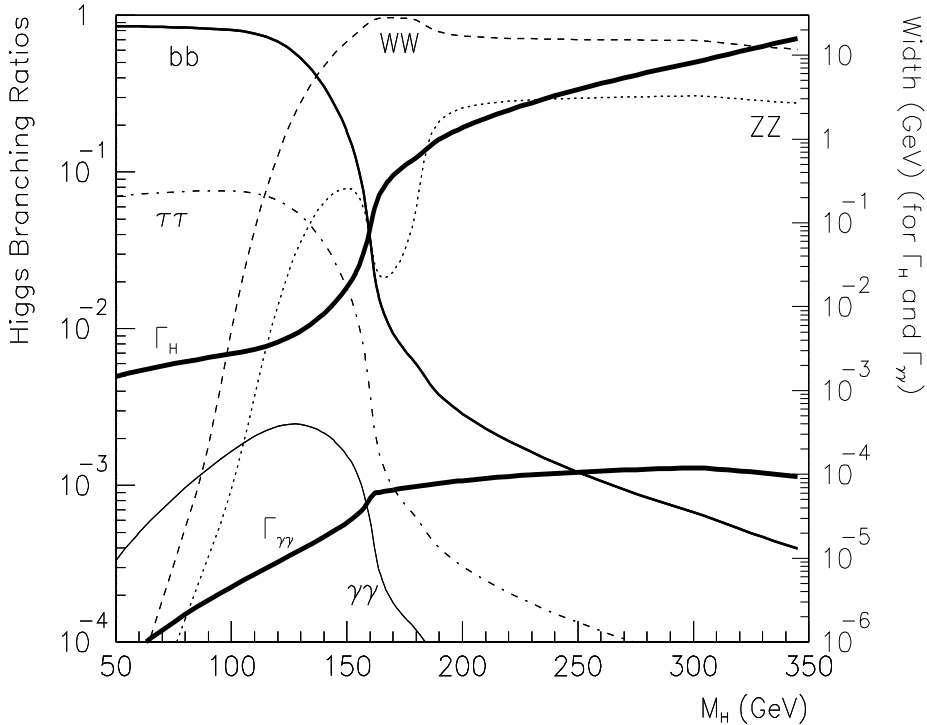
¹¹The choice of this scheme tacitly assumes that the mass of the Higgs has been determined in the e^+e^- mode and that $\sqrt{s_{ee}} = 500$ GeV would, in any way, be available.

Anyway, we feel it is essential to address the issue of whether the intermediate mass Higgs could be observed as a resonance in a setting with a spectrum that allows a whole and self-contained physics program to be conducted.

The issue of seeing the heavy Higgs in the WW and ZZ channels has been addressed in sections 6 and 7 and discussed in the talk of D. Zappala and H. Veltman[32, 88]. In this section we only reassess the $\gamma\gamma$ discovery potential of the \mathcal{SM} Higgs, readdress the question of different backgrounds and how one could reduce their effect to a minimum. A few investigations of this aspect have been done with different emphasis and approaches [51, 52, 16, 64, 89].

The IMH, as is known, will decay predominantly into a $b\bar{b}$ pair and has an extremely narrow width (see Fig. 15). This width, $\Gamma_H = \Gamma_{total}$, is of order of a few MeV.

Figure 15: *Some of the \mathcal{SM} branching ratios of the Higgs as a function of the Higgs mass calculated with a top mass of 150GeV. Also shown (thick lines) the total width and the $\gamma\gamma$ width.*



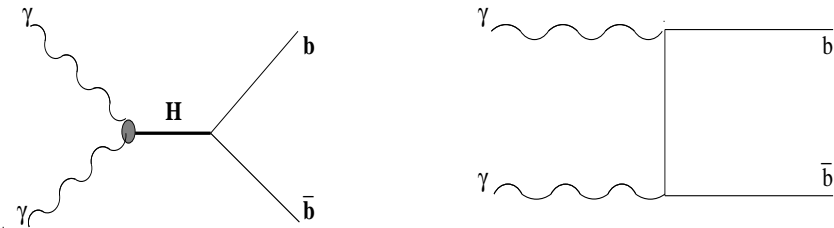
In the rest frame of the Higgs, the fermions are produced isotropically in the $J_Z = 0$

state. The corresponding cross-section is described by the Breit-Wigner formula[51, 64]

$$\sigma(\gamma\gamma \xrightarrow{H} b\bar{b}) = \frac{8\pi\Gamma(H \rightarrow \gamma\gamma)\Gamma(H \rightarrow b\bar{b})}{(\hat{s} - M_H)^2 + \Gamma_H^2 M_H^2} (1 + \lambda_1 \lambda_2) \quad (8.1)$$

The exact expressions for the branching ratios of the Higgs and the $\Gamma(H \rightarrow \gamma\gamma)$ width that we will use in our analysis are taken from[90]¹². A top mass of 150 GeV has been assumed. One obvious background is the direct QED $\gamma\gamma \rightarrow q\bar{q}$ production where $q = b$.

Figure 16: *The Higgs signal into $b\bar{b}$ and its QED background*



One should also worry about other light quark flavours if no b -tagging is possible, charm causing much problem. A glance at the expression of the differential cross-section gives the clue as to how one could efficiently suppress this background. For the quark of charge e_f and with $N_c = 3$ we have, in the $\gamma\gamma$ cms with θ^* being the q scattering angle and $x = \cos \theta^*$:

$$\frac{d\sigma_{QED}}{dx} = \frac{2\pi\alpha^2 e_f^4 N_c \beta}{\hat{s}(1 - \beta^2 x^2)^2} \left\{ (1 + \lambda_1 \lambda_2)(1 - \beta^4) + (1 - \lambda_1 \lambda_2)\beta^2(1 - x^2)(2 - \beta^2(1 - x^2)) \right\} \quad (8.2)$$

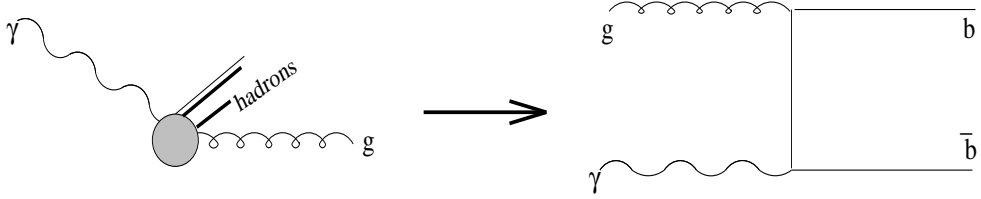
It is clear that the bulk of the cross-section is from the extreme forward-backward region. A modest cut on $\cos \theta^*$ will reduce the continuum substantially and will almost totally eliminate its $J_Z = 0$ contribution (note its $(1 - \beta^4)$ chiral factor). Therefore, choosing a spectrum with a predominantly $J_Z = 0$ component[51] and applying a cut on $\cos \theta^*$ should do the trick. It is instructive to note that the $J_Z = 2$, because of angular momentum conservation, vanishes in the exact forward region.

It has recently been pointed out[89] that, unfortunately, this is not the whole story. Owing to the fact that the photon has a hadronic structure[91] it can “resolve”¹³ into a gluon with some spectator jets left over. One then has to worry about $q\bar{q}$ production through γg . Although the photon transfers only a small fraction, x_g , of its energy to the gluon, at $\sqrt{s_{ee}} \sim 500$ GeV the overall energy can be large enough for this gluon to combine with a

¹²We thank Abdel Djouadi for providing us with the Fortran code.

¹³This terminology has been introduced by Drees and Godbole [92].

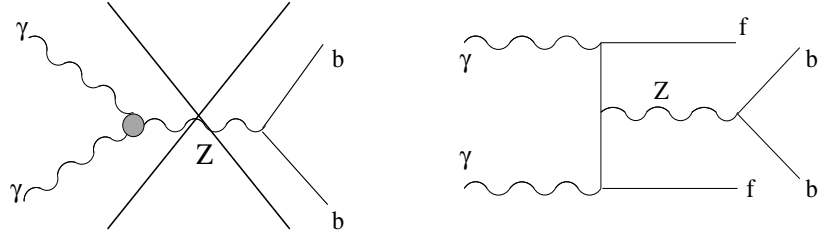
Figure 17: Bottom pair production through the “once-resolved” photon.



photon so that the subsystem energy is enough for the IMH production. At 500 GeV with a spectrum with $x_0 = 4.82$ so that $\sqrt{s_{\gamma\gamma}^{\text{max}}} \sim 400$ GeV, this is an annoying background. Of course, if the photon transferred all of its polarisation to the gluon then there will be not much problem as we will be in the same situation as with the polarised $\gamma\gamma$ initiated process. Unfortunately, we expect the polarisation to be diluted in the transfer. In principle, one could discriminate the gluon initiated processes from the direct production through the presence of the spectator jets. However, it seems to be very difficult to tag these spectator jets in the $\gamma\gamma$ environment¹⁴. As rightly remarked by [89], in the γg initiated process, the gluon has in general much less energy than the photon since the gluon distribution inside the photon comes essentially from the low x_g region. This will lead to a larger boost of the $q\bar{q}$ system along the photon direction leading to a system with a much larger rapidity than in the direct processes. Thus the authors of [89] have suggested to apply a cut to reject b 's with large rapidities. It is to be noted that the twice resolved (both photons resolving into gluons), contribution, is negligible at 500 GeV and *a fortiori* at lower energies. We have not included the “2-resolved” contribution.

When the mass of the Higgs is around that of the Z we have another non-negligible background[93]: Z radiation off a fermion pair while the external fermions go down the beam undetected. The Z subsequently decays in $b\bar{b}$. We will not cover this particular case here. We concentrate on two cases: $M_H = 120, 140$ GeV.

Figure 18: The fake $Z \rightarrow b\bar{b}$ in $\gamma\gamma$ through the untagged fermions. Note that the first diagram, $\gamma\gamma \rightarrow Z$, is forbidden by Yang’s theorem.



We have reanalysed the issue of the background suppression and considered different

¹⁴For a more optimistic view, see [64].

$\gamma\gamma$ spectra. To illustrate the fact that the resolved photon problem is much less severe at lower e^+e^- cms we also take the case of $\sqrt{s_{ee}} = 300$ GeV. We also differ from[89] in the set of cuts. First, instead of a cut on $\cos\theta^*$ we required that both quarks have a transverse momentum such that

$$p_T^b > \max(30 \text{ GeV}, 0.375 M_{b\bar{b}}) \quad (8.3)$$

with $M_{b\bar{b}}$ the invariant mass of the $b\bar{b}$ system. To reduce the resolved photon contribution we have applied cuts on the reconstructed energy fractions of the initial γ or g , x_g^{\min} and x_g^{\max} .

$$x_g = \frac{1}{\sqrt{s_{ee}}} \left((E_b + E_{\bar{b}}) \pm \sqrt{(E_b + E_{\bar{b}})^2 - M_{b\bar{b}}^2} \right) \quad (8.4)$$

The resolved contribution has on average a much smaller x_g^{\min} and a larger x_g^{\max} . We have therefore cut on x_g^{\min} and x_g^{\max} and have found that the optimised values for the cuts were

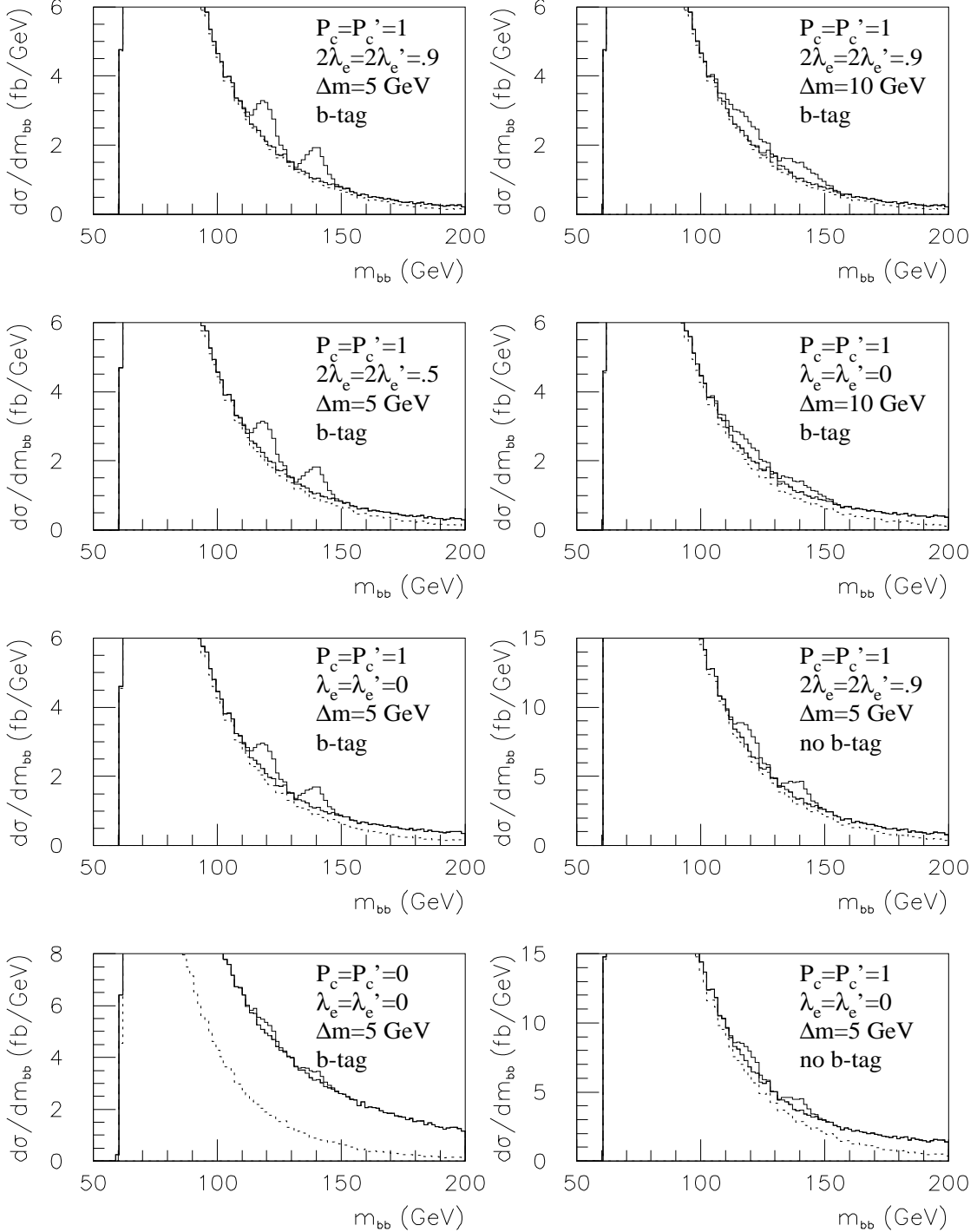
$$x_g^{\min} > \sqrt{\widetilde{M}_{b\bar{b}}^3 / y_{\max}} ; \quad x_g^{\max} < \sqrt{y_{\max} \widetilde{M}_{b\bar{b}}} ; \quad \widetilde{M}_{b\bar{b}} = M_{b\bar{b}} / \sqrt{s_{ee}} ; \quad y_{\max} = \frac{x_0}{1 + x_0} = 0.83 \quad (8.5)$$

For the gluon distribution inside the photon we have taken the GRV[94] parameterisation with $Q^2 = (60 \text{ GeV})^2$. This Q^2 is such that $Q^2 \sim (M_H/2)^2$. We would like to point out that the effect of this cut is another lucky strike: besides allowing to get rid of large rapidities it improves on the rejection of the $J_Z = 2$ from the *direct* $b\bar{b}$ process. This is so because it forces the two photons to have equal energies. Therefore, even if no electron polarisation were available and if $P_c = P'_c$, each of the colliding photons will have the same degree of polarisation (Eq. 3.6) hence providing a dominant $J_Z = 0$ setting. This is in fact the message that Fig. 6b conveys.

Moreover, we emphasize the importance of the resolution on the invariant $b\bar{b}$ mass. To simulate the resolution we have introduced a Gaussian smearing onto the Higgs signal. We consider two values for the resolution: $\Delta M = 5$ GeV and $\Delta M = 10$ GeV. The conclusions depend critically on the would-be achieved resolution.

The issue of b -tagging was also investigated. We have generated both $c\bar{c}$ and $b\bar{b}$ final states, considering two different possibilities: no b -tagging and a realistic efficiency of $\epsilon_b = .47$ and $\epsilon_c = .11$ as would be the case with a micro-vertex detector with a modest performance. Our meaning of no b -tagging is that there is a total confusion between b and c only but that the other light flavours cannot be confused. Needless to say that if one has no distinction at all between the flavours the situation is much worse than in the case of no b -tagging (in fact it is hopeless). We applied the single-jet tag strategy[95] which gives a global efficiency of $\epsilon_{b\bar{b}} = .72$ and $\epsilon_{c\bar{c}} = .21$. Probably by the time (or even before) this machine

Figure 19: *The fate of the Higgs resonance at 500 GeV assuming different polarisation settings, resolutions and b-tagging efficiencies. The contribution of the resolved photon is shown as a dashed line.*



is built one could achieve better efficiencies, but it is not clear how these detectors will perform in the $\gamma\gamma$ mode.

Since we need a broad spectrum for the search, with a dominance of the $J_Z = 0$ we will take $P_c = P'_c = 1$ with $2\lambda_e P_c = 2\lambda'_e P'_c \geq 0$ and compare with the case of no polarisation.

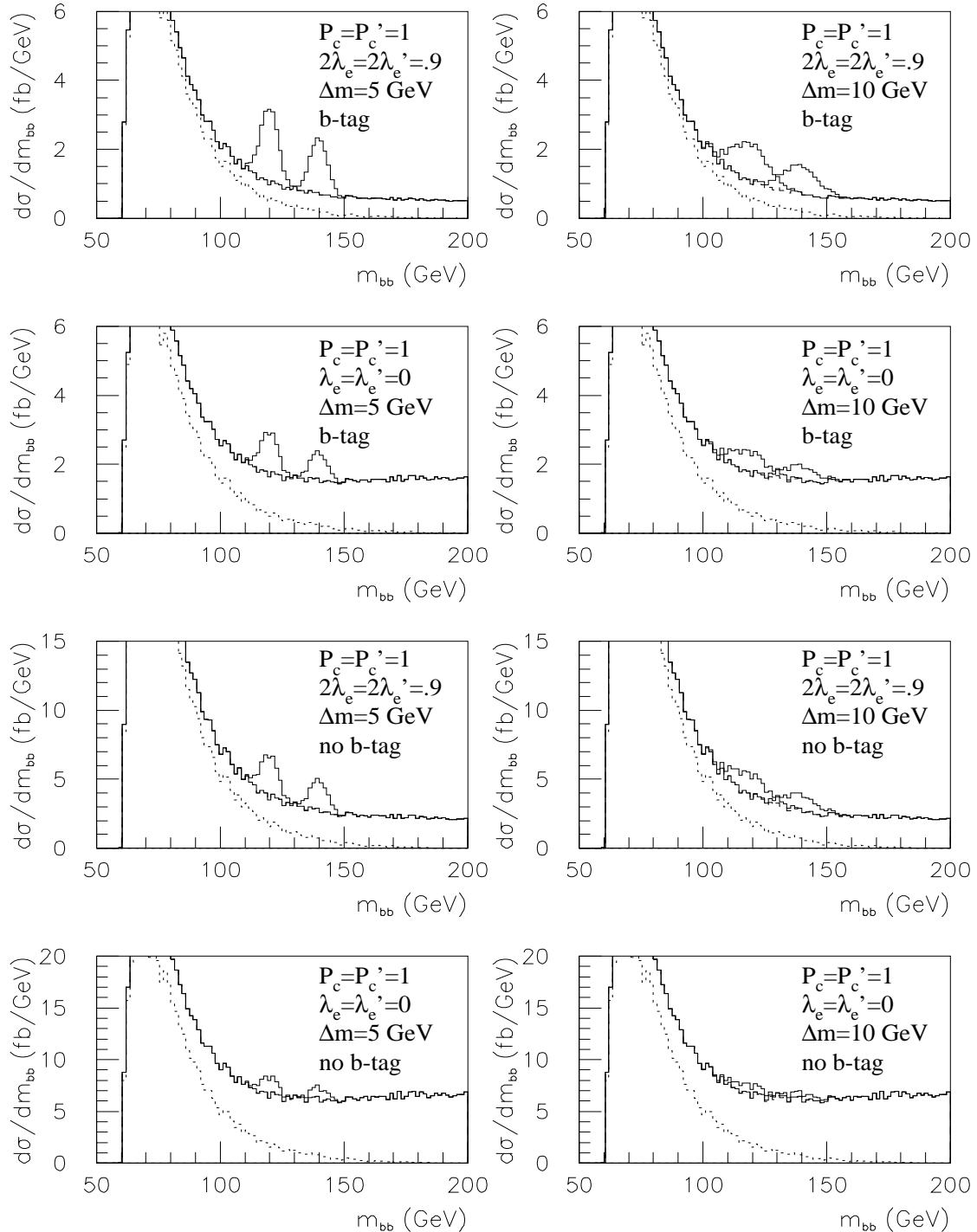
8.1 The case of a 500 GeV e^+e^-

The first remark is that, as shown on Fig. 19, even after the cuts have been applied the bulk of the background is due to the resolved contribution (dotted line). With a good resolution (5 GeV) and a realistic b -tagging efficiency together with 90% longitudinal polarisation for the electrons we obtain a good signal with a significance $\sigma = S/\sqrt{B} = 4.7$ ($\sigma = 5.3$) for $M_H = 120$ GeV ($M_H = 140$ GeV). These numbers and the following values of the significance assume an integrated luminosity of 10fb^{-1} only. This is slightly reduced when only 50% e^- polarisation is achieved. What we find is that there is not much further reduction in the significance if no electron polarisation were available. This result, as explained above, is due to the fact that the cuts filter photons with sensibly the same energies and hence we are in a setting that corresponds to the spectrum in Fig. 6b. In the case of no polarisation at all, which is very unlikely for the lasers, the situation seems hopeless. The change in the resolution from 5 GeV to 10 GeV has a more dramatic effect. Even when the electron polarisations are at 90% the nice peak structure has almost disappeared. Assuming b -tagging, the above significances change to $\sigma = 3.5$ (4.1) for 120 GeV (140 GeV). Further reduction occurs with no linac polarisation.

In the case of no b -tagging at all the event sample increases but the significance of the signal diminishes. A signal is clearly seen with a good resolution and 90% e^- longitudinal polarisation. For $M_H = 120$ GeV we get $\sigma = 3.9$ and even better for $M_H = 140$ GeV ($\sigma=4.7$ (5 GeV)). This significance does not degrade dramatically if no linac polarisation were available. However, with a resolution of 10 GeV even with optimum polarisation the situation is desperate.

To conclude, we stress the primary importance of aiming at having a good resolution. The polarisation settings seem to be achievable without much problem since an excellent degree of e^- longitudinal polarisation is not absolutely essential, though helpful. Good (present-day LEP performances) b -tagging must be provided. In fact, a good μvx could even help in a better reconstruction of the invariant $b\bar{b}$ mass. It rests to see how a μvx would perform in the unusual environment of the laser scheme.

Figure 20: *The fate of the Higgs resonance at 300 GeV assuming b-tagging and different resolutions. The dashed line shows the resolved contribution.*



8.2 The case of a 300 GeV e^+e^-

Here the situation is far better: see Fig. 20. This is mainly because the resolved contribution has dropped. With 90% longitudinal electron polarisation and 5 GeV resolution we obtain beautiful peaks. These peaks are still very clear with no electron polarisation. Even when c and b are totally confused, provided one has a good resolution, the resonant structure is evident even when the electrons are unpolarised. In this non optimal case we obtain $\sigma = 4.1$ for $M_H = 120$ GeV (with $\int \mathcal{L} = \infty / \{ |^{-\infty} \text{ only}\}$). Taking a larger resolution (10 GeV) the signal has an excellent statistical significance if a very good degree of longitudinal polarisation for the e^- ($2\lambda_e = 2\lambda'_e = 90\%$) can be achieved together with b -tagging. In the case of no b -tag the same polarisation setting and $\Delta M = 10$ GeV leads to a good significance $\sigma = 7.2$ (6.5) for $M_H = 120$ GeV (140 GeV). Unfortunately, even at 300 GeV, the IMH is lost if no b -tag is provided and if the resolution is large without much electron polarisation. But this is the most pessimistic scenario.

In view of these results it is important to realise that at 300 GeV e^- polarisation is a top priority and that we could, in this case, make do with a not so good resolution, $\Delta M = 10$ GeV. At 500 GeV, we could not, in all cases, afford having such values of the resolution. On the other hand, although polarisation is very helpful it is not as important as at lower energies. This is easily explained by the fact that as we go higher in energy the contribution of the resolved photon becomes more and more important. This contribution is not killed by the choice of polarisation as is the direct contribution whose yield is more important at lower energies.

9 Non resonant Higgs production: the importance of the WWH process

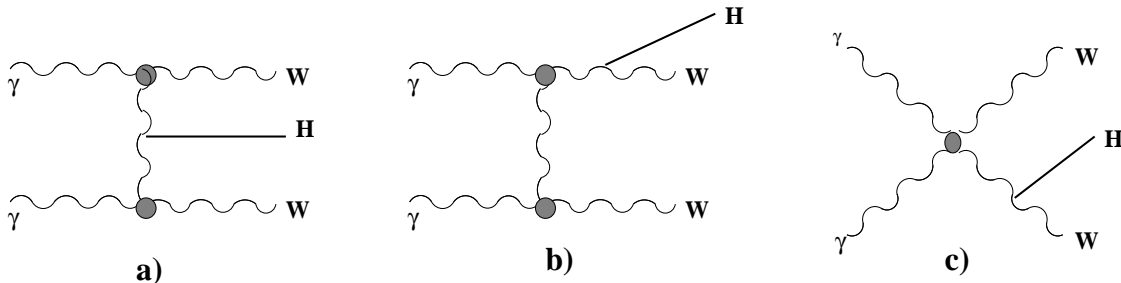
9.1 Comparison with other Higgs production mechanisms

Unless one chooses a very monochromatic spectrum designed to cover a narrow band around the mass of the IMH, the nice resonance structure of the Higgs is not so conspicuous. As we have seen, this production suffers from large backgrounds at 500 GeV and for higher energies it seems extremely laborious if not impossible to extract a signal. For a Higgs heavier than about 400 GeV at $\sqrt{s_{ee}} \geq 500$ GeV, it seems to be impossible to unravel a peak formation in the most favourable channel: ZZ . As in the case of the IMH, the situation gets worse as the e^+e^- energy increases. It is, therefore important to

see whether other mechanisms for Higgs production are possible and survive over their corresponding backgrounds. Once again, the backbone WW reaction should provide for an efficient Higgs production. The fact that the WW cross-section is so large and that the Higgs couples preferentially to the weak bosons, one expects WW to trigger a good Higgs yield. We have found [81, 3] that at high enough energy this is one of the most important reactions for Higgs production even when compared to the usual e^+e^- mode. We concentrate essentially on the case of the IMH.

We find that for a Higgs mass of 100 GeV we obtain a cross-section, before folding with

Figure 21: *Typical diagrams for WWH production in $\gamma\gamma$. Diagram a) is of the fusion type.*



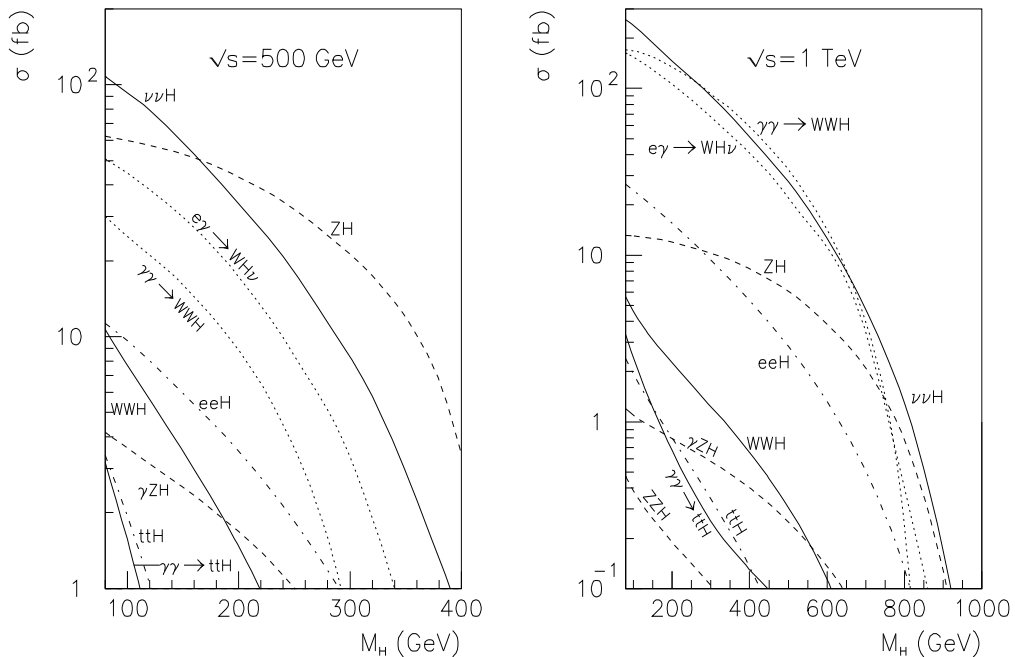
the photon luminosity spectrum, of about 20fb at $\sqrt{s_{\gamma\gamma}} = 500$ GeV. The WWH cross-section quickly rises to yield $\simeq 400\text{fb}$ at 2 TeV (for $m_H = 100$ GeV). The importance of this mechanism at TeV energies is best illustrated by contrasting it with top pair production (see Fig. 2). For $m_H = 100$ GeV and $m_t = 130$ GeV the two processes have the same threshold energy and lead to the same final state (IMH decays predominantly into $b\bar{b}$). While at $\sqrt{s_{\gamma\gamma}} \simeq 500$ GeV top pair production is almost two-orders of magnitude larger than WWH , the latter which is a third order process is twice as large at 2 TeV. Nonetheless, the WWZ cross-section is about an order-of-magnitude larger than the “IMH- WWH ” for all centre-of-mass energies. Another non resonant Higgs mechanism that has recently been suggested [96] is Higgs production in association with a top pair in analogy to $t\bar{t}H$ production in hadron machines. Unfortunately, the IMH yield does not exceed $1 - 3\text{fb}$ (for $m_t \leq 150$ GeV). The $t\bar{t}H$ cross-section decreases very slowly with $\sqrt{s_{\gamma\gamma}}$.

To see the importance of this process we first compare it, before folding with a luminosity spectrum, with other Higgs processes that take part in the e^+e^- environment (including $e\gamma$ and of course $\gamma\gamma$ modes). This is shown in Fig. 22. For e^+e^- the standard dominant reactions are the Bjorken process and the WW fusion processes. Other e^+e^- processes (Higgs in association with two vector bosons) have been studied but they yield smaller cross-sections[95, 12].

An efficient mechanism for Higgs production in an $e\gamma$ environment is through $e\gamma \rightarrow \nu WH$ [97, 98]. Comparing at the same $\sqrt{s}_{\gamma\gamma}$ and $\sqrt{s}_{e\gamma}$ centre-of-mass, in the *IMH* case, the cross-sections for WWH start becoming larger than those of $e\gamma \rightarrow \nu WH$ for energies around 700 GeV. At lower energies the $e\gamma$ mode benefits from a larger phase space (see Fig. 1 and Fig. 22).

In the *IMH* case, taking for illustration $M_H = 80$ GeV, at 500 GeV, $\sigma(\gamma\gamma \rightarrow WWH) \simeq$

Figure 22: *Comparison between different mechanisms of Higgs production in e^+e^- , $e\gamma$ and $\gamma\gamma$ at 500 GeV and 1 TeV. No folding with the luminosity spectrum has been performed. e^+e^- processes are, in the figure, only characterised by their final state.*



30fb which is by only a factor 2 smaller than $\sigma(e\gamma \rightarrow \nu WH)$ and a factor 3.3 compared to the dominant WW fusion process in e^+e^- . On the other hand, $\sigma(\gamma\gamma \rightarrow WWH)$ is larger than all the VVH ($WWH, ZZH, ZH\gamma$) processes in e^+e^- by at least a factor 3[95]. Higgs production from top bremsstrahlung ($t\bar{t}H$ final state), either in e^+e^- [99] or $\gamma\gamma$ [96] is abysmally small. At 1 TeV our $\gamma\gamma \rightarrow WWH$ process becomes very comparable to $e\gamma \rightarrow \nu WH$ and is only about a factor 2 smaller than the dominant WW fusion process in e^+e^- . Nonetheless, the fact that in $\sigma(\gamma\gamma \rightarrow WWH)$, unlike the WW fusion in e^+e^- or the corresponding one at $e\gamma$, all final particles can be observed or reconstructed (hence alleviating the lack in energy constraints) makes this reaction worth considering especially at a TeV $\gamma\gamma$ collider. But of course, this statement tacitly assumes an ideal monochromatic $\gamma\gamma$ collider. We will now turn to more realistic photon luminosity spectra. Before so doing, it is worth pointing out that an almost equal number of H is produced in the

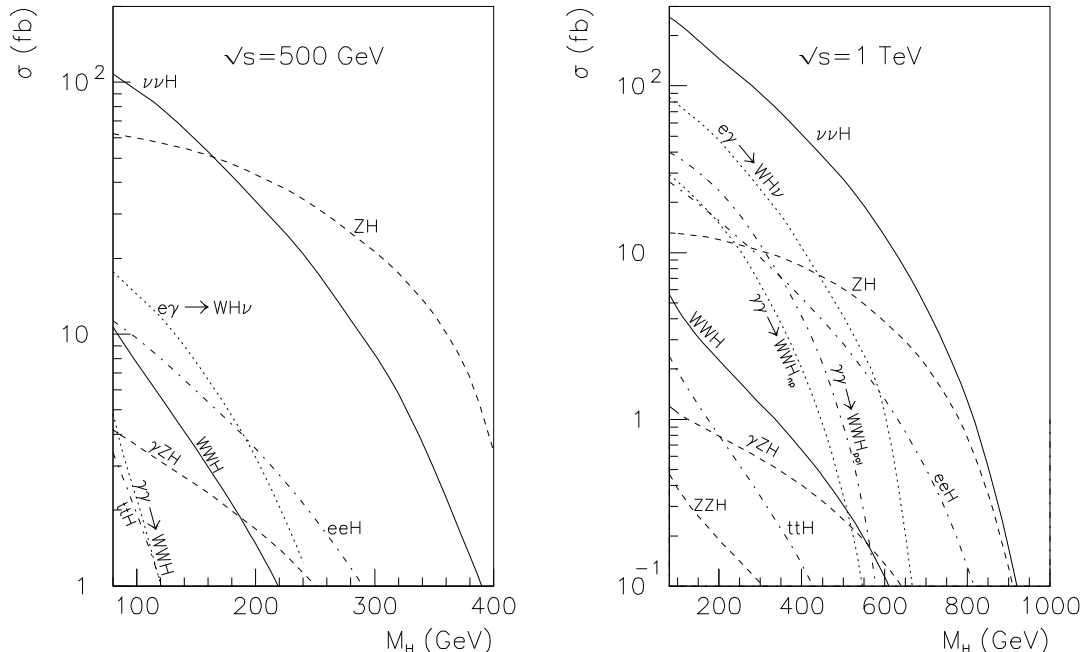
$J_Z = 0$ or the $J_Z = 2$ with both W being essentially transverse.

9.2 Folding with the luminosity spectra

With $\sqrt{s}_{ee} = 500$ GeV, the inclusion of the spectra changes the WWH yield significantly due to the fact that the maximum $\sqrt{s}_{\gamma\gamma} \simeq 400$ GeV leaves a small phase space for the IMH . Even when we choose the polarisation of the primary beams to give the peaked $J_Z = 2$ dominating spectrum, the cross-section does not exceed 4fb and is therefore almost two orders of magnitude below the WW fusion process in the e^+e^- mode and an order of magnitude smaller than νWH production in the $e\gamma$ mode (See Fig. 23).

The situation is much more favourable at 1 TeV. Up to $M_H \simeq 300$ GeV this mode

Figure 23: *As in the previous figure but where we have included the luminosity spectra. For all $\gamma\gamma$ and $e\gamma$ processes we have considered a broad spectrum with unpolarised laser and e^- . In the case of WWH at $\gamma\gamma$ we also show the effect of a “ $J_Z = 0$ -dominated” spectrum (see text).*



produces almost twice as many Higgses as the conventional Bjorken process. For $M_H = 100$ GeV and choosing a setting which gives a “0-dom”, we obtain ~ 37.5 fb (compared to 37.2 in the “2-dom”) and 26.3 fb with no polarisation for the primary beams. The advantage of a polarised spectrum is undeniable. The two cross-sections for νWH (in $e\gamma$) and $H\nu\nu$ (in e^+e^-) are respectively about 2 and 5 times larger in the IMH case. A comparison between the variety of Higgs production modes in the NLC(1TeV) environment is shown in Fig. 23 which clearly brings out the importance of WWH in $\gamma\gamma$.

Considering the large WWZ yield, b tagging is almost necessary for the IMH search. Another dangerous background, even with b -tagging is due to top pair production: $\gamma\gamma \rightarrow t\bar{t} \rightarrow W^+W^-b\bar{b}$. For instance, at $\sqrt{s}_{ee} = 500 \text{ GeV}$, this is about two-orders of magnitude larger than $WWH_{\rightarrow b\bar{b}}$. Fortunately, one can eliminate this huge contamination by rejecting all those WWH events where the simultaneous cuts on the invariant mass of the two Wb is such that the Wb does not reconstruct the top mass (within 15 GeV)

$$\begin{aligned}
m_t - 15 \text{ GeV} < M_{W+b} < m_t + 15 \text{ GeV} \quad \text{and} \quad m_t - 15 \text{ GeV} < M_{W-b'} < m_t + 15 \text{ GeV} \\
\text{or} \\
m_t - 15 \text{ GeV} < M_{W+b'} < m_t + 15 \text{ GeV} \quad \text{and} \quad m_t - 15 \text{ GeV} < M_{W-b} < m_t + 15 \text{ GeV}
\end{aligned} \tag{9.6}$$

The reason we try both combinations W^+b or W^+b' is that we do not want to rely on charge identification, for the b especially, which necessarily entails a reduction in the b sample (and hence our signal). A good vertex detector should be sufficient ¹⁵. In carrying the vetoing in our Monte-Carlo sample we made the Higgs decay isotropically in its rest frame. The effective loss at 500 GeV is about a mere 0.3fb while at 1 TeV, where we have a “healthy” cross-section, the percentage loss is only about 4% for all choices of the polarisation. Table 4 shows the cross-sections taking a Higgs mass of $M_H = 100 \text{ GeV}$ with $Br(H \rightarrow b\bar{b}) \sim 80\%$, $|\cos\theta| < 0.8$ for all angles between two particles and assuming $m_t = 150 \text{ GeV}$.

Once the “faked” top events have been dealt with, the $WWZ_{\rightarrow b\bar{b}}$ do not bury the signal (for $M_H \sim M_Z \pm 10 \text{ GeV}$). These WWZ can be further reduced by judiciously switching the “2-dom.” setting, both at 500 GeV and at 1 TeV. Although at the former energy the event rate is probably too small to be useful, at 1 TeV, in the “2-dom.”, we have, after including the cuts and the branching fractions into b , 30fb of signal compared to 60fb from WWZ . With one W , at least, decaying into jets and not taking into account decays into τ ’s, the number of WWH with the contemplated integrated luminosity of $\mathcal{L} = 60 \text{ fb}^{-1}$ will be about 1400 events. Even if one allows for an overall efficiency of 50% this is a very important channel to look for the Higgs. There is one background which we have not considered, the $W^+W^-b\bar{b}$ final state with $b\bar{b} \rightarrow W^+W^-$ as a sub-process. We expect this to be negligible once one puts a high p_T cut on both b ’s and require $m_{bb} \sim M_H$.

¹⁵We have not tried to cut the $t\bar{t}$ by demanding that $m_{b\bar{b}} = M_H \pm 10 \text{ GeV}$, as the cut above is very efficient. Moreover, based on our previous analysis of WWH in e^+e^- [95], the Wb cut was by far more efficacious.

Table 4: *Cross-section in fb for three-boson (and $t\bar{t}$) productions with $M_H = 100\text{GeV}$ and $m_t = 150\text{ GeV}$. The $WW\gamma$ includes a p_T^γ cut of 20GeV at 500 GeV and 40GeV at 1TeV . “non-top” means all Higgs events with Higgs decaying into $b\bar{b}$ and where the simultaneous Wb invariant mass has been applied as explained in the text. “direct” means that we have not taken into account top pairs produced through the gluons inside the photon, i.e., the “resolved” photons contribution has not been considered.*

	500 GeV			1 TeV		
	non pol.	0-dom.	2-dom	non pol.	0-dom.	2-dom
WWH	1.0	1.7	2.24	26.3	37.5	37.2
$WWH_{\rightarrow b\bar{b}}$	0.8	1.4	1.8	21	30	29.8
$WWH_{\rightarrow b\bar{b}}$ “non-top”	0.7	1.1	1.5	20.2	28.9	28.7
WWZ	24.2	55.3	36.9	342	473	408
$WWZ_{\rightarrow b\bar{b}}$	3.6	8.3	5.53	51.3	70.9	61.2
$WW\gamma$	205	321	272	483	592	560
$t\bar{t}$ (“direct”)	207	458	250	620	525	687

To conclude, this new mechanism of Higgs production in a $\gamma\gamma$ mode of $\sim 1\text{ TeV}$ e^+e^- collider is a very promising prospect. The oft discussed intermediate mass Higgs production, as a narrow resonance in $\gamma\gamma$ collisions, relies on a spectrum which is peaked around the Higgs mass in a $J_Z = 0$ dominated setting. The extensive study in [16] finds that with $\int \mathcal{L}_{ee} = 10\text{fb}^{-1}$, one expects between about 500 Higgs events for $M_H \sim M_Z$ to about 600 events for $M_H \sim 140\text{ GeV}$. This is 2 – 3 times more than what we get with WWH at $\sqrt{s}_{ee} = 1\text{ TeV}$ if only $\int \mathcal{L}_{ee} = 10\text{fb}^{-1}$ is assumed. However, as we have stressed repeatedly, the resonance scheme means that the available $\gamma\gamma$ invariant mass covers a very narrow, and in the case of the *IMH*, low range of energies. Hence, while allowing a precise study of the $H\gamma\gamma$ coupling it forbids the study of a wealth of interesting processes in the $\gamma\gamma$ mode of the NLC. Higgs detection through WWH at 1 TeV will be one aspect among a variety of studies of weak processes (WW, ZZ, WWZ, \dots etc). At 500 GeV this mechanism does not offer much prospect with a nominal integrated luminosity of 10fb^{-1} . However, in this case we have shown that with a broad spectrum -provided optimal values for the mass resolution, the polarisation and the tagging efficiencies are achieved- the Higgs can be observed through the resonant mechanism. Therefore, as far as the IMH is concerned, it will always be possible to discover the Higgs in a $\gamma\gamma$ machine without having recourse to the peaked-narrow spectrum. The latter, of course, assumes a knowledge of the Higgs mass.

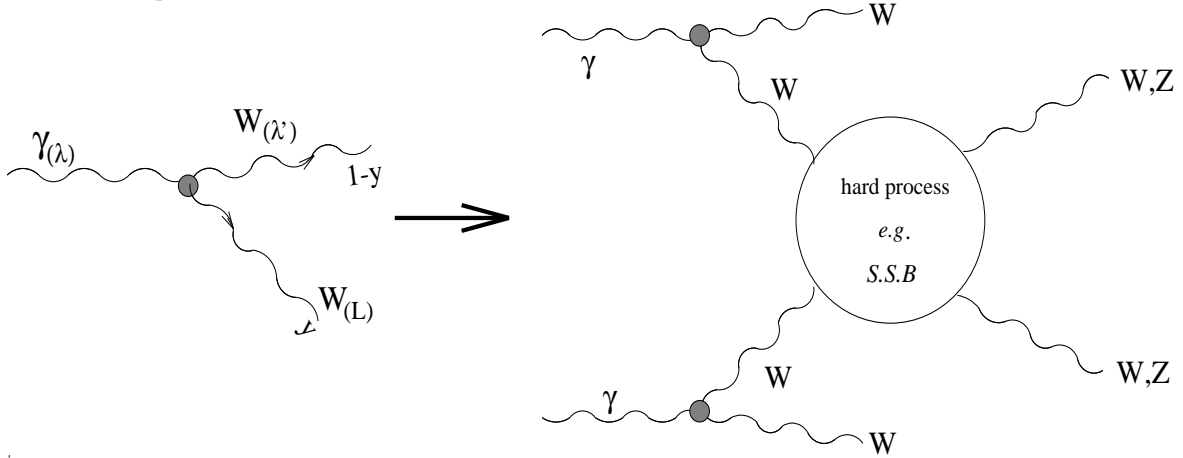
10 The W content of the photon and the prospect of WW scattering in the $\gamma\gamma$ mode

We have seen that with W pair production we could investigate the symmetry breaking sector of the \mathcal{SM} through, for instance, the chiral Lagrangian parameterisation. This reaction, together with the ZZ process, could be regarded as the testing ground of possible rescattering effects in $WW \rightarrow VV$ ($VV = WW, ZZ$) that originate from the symmetry breaking sector. Unfortunately, at high energies, *i.e.*, at high VV invariant masses, where the effect of the New Physics would be most evident, one has to fight extremely hard against the pure gauge sector that produces large cross sections for transverse W and Z . At the pp collider(s) and in the usual e^+e^- mode one often relies, at TeV energies, on WW scattering processes. Ideally, the symmetry breaking sector would be most efficiently probed through the reactions $V_L V_L \rightarrow V_L V_L$ but then one needs a source of longitudinal vector bosons. Lacking such a source, the $V_L V_L$ subprocesses are embedded in a large class of diagrams which, not only have not much to do with the physics one wants to get at, but also complicate the computational task. It has become customary to rely on some approximation [100, 101, 102, 103, 104, 105], with various degree of accuracy, whose aim is to isolate the interesting subprocess and convolute the cross section with an effective luminosity of longitudinal vector bosons. The latter are regarded as partons or constituents of the light fermion. The approximation (effective W approximation or EWA [100, 101, 102, 103, 104, 105]) is really an adaptation of the Weiszäcker-Williams approximation[13], the effective photon approximation (EPA). Still, in the context of non-Abelian QCD, this has to be paralleled with the splitting or structure function language. The latter analogy is more to the point for the application to the $\gamma\gamma$ collider where we would like to find out the splitting of the photon into W^\pm that emanates solely from the non Abelian part (as in $g \rightarrow gg$). A novelty, here, being of course the longitudinal W content (see Fig. 24).

An expression for the longitudinal W content inside the photon has been derived [97]. It was found that the photon has a relatively larger W_L component than the electron. In view of this encouraging result, it has been pointed out that one could hope[106, 107], at TeV energies, to study WW scattering more efficiently than in the e^+e^- mode. Here, we will argue that great care should be exercised in the use of the expression derived in[97] to applications to other processes. We will then present a new set of polarised structure functions of the W_L content of the photon. In a nut-shell, we have identified a Q^2 dependent part in the splitting function that is not interpreted as such in [97].

Having in view the extraction of the longitudinal W component of the photon, it is

Figure 24: A photon of helicity λ “splits” into a longitudinal W that carries a fraction y of its momentum and a spectator W with helicity λ' . The longitudinal W then takes part in the hard process.



worth recalling the extraction of the analog component of the light fermion. The problem in the fermion case is simplified because it is possible to find processes that are described by a single diagram. This diagram is then amenable to an interpretation in terms of structure functions. In the all-bosonic sector and especially when one is dealing with the longitudinal vector bosons it is difficult to isolate a single diagram since it is not gauge invariant by itself. As a consequence one has to tackle the problem of unitarity first and extract the part of the single diagram which is well behaved and reflects the dominant contribution of the whole set of diagrams.

Another aspect common to both the fermion and the photon splittings is that the validity of the effective boson approximation exploits the fact that the parton virtuality is small (so that its propagator is large) and that the subprocess (the hard scattering part) has a smooth limit in the small virtuality. The smooth mass limit in Abelian QED exists and explains the success of the EPA. Unfortunately, the off-shell hard scattering diagrams in the electroweak theory do not have a “smooth mass limit” and are not element of the S -matrix. This is especially acute for the “longitudinal” states where the very delicate gauge theory cancellations are no longer operative. This problem of the virtuality versus unitarity that is present in the fermion case of the EWA is also unavoidable in the photon to W splitting. This first aspect of the unitarity problem has to do with the bad high energy behaviour of the off-shell hard scattering process [108]. In the photon case, there is another potential complication with unitarity which concerns the splitting part and has to do with the spectator W . Take a polarised photon that splits into two W ’s. The case where both W are transverse, $\gamma \rightarrow W_T W_T$, should be quite similar to the gluon

splitting into two gluons, P_{GG} [109]. This component has not much incidence on what we want to study, the \mathcal{SB} mechanism. As for the W_L component, it consists of two parts: one when the spectator W is transverse, $\gamma \rightarrow W_L(W_T)$ and one when it is longitudinal ($\gamma \rightarrow W_L(W_L)$). The extraction of the latter poses more problems. The reason is the following. In the diagrammatic identification of the spectator W_L , this is an on-shell external W_L . As with most processes that involve vector bosons, the problem of unitarity is more severe with W_L than with W_T . Subtle cancellations between different diagrams have to take part before arriving at a unitary result. Therefore, in general, even when one isolates the single diagram that should capture the essence of the EWA (t -channel diagram), there is some “kneading” to do. One should first subtract any potential ultraviolet part that it may contain. When this is done, the “universality” of the remaining “collinear-sensitive” term is not so obvious.

In[97] the W_L content of the photon is extracted, in a heuristic way, by studying the process $\gamma W_L \rightarrow HW$. From the high-energy asymptotic cross section of this process

$$\sigma(\gamma W_L \rightarrow WH) \xrightarrow{M_W^2 \ll s, M_H^2} \frac{\pi \alpha^2}{s_w^2 M_W^2} \left(1 - \frac{M_H^2}{s}\right) \left\{ 1 + \frac{M_H^4}{2s^2} \left(-2 + \log \frac{(s - M_H^2)^2}{s M_W^2} \right) \right\} \quad (10.1)$$

the following W_L distribution inside the photon is identified

$$D_{W_L/\gamma}(y) = \frac{\alpha}{\pi} \left\{ \frac{1-y}{y} + \frac{y(1-y)}{2} \left(-2 + \log \frac{s(1-y)^2}{M_W^2} \right) \right\} \quad (10.2)$$

where y is the momentum fraction of the photon transferred to the W (see Fig. 24). Note that in this result, one has summed over all helicity states of the spectator W .

We have rederived the asymptotic form $\sigma(\gamma W_L \rightarrow WH)$, our aim being to isolate the different helicity states of the spectator W and to check that, indeed, there is a subtle cancellation in the W_L spectator (the outgoing W). In order not to unduly complicate the cancellation mechanism, we have chosen (once again) to work in the non-linear gauge since we keep the same number of diagrams as in the unitarity case while the W propagator is as in the t’Hooft-Feynman gauge. Power counting (in the ultraviolet sense) is trivial and shows that when the would-be spectator W is transverse, taking only the t -channel diagram suffices to reproduce the leading term in the cross section. When the spectator W is longitudinal it is crucial to subtract a part that corresponds to the annihilation diagram in order not to violate unitarity. For the transverse spectator W one could then identify

$$D_{W_L/\gamma\lambda}^{(W_\lambda)}(y) = \frac{\alpha}{\pi} \frac{1-y}{y} \quad (10.3)$$

For this part we arrive at the same identification as [97]. We note that in this case the photon transfers its helicity, λ , to the spectator W . The contribution from the W with the opposite helicity, $-\lambda$, is non leading. The important observation is that $D_{W_L/\gamma_\lambda}^{(W_\lambda)}(y)$ is of exactly the same form and strength (allowing for the overall strength of the $W e \nu_e$ coupling) as the W_L distribution inside the electron:

$$D_{W_L/e}^{(W_\lambda)}(y) = \frac{\alpha}{4\pi s_W^2} \frac{1-y}{y} \quad (10.4)$$

This is already a hint that $D_{W_L/\gamma_\lambda}^{(W_\lambda)}(y)$ qualifies as a universal distribution. The remaining (W_L) contribution can be read-off from the M_H^4 term in Eq. 10.1. If one makes the same identification as the authors of ref. [97] one would arrive at

$$\widetilde{D}_{W_L/\gamma_\lambda}^{(W_L)}(y) = \frac{\alpha}{\pi} \frac{y(1-y)}{2} \left(-2 + \log \frac{s(1-y)^2}{M_W^2} \right) \quad (10.5)$$

We would like to argue that this expression could be misleading when applied to other processes. First of all, it does not have the $y \leftrightarrow (1-y)$ symmetry as it should for $\gamma \rightarrow W_L W_L$. In fact, the argument of the logarithm, which is precisely the non-symmetric part, depends on the kinematics and the nature of the hard sub-process. The argument of the logarithm comes solely from integrating over the virtuality $Q^2 = M_W^2 - (k_\gamma - k_W^{spec.})^2$; where $k_W^{spec.}$ is the momentum of the spectator W and k_γ that of the incoming photon. It is best to write the logarithm in Eq. 10.1 as

$$\log \left(\frac{(s - M_H^2)^2}{s M_W^2} \right) = \log \left(\frac{Q_{max.}^2}{Q_{min.}^2} \right) \quad (10.6)$$

where $Q_{max.,min.}^2$ are the minimum and maximum value of Q^2 . For the validity of the EWA in the photon splitting we have warned that the virtuality must be very small, so that in the identification Q^2 should be kept small. We note that our observation has some similarities with the so-called modified EPA [110]. We thus suggest to replace

$$\log \left(\frac{Q_{max.}^2}{Q_{min.}^2} \right) \longrightarrow \log \left(\frac{Q^2}{Q_{min.}^2} \right) \longrightarrow \log \left(\frac{Q_p^2}{M_W^2} \right) \quad (10.7)$$

where as a further approximation we have taken Q_p^2 to be a typical Q^2 of the hard subprocess under study. Therefore, we arrive at the approximate parameterisation with a fixed Q_p^2

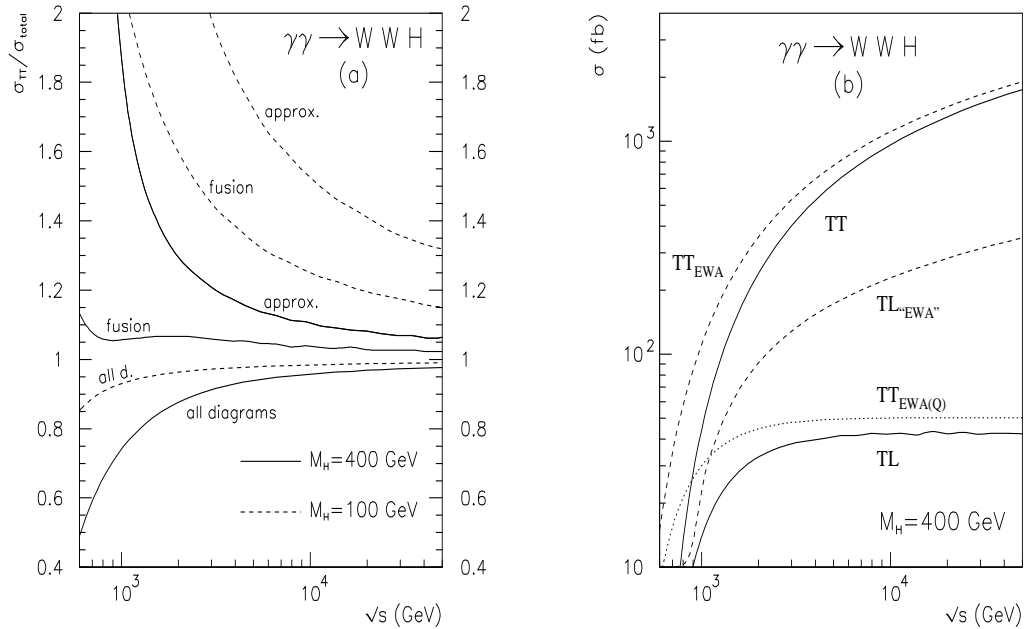
$$D_{W_L/\gamma_\lambda}^{(W_L)}(y, Q_p^2) = \frac{\alpha}{\pi} \frac{y(1-y)}{2} \left(-2 + \log \frac{Q_p^2}{M_W^2} \right) \quad (10.8)$$

Because of the various subtleties involved in the extraction of the W component inside the photon it is worth reconsidering the issue by studying another process. We have looked

at $\gamma\gamma \rightarrow W^+W^-H$. We leave the full details for another paper and only present the main points.

To be able to formulate the problem in terms of a distribution function, we will consider

Figure 25: a) The ratio $\sigma_{TT}/\sigma_{total}$ in the case $M_H = 400$ GeV (full line) and $M_H = 100$ GeV dashed line. The total refers to the exact numerical result including all the diagrams and summing over all polarisations. The lines “all diag.” are for the exact TT result. The fusion refers to taking only the fusion diagrams with the W being transverse while the “approx.” curves are the approximate analytical expression for TT (see text). b) Comparing the exact TT and TL cross sections for WWH with $M_H = 400$ GeV with the result of using the structure function. For TL we show the result of taking the structure function with $Q^2 = M_H^2$ (EWA(Q^2)) as well as the harder distribution “EWA” [97].



the particular case of a heavy Higgs of mass 400 GeV that couples almost exclusively to the longitudinal vector bosons. We recall that $\gamma\gamma \rightarrow W^+W^-H$ cross section is dominated, at high energy, by the production of both W being transverse. W_TW_LH represents a small fraction, about 10% for a Higgs mass of 400 GeV and for $\sqrt{s_{\gamma\gamma}} > 2$ TeV. The LL contribution is dismal. This is a good sign since the contribution that requires the most delicate cancellation between the different diagrams, W_LW_LH , is the smallest[3]. Therefore, at high energy and in the case of a heavy Higgs (that we expect to couple almost exclusively to the internal quasi-real longitudinal W 's) we can afford to keep only the fusion diagrams and restrict ourselves to the transverse modes of the final W . We find that this is indeed the case (see Fig. 25a). At energies around 2 TeV, Fig. 25a shows

that our expectation is borne out by the result of the exact calculation. Indeed, we see that the TT are dominating and that taking only the TT fusion diagrams reproduce the total cross section extremely well. Note, however, that there is a slight overestimate of the cross section by only keeping the fusion diagrams. In this figure we have plotted the ratio $\sigma_{TT}/\sigma_{total}$ where σ_{total} is the exact result (all diagrams included) with all final polarisation summed over. Fig. 25a shows also the case of a light (IMH) Higgs where we learn that, as expected, the approximation of keeping only the fusion diagrams is not as good especially at lower energies. Nonetheless, the TT cross section dominates (with all diagrams included) and almost reproduces the total cross section.

Having isolated the dominant topology, the fusion diagrams, it becomes easier to find an analytic approximation for $W_T W_T H$. The analysis is quite simple in the non linear gauge. By neglecting non-leading M_W and P_T^W terms we find, independently of the Higgs mass,

$$\sigma_{\gamma\gamma \rightarrow W^+ W^- H} \sim \sigma_{\gamma\gamma \rightarrow W_T W_T H} \sim \frac{\alpha}{4\pi \sin \theta_W^2} \left\{ \left(1 + \frac{M_H^2}{s}\right) \ln \frac{s}{M_H^2} - 2\left(1 - \frac{M_H^2}{s}\right) \right\} \sigma_{\gamma\gamma \rightarrow W^+ W^-} \quad (10.9)$$

We show in Fig. 25a how well this analytic approximation of the fusion diagrams performs (σ_{total} once again is the exact result). We see that for the 400 GeV Higgs the approximation is quite good, already at 2 TeV it is within 10% of the exact result and gets better with increasing energy. For the IMH, only the order of magnitude is reproduced by using the approximation.

In fact, once we have brought the problem down to the fusion diagrams and the transverse external W 's, the situation is quite similar to the study of heavy Higgs production in $e^+ e^- \rightarrow \nu\bar{\nu} H$ which is a pure fusion process[111].

Of course, the above formula 10.9 being for transverse external W we can only extract the part of the structure function that corresponds to a transverse spectator W : $D_{W/\gamma\lambda}^{(W_\lambda)}$. It is easy to obtain that the leading term is indeed given by Eq. 10.3. Therefore, this gives more credence to the fact that this part can be considered universal. We show in Fig. 25b how good the use of the structure function with the transverse spectator W is by comparing it with the *exact* $W_T W_T H$. We have not attempted to extract the $W_L W_T$ part from this process, however we have tried the Q^2 parameterisation suggested above (Eq. 10.8). We have taken the typical $Q_p^2 = M_H^2$ for the hard process since this is the only scale at hand, if we take M_W to be an “infrared” scale. The “ Q_p^2 -EWA” is excellent and reproduces the energy dependence of the cross section very well, this is not the case of the harder distribution suggested in [97] as Fig. 25b makes clear.

As a conclusion we would like to emphasize that care must be taken in applying the

structure function formalism to WW scattering in a $\gamma\gamma$ option. The encouraging aspect is that there is indeed more W_L 's inside the photon than in the electron due to the additional degree of freedom provided by the longitudinal spectator W . Unfortunately, the bulk of the contribution is from the transverse spectator part that has exactly the same distribution as that of the W_L inside the electron. The strength of the latter (W_L inside the e^-) is in fact a little larger than the former (W_L inside the γ) because of the slightly larger $W\bar{e}\nu$ coupling.

An application of the W content inside the photon to models of a strongly interacting Higgs has been done in [112] by taking the very hard distribution, Eq. 10.2. Apart from the choice of the distribution, the most worrying aspect that we foresee is the problem of the expected large background with $4W$ or $WWZZ$ final states[113], all vectors being transverse. We have seen that the production of three vector bosons within the \mathcal{SM} is quite large and growing. Hence we might have to face the same recurring problem, *i.e.*, that of trying to get rid of the annoying gauge transverse sector contribution.

11 Conclusions

The laser induced $\gamma\gamma$ collider at sub-TeV or TeV energies offers a rich and attractive physics program especially as regards the physics of W 's and the concomitant symmetry breaking phenomenon. Such machines are ideal W factories and enviable laboratories for precision tests on the Higgs properties. As we have shown, one should, perhaps, add a slight undertone as concerns W physics. This is because, while we have plenty of cross section as compared to the usual e^+e^- and a host of appealing processes , the preliminary studies indicate that the most interesting part of the W (that has a stronger link to symmetry breaking) has a somehow larger “intrinsic self-background” from the “gauge-transverse” sector than at the usual e^+e^- mode.

Of course, more physics can be done than the aspects we have covered here. For instance, one could mention the search for new particles like those of susy [114, 115] or those that signal a new layer of matter [116, 117] and how these searches could complement those in the e^+e^- mode. The ability to access the $J_Z = 0$ quite naturally is a strong asset, as is the possibility to produce in an almost democratic way any charged particle.

There is, though, still much work to be done in this nascent domain. Leaving aside the technical feasibility, thorough investigations and simulations of the interaction region should be performed. One will have an unusual environment where the backgrounds could be more severe than those we encounter in the usual e^+e^- mode. For instance, we have not addressed the subject of the hadronic cross-section and the minijet problem[118].

Although, at the present time, this problem does not look as dramatic[119, 120] as it first appeared three years ago, it is nonetheless more severe in a $\gamma\gamma$ mode than in the e^+e^- mode of the next linear collider especially at TeV energies[120]. At a $\gamma\gamma$ version of a 500GeV linear collider the situation looks quite “bright”[120]. In any case, one should strive to further reduce any of these backgrounds even at TeV energies or be able to efficiently simulate them. Another potential problem that we have alluded to a few times, is the purity of the $\gamma\gamma$ state and the rejection of the soft electrons which could also, through multiple interactions with the laser beam, lead to further disruption. The incidence, on the design of a dedicated detector, of a large magnetic field to sweep these unwanted relicts deserves an urgent and critical clarification.

Although, at present, one does not have the ideal laser that embodies all the requirements (high power, high repetition, short pulse length at the appropriate frequencies) [52, 16] for the conversion of the e^+e^- NLC into the $\gamma\gamma$ mode, there is all reason to believe that such a device will be available. Free Electron Lasers (FEL)[16] seem to be a hopeful prospect. Because of all these critical machine/detector issues it would very gratifying to have an unexpensive test-machine to convince us of the feasibility of the scheme. It has been suggested[16] to build a low energy prototype.

Once the “shadows” associated with the technical feasibility have been dispelled, the physics program that such a collider offers are so enthralling that every effort should be made to turn this “bright” idea into practice. Also, one can not help over-emphasizing that such a scheme will be most beneficial as part of a package with a normal mode of the e^+e^- and that it is the combination and the complementarity of the two modes which will make the NLC a dream machine.

Acknowledgments

We have greatly enjoyed our lengthy and valuable discussions with Ilya Ginzburg, George Jikia and Valeri Serbo. On QCD issues, we were lucky to have Patrick Aurenche and Jean-Philippe Guillet a few doors away from our offices. We acknowledge helpful discussions with Michel Fontannaz and Peter Zerwas concerning the “resolved” photon problem. We also wish to thank Edward Boos, Misha Dubinin and Slava Ilyin for confirming our results on the three body processes and for discussions. We also benefited from discussions with André Courau, Abdel Djouadi, George Gounaris, David Miller and Tran Truong. We are indebted to Abdel Djouadi for sending us the Fortran code for the Higgs branching ratios, George Jikia for making available the figures for $\gamma\gamma \rightarrow ZZ$

and Misha Bilenky for adapting the $e^+e^- \rightarrow W^+W^-$ BMT program to the case of the chiral Lagrangian. MB and GB wish to express their gratitude for the hospitality LAPP extended to them.

A Appendix

The formulae for the helicity amplitudes of the anomalous trilinear couplings, $\Delta\kappa$ and λ_γ are collected here. The reduced amplitude $\mathcal{N}_{\lambda_1\lambda_2\lambda_3\lambda_4}^{ano}$ is defined in the same way as the \mathcal{SM} ones, *i.e.* in 5.13, $\mathcal{N}^{sm} \rightarrow \mathcal{N}^{ano}$

$$-2 \sin^2 \theta (\gamma - 2) (\sin^2 \theta + 2 P_{34}^+) - 4 \cos^2 \theta (\sin^2 \theta + 4 P_{34}^+) \Biggr) \quad (A.2)$$

$$\begin{aligned}
\mathcal{N}_{+-;\lambda_3\lambda_4} &= \frac{\Delta\kappa}{2} \left[P_{34}^+ \sin^2 \theta + P_{34}^- (1 + \lambda_3 \cos \theta)^2 \right] + \lambda_\gamma P_{34}^+ (\gamma - 4) \sin^2 \theta + \\
&\quad \frac{\Delta\kappa^2}{8} \left\{ 6P_{34}^+ \sin^2 \theta + P_{34}^- (1 + \lambda_3 \cos \theta)^2 (\gamma + 2 - (\gamma - 4)\lambda_3 \cos \theta) \right\} + \\
&\quad \frac{\Delta\kappa\lambda_\gamma}{16} \left\{ 2P_{34}^+ \sin^2 \theta (\gamma - 3) + P_{34}^- (1 + \lambda_3 \cos \theta)^2 (\gamma - 2 - (\gamma - 4)\lambda_3 \cos \theta) \right\} + \\
&\quad \frac{\lambda_\gamma^2}{16} \left\{ 2P_{34}^+ \sin^2 \theta [2 - \sin^2 \theta (\gamma - 4)] + P_{34}^- (1 + \lambda_3 \cos \theta)^2 \times \right. \\
&\quad \left. \left[\gamma^2 (1 - \lambda_3 \cos \theta) (3 - \lambda_3 \cos \theta) - 4(1 - 6\lambda_3 \cos \theta + 2 \cos^2 \theta) - \right. \right. \\
&\quad \left. \left. 2\gamma(6 - 11\lambda_3 \cos \theta + 3 \cos^2 \theta) \right] \right\} \quad (A.3)
\end{aligned}$$

where $P_{34}^{\pm} = (1 \pm \lambda_3 \lambda_4)/2$ are operators projecting onto the W states with same (opposite) helicities respectively. The amplitudes not written explicitly above are simply obtained with the relation,

$$\mathcal{M}_{\lambda_1\lambda_2;\lambda_3\lambda_4} = \mathcal{M}_{-\lambda_1-\lambda_2;-\lambda_3-\lambda_4}^* \quad \theta \rightarrow -\theta \quad (\text{A.4})$$

Apart for various signs due to a different labelling of the polarisation vectors, these amplitudes agree with those of Yehudai[31] save for the dominant term (in $s_{\gamma\gamma}$) in the λ_{γ}^2 term of the $J_Z = 0$ amplitude for transverse W's, *i.e.* $(1 - 3 \cos^2 \theta) \rightarrow (3 - \cos^2 \theta)$. This is probably just a misprint.

References

- [1] I. F. Ginzburg, G. L. Kotkin, S. L. Panfil and V. G. Serbo, *Nucl. Phys.* **B228** (1983) 285.
- [2] G. Bélanger and F. Boudjema, *Phys. Lett.* **B288** (1992) 210.
- [3] M. Baillargeon and F. Boudjema, *Phys. Lett.* **B317** (1993) 371.
- [4] L.N. Lipatov and G.V. Frolov, *Sov. J. Nucl. Phys.* **13** (1971) 333
H. Cheng and T.T. Wu, *Phys. Rev.* **D1** (1970) 3414.
- [5] G.V. Jikia, *Phys. Lett.* **B298** (1993) 224; *Nucl. Phys.* **B405** (1993) 24.

- [6] B. Bajc, *Phys. Rev.* **D48** (1993) 1907.
- [7] M.S. Berger, *Phys. Rev.* **D48** (1993) 5121.
- [8] D.A. Dicus and C. Kao, *Phys. Rev.* **D49** (1994) 1265.
- [9] H. Veltman, SACLAY-SPHT-93-111, hep-ph-9311261.
- [10] G. Bélanger and F. Boudjema, *Phys. Lett.* **B288** (1992) 201.
- [11] V. Barger, T. Han and R.J.N. Phillips, *Phys. Rev.* **D39** (1989) 146.
- [12] V. Barger, T. Han and A. Stange, *Phys. Rev.* **D42** (1990) 777.
- [13] E. Fermi, *Z. Phys.* **29** (1924) 315.
 C. Weizsäcker *Z. Phys.* **88** (1934) 612
 E.J. Williams, *Phys. Rev.* **45** (1934) 729.
- [14] F.R. Arutyunian and V.A. Tumanian, *Phys. Lett.* **4** (1963) 176
 R.H. Milburn, *Phys. Rev. Lett.* **10** (1963) 75.
- [15] I.F. Ginzburg, G.L. Kotkin, V.G. Serbo and V.I. Telnov, *Sov. ZhETF Pis'ma* **34** (1981) 514 [JETP Lett. **34** 491 (1982)];
 I.F. Ginzburg, G.L. Kotkin, V.G. Serbo and V.I. Telnov, *Nucl. Instrum. Methods* **205** (1983) 47;
 I.F. Ginzburg, G.L. Kotkin, S.L. Panfil, V.G. Serbo and V.I. Telnov, *ibid* **219** (1984) 5;
 V.I. Telnov, *ibid* **A294** (1990) 72.
 V.I. Telnov, Proc. of the Workshop on “*Physics and Experiments with Linear Colliders*”, Saariselkä, Finland, eds. R. Orawa, P. Eerola and M. Nordberg, World Scientific, Singapore (1992) 739.
 V.I. Telnov, in *Proceedings of the IXth International Workshop on Photon-Photon Collisions.*, edited by D.O. Caldwell and H.P. Paar, World Scientific, (1992) 369.
- [16] D.L. Borden, D.A. Bauer, D.O. Caldwell, SLAC-PUB-5715, UCSB-HEP-92-01 (1992).
 D.L. Borden, Proceedings of *Workshop on Physics and Experiments with Linear e^+e^- Colliders*, Eds. F.A. Harris *et al.* (World Scientific, 1994) 323.
- [17] B. Grzadkowski and J.F. Gunion, *Phys. Lett.* **B294** (1992) 361.
- [18] G. Bélanger and G. Couture, UdeM-LPN-TH-93-163, UQAM-PHE-9305.

[19] G. Bélanger and F. Boudjema, in *Proceedings of the IXth International Workshop on Photon-Photon Collisions.*, eds. D. O. Caldwell and H. P. Paar, World Scientific (1992) 402.

[20] V. Telnov, Proceedings of *Workshop on Physics and Experiments with Linear e^+e^- Colliders*, Eds. F.A. Harris *et al.* (World Scientific, 1994) 551.

[21] Y. Yasui, I. Watanabe, J. Kodaira and I. Endo, *Nucl. Instrum. Meth.* **A335** (1993) 385.

[22] A. Aeppli, F. Cuypers and G. J. van Oldenborgh, *Phys. Lett.* **B314** (1993) 413.

[23] G. Bélanger and F. Boudjema, in progress.

[24] K. Fujikawa, *Phys. Rev.* **D7** (1973) 393
 M. Base and N.D. Hari Dass, *Ann. Phys.* **94** (1975) 349
 M.B. Gavela, G. Girardi, C. Malleville and P. Sorba, *Nucl. Phys.* **B193** (1981) 257
 N.G. Deshpande and M. Nazerimonfared, *Nucl. Phys.* **B213** (1983) 390
 F. Boudjema, *Phys. Lett.* **B187** (1987) 362.

[25] Z. Bern and D.A. Kosower, *Phys. Rev. Lett.* **66** (1991) 1669.
 Z. Bern and D.A. Kosower, *Nucl. Phys.* **B379** (1992) 451.
 Z. Bern and D.C. Dunbar, *Nucl. Phys.* **B379** (1992) 562.

[26] M. Baillargeon and F. Boudjema, *Phys. Lett.* **B272** (1991) 158.

[27] P.D. Pesic, *Phys. Rev.* **D8** (1973) 945.

[28] K. J. Kim and Y. S. Tsai, *Phys. Rev.* **D8** (1973) 3109.

[29] G. P. Sushkov, V. V. Flambaum and S. B. Khriplovich, *Sov. J. Nucl. Phys.* **20** (1975) 537.

[30] G. Tupper and M. A. Samuel, *Phys. Rev.* **D23** (1981) 1933.

[31] E. Yehudai, *Phys. Rev.* **D44** (1991) 3434.
 E. Yehudai, Ph.D. thesis, August 1991, SLAC-383.

[32] D. Zappala, these proceedings and D.A. Morris, T.N. Truong and D. Zappala, *Phys. Lett.* **323** (1994) 421.

[33] K. Hagiwara, R. Peccei, D. Zeppenfeld and K. Hikasa *Nucl. Phys.* **B282** (1987) 253.

[34] *BMT*: G.J. Gounaris *et al.*, in *Proc. of the Workshop on e^+e^- Collisions at 500 GeV: The Physics Potential*, ed P. Zerwas, DESY-92-123B (1992) 735.
BM2: M. Bilenky, J.L. Kneur, F.M. Renard and D. Schildknecht, *Nucl. Phys.* **409** (1993) 22.

[35] F. Boudjema, Proceedings of *Workshop on Physics and Experiments with Linear e^+e^- Colliders*, eds. F.A. Harris *et al.* (World Scientific, 1994) 712.

[36] J. P. Ma and B. H. J. Mckellar, *Phys. Lett.* **B319** (1993) 533.

[37] H. Aronson, *Phys. Rev.* **186** (1969) 1434.

[38] W. Buchmüller and D. Wyler, *Nucl. Phys.* **B268** (1986) 621.

[39] A. de Rújula, M.B. Gavela, P. Hernandez and E. Massó, *Nucl. Phys.* **B384** (1992) 3.

[40] T. Appelquist and C. Bernard, *Phys. Rev.* **D22** (1980) 200; A. Longhitano, *Nucl. Phys.* **B188** (1981) 118.

[41] B. Holdom, *Phys. Lett.* **B258** (1991) 156.

[42] D. Espriu and M.J. Herrero, *Nucl. Phys.* **B373** (1992) 117.

[43] A. Falk, M. Luke and E. Simmons, *Nucl. Phys.* **B365** (1991) 523.

[44] J. Bagger, S. Dawson and G. Valencia, *Nucl. Phys.* **B399** (1993) 364.

[45] F. Feruglio, *Int. J. of Mod. Phys.* **A28** (1993) 4937.

[46] T. Appelquist and G.H. Wu, *Phys. Rev.* **D48** (1993) 3235.

[47] S.Y. Choi and F. Schrempp, *Phys. Lett.* **B272** (1991) 149.

[48] M. Herrero and E. Ruiz-Morales, *Phys. Lett.* **B296** (1992) 397.

[49] C. Grosse-Knetter and I. Knuss, Bielefeld preprint BI-TP 94/10, hep-ph 9403291.

[50] A. Dobado and J. R. Pelaez, Madrid preprint FT/UCM/2/94, hep-ph/9404239.

[51] J.F. Gunion and H.E. Haber, in *Research Directions for the Decade*, Proc. of the 1990 DPF Summer Study on High Energy Physics, Snowmass, July 1990, edited by E.L. Berger, World Scientific, Singapore, p. 469.
Also, *Phys. Rev.* **D48** (1993) 5109.

[52] F. Richard, in Proc. of the *Workshop on e^+e^- Collisions at 500 GeV: The Physics Potential*, ed P. Zerwas, DESY-92-123B (1992) p. 883.

[53] J. Bijnens and F. Cornet, *Nucl. Phys.* **B296** (1988) 557.

[54] J. F. Donoghue, B. R. Holstein and Y. C. Lin, *Phys. Rev.* **D37** (1988) 2423.

[55] D. Morgan and M.R. Pennington, *Phys. Lett.* **B272** (1991) 134.

[56] T.N. Truong, *Phys. Lett.* **B313** (1993) 221.

[57] Crystal Ball Collaboration, H. Marsiske *et al.*, *Phys. Rev.* **D41** (1990) 3324.

[58] H. Fanchiotti, H. O. Girotti and A. Sirlin, *Lett. Nuov. Cim.* **4** (1972) 826.

[59] F. Boudjema, *Phys. Lett.* **B187** (1987) 362.

[60] F.-X. Dong, X.-D. Jiang and X.-J. Zhou, *Phys. Rev.* **D46** (1992) 5074.

[61] E.W.N. Glover and A.G. Morgan, *Z. Phys.* **C60** (1993) 175.

[62] G. Jikia and A. Tkabladze, IHEP preprint, IHEP-93-151, hep-ph/9312274, December 1993.

[63] G. Jikia and A. Tkabladze, *Phys. Lett.* **B323** (1994) 453.

[64] D.L. Borden, D.A. Bauer, D.O. Caldwell, *Phys. Rev.* **D48** (1993) 4018.

[65] D. Bowser-Cho and K. Cheung, *Phys. Rev.* **D48** 89 (1993).

[66] E. .E. Boos and G. V. Jikia, *Phys. Lett.* **B275** (1992) 164.

[67] M.V. Terent'ev, *Sov. J. Nucl. Phys.* **16** (1972) 87.

[68] J. Bijnens, S. Dawson and G. Valencia, *Phys. Rev.* **D44** (1991) 3555.

[69] J. F. Donoghue, C. Ramirez and G. Valencia , *Phys. Rev.* **D39** (1989) 1947.

[70] R. Rosenfeld, NUB-3074-93-TH, hep-ph-9310217.

[71] M.S. Chanowitz, *Phys. Rev. Lett.* **69** (1992) 2037.

[72] G. Gounaris and F. M. Renard, *Phys. Lett.* **B236** (1994) 131; *ibid Z. Phys.* **C59** (1993) 143.

[73] M. Bando, T. Kugo and K. Yamawaki, *Phys. Rep.* **164** (1988) 217.

- [74] G. Ecker, A. Pich and E. de Rafael, *Phys. Lett.* **B237** (1990) 481.
- [75] R. Casalbuoni, S. De Curtis, D. Dominici and R. Gatto, *Phys. Lett.* **B155**, 95 (1985); *Nucl. Phys.* **B282** (1987) 235 .
- [76] P. Ko, *Phys. Rev.* **D41** (1990) 1531.
- [77] R. Rosenfeld, NUB-3086-94-TH, hep-ph-9403356.
- [78] A. Abbasabadi, D. Bowser-Chao, D.A. Dicus and W.W. Repko, *Phys. Rev.* **D49** (1994) 547.
- [79] M. Peskin in *Proc. of Workshop on Physics and Experiments with Linear Colliders*, ed. by R. Orava, P. Eerola and M. Nordberg, World Scientific (1992) 1.
- [80] O.J. P. Eboli, M.C. Gonzalez-Garcia and S. F. Novaes, *Nucl. Phys.* **B411** (1994) 381.
- [81] M. Baillargeon and F. Boudjema, in *Proceedings of Beyond the SM III*, Ottawa , edited by S. Godfrey, World Scientific (1993) 387.
- [82] A. Ringwald, CERN-TH-6862-93, hep-ph-9305280.
- [83] E. Boos , M. Dubinin, V. A. Ilyin and A. E. Pukhov, in *Proc. of the Workshop on “ e^+e^- Collisions at 500 GeV. The Physics Potential”*, ed. P. M. Zerwas, DESY 92-123C (1994) 561.
- [84] F. T. Brandt, O. J. P. Eboli, E. M. Gregores, M. B. Magro, P. G. Mercadante and S. F. Novaes, IFUSP-P 1065, IFT-P.053/93, hep-ph/9308353.
- [85] M. Krämer, J. Kühn, M. L. Stong and P. M. Zerwas, DESY 93-174, TTP 93-41, hep-ph/9404280.
- [86] J.F. Gunion and J. G. Kelly, UCD-94-20, hep-ph/9404343.
- [87] B. Wiik, Summary Talk, Workshop “*Physics and Experiments with Linear Colliders*”, Saariselkä, Finland, 10-14 Sept. 1991.
- [88] see Hélène Veltman’s contribution in these proceedings.
- [89] O.J. P. Eboli, M.C. Gonzalez-Garcia, F. Halzen and D. Zeppenfeld, *Phys. Rev.* **D48** (1993) 1430.

[90] A. Djouadi *et al.*, Proc. of the Workshop on “ e^+e^- Collisions at 500 GeV. The Physics Potential”, ed. by P.M. Zerwas, DESY 92-123A/B (1992) 11.

[91] E. Witten, *Nucl. Phys.* **B120** (1977) 189.
C.H. Llewellyn-Smith, *Phys. Lett.* **B79** (1978) 83.

[92] M. Drees and R.M. Godbole, *Nucl. Phys.* **B339** (1990) 355.

[93] I.F. Ginzburg and V.G. Serbo, *Phys. Rev.* **D49** (1994) 49.

[94] M. Glück, E. Reya and A. Vogt, *Phys. Rev.* **D46** (1992) 1973.

[95] M. Baillargeon *et al.*, CERN-TH-6932-93, hep-ph-9307225, *Nucl. Phys.* **B** in Press.

[96] E. Boos *et al.*, *Z. Phys.* **C56** (1992) 487.
K. Cheung, *Phys. Rev.* **D47** (1993) 3750.

[97] K. Hagiwara, I. Watanabe, P.M. Zerwas, *Phys. Lett.* **B278** (1992) 187.

[98] E. Boos *et al.*, *Phys. Lett.* **B273** (1991) 173.

[99] A. Djouadi, J. Kalinowski and P. Zerwas, *Z. Phys.* **C54** (1992) 255.

[100] R.N. Cahn and S. Dawson, *Phys. Lett.* **B136** (1984) 196.

[101] S. Dawson, *Nucl. Phys.* **B249** (1984) 42.

[102] M.S. Chanowitz and M.K. Gaillard, *Phys. Lett.* **B142** (1984) 196.

[103] G.L. Kane, W.W. Repko and W.B. Rolnick, *Phys. Lett.* **B148** (1984) 367.

[104] J. Lindfors, *Z. Phys.* **C28** (1985) 427.

[105] W.B. Rolnick, *Nucl. Phys.* **B274** (1986) 171.

[106] This has first been suggested by F. Boudjema, Convener’s talk (*W* Working Group), 1st meeting of the Workshop on “ e^+e^- Collisions at 500 GeV. The Physics Potential”, Munich-Annecy-Hamburg, Munich, Nov. 1992.

[107] S. Brodsky, Proceedings of *Workshop on Physics and Experiments with Linear e^+e^- Colliders*, Eds. F.A. Harris *et al.* (World Scientific, 1994) 295.

[108] R. Kleiss and W.J. Stirling *Phys. Lett.* **B182** (1986) 75.

[109] G. Altarelli and G. Parisi, *Nucl. Phys.* **B126** 298 (1977).

[110] S. J. Brodsky, T. Kinoshita and H. Terazawa, *Phys. Rev.* **D4** (1971) 1532
 V.M. Budnev *et al.*, *Phys. Rep.* **15** (1975) 183
 V.N. Baier *et al.*, *Phys. Rep.* **78** (1981) 293
 K. Hagiwara *et al.*, *Nucl. Phys.* **B365** (1991) 544.

[111] R.N. Cahn, *Nucl. Phys.* **B255** (1985) 341.

[112] K. Cheung, *Phys. Lett.* **B323** (1994) 85.

[113] G. Jikia, work in progress. Private communication.

[114] A. Goto and T. Kon, *in Europhys. Lett. Phys. Lett.* **13** (1990) 211; *Erratum, ibid* **14** (1991) 281.
 T. Kon, *Phys. Lett.* **B316** (1993) 181.

[115] F. Cuypers, G. J. van Oldenborgh and R. Rückl, *Nucl. Phys.* **B409** (1993) 144.

[116] I. F. Ginzburg and D. Yu. Ivanov, *Phys. Lett.* **B276** (1992) 214.

[117] F. Boudjema, A. Djouadi and J. L. Kneur, *Z. Phys.* **C57** (1993) 425.

[118] M. Drees and R.M. Godbole, *Phys. Rev. Lett.* **67** (1991) 1189.
 In Proc. of the *Workshop on e^+e^- Collisions at 500GeV: The Physics Potential*, ed P. Zerwas, DESY-92-123B (1992) p. 863.

[119] J.R. Forshaw and J.D. Storrow, *Phys. Lett.* **B278** (1992) 193.

[120] P. Chen, T. L. Barklow and M. Peskin *Phys. Rev.* **D49** (1994) 3209.